

NOTE TO USERS

This reproduction is the best copy available.

UMI[®]

**Fluorescence Based Trace Detection of Pesticides Using Supramolecular Hosts, UV Photolysis
and Synchronous Scanning**

A Thesis

Submitted to the Graduate Faculty

In Partial Fulfillment of the Requirements

For the Degree of

Master of Science

in the Department of Chemistry

Faculty of Science

University of Prince Edward Island

Shawn A. MacDougall

Charlottetown, P.E.I.

March, 2010



Library and Archives
Canada

Published Heritage
Branch

395 Wellington Street
Ottawa ON K1A 0N4
Canada

Bibliothèque et
Archives Canada

Direction du
Patrimoine de l'édition

395, rue Wellington
Ottawa ON K1A 0N4
Canada

Your file Votre référence
ISBN: 978-0-494-64465-2
Our file Notre référence
ISBN: 978-0-494-64465-2

NOTICE:

The author has granted a non-exclusive license allowing Library and Archives Canada to reproduce, publish, archive, preserve, conserve, communicate to the public by telecommunication or on the Internet, loan, distribute and sell theses worldwide, for commercial or non-commercial purposes, in microform, paper, electronic and/or any other formats.

The author retains copyright ownership and moral rights in this thesis. Neither the thesis nor substantial extracts from it may be printed or otherwise reproduced without the author's permission.

In compliance with the Canadian Privacy Act some supporting forms may have been removed from this thesis.

While these forms may be included in the document page count, their removal does not represent any loss of content from the thesis.

AVIS:

L'auteur a accordé une licence non exclusive permettant à la Bibliothèque et Archives Canada de reproduire, publier, archiver, sauvegarder, conserver, transmettre au public par télécommunication ou par l'Internet, prêter, distribuer et vendre des thèses partout dans le monde, à des fins commerciales ou autres, sur support microforme, papier, électronique et/ou autres formats.

L'auteur conserve la propriété du droit d'auteur et des droits moraux qui protège cette thèse. Ni la thèse ni des extraits substantiels de celle-ci ne doivent être imprimés ou autrement reproduits sans son autorisation.

Conformément à la loi canadienne sur la protection de la vie privée, quelques formulaires secondaires ont été enlevés de cette thèse.

Bien que ces formulaires aient inclus dans la pagination, il n'y aura aucun contenu manquant.



Canada

The author has agreed that the Library, University of Prince Edward Island, may make this thesis freely available for inspection. Moreover, the author has agreed that permission for extensive copying of this thesis for scholarly purposes may be granted by the professor of professors who supervised the thesis work recorded herein or, in their absence, by the Chair of the Department or the Dean of the Faculty in which the thesis work was done. It is understood that due recognition will be given to the author of this thesis and to the University of Prince Edward Island in any use of the material in this thesis. Copying or publication or any other use of the thesis for financial gain without approval by the University of Prince Edward Island and the author's written permission is prohibited.

Requests for permission to copy or to make any other use of material in this thesis in whole or in part should be addressed to:

Chair of the Department of Chemistry

Faculty of Science

University of Prince Edward Island

Charlottetown, P.E.I.

Canada, C1A 4P3

SIGNATURE PAGE

(iii) & (iv)

REMOVED

Table of Contents

Acknowledgments	-ix-
List of Figures	-xi-
List of Tables	-xiii-
List of Abbreviations	-xiii-
Abstract	-xv-
I. INTRODUCTION	1
<i>I.1. Standard Methods of Pesticide Detection on Prince Edward Island</i>	4
<i>I.2. Enhancement of Natural Fluorescence</i>	6
I.2.1 Supramolecular Host-Guest Inclusion Complexes	10
I.2.2. Photochemically Induced Fluorescence	17
<i>I.3. Pesticides of Interest</i>	18
<i>I.4. Overall Project Goals</i>	23
II. EXPERIMENTAL	25
<i>II.1. Materials Used</i>	25
<i>II.2. Instrumentation</i>	26
II.2.1. UV-Visible Absorption Spectroscopy	26
II.2.2. Steady-State Fluorescence	27
II.2.3. UV Photochemistry	28
<i>II.3. Pesticide Stock Solution Preparation</i>	29
<i>II.4 Determination of the Percent Water in the Cavity of Various Cyclodextrins</i>	30
<i>II.5. Fluorescence Quantum Yields and Extinction Coefficients</i>	31
II.5.1. Solution Preparation	32
II.5.2. QY and EC Procedure	33

II.6. Photochemically Induced Fluorescence	35
II.6.1. Imidacloprid Photolysis and Steady State Fluorescence	34
II.6.2. Azoxystrobin Photolysis and Steady State Fluorescence	35
II.7. Host:Guest Enhanced Fluorescence	36
II.7.1. Determination of Binding Constant, K	36
II.7.2. Calibration Curves	37
II.7.3. Limit of Detection and Quantification	38
II.8. HPLC Experiments	39
II.8.1. Solution Preparation	39
II.8.2. HPLC Analysis	40
II.9. 1H NMR Experiments	41
II.10. Synchronous Scanning Fluorescence Experiments	41
II.10.1. Sample Preparation	41
II.10.2. Synchronous Scanning Procedure	42
III. RESULTS AND DISCUSSIONS-	Cyclodextrin Enhanced Fluorescence of
	Pesticides in Water
	44
III.1. Determination of the Percent Water in the Cavity of Various Cyclodextrins	44
III.2. Carbofuran	45
III.2.1. Absorption and Fluorescence Measurements	45
III.2.2. Fluorescence Enhancement by CD Inclusion	47
III.2.3. Investigation into the Mechanism for the Enhancement of CAF Fluorescence	48
III.2.4. Fluorescence Titrations	52
III.2.5. Calibration Curve, LOD and LOQ	54
III.2.6. Spiked Samples	57
III.3. Chlorothalonil	59

III.3.1. Absorption and Fluorescence Measurements	59
III.3.2. Fluorescence Enhancement by CD Inclusion	60
III.3.3. Fluorescence Titrations	61
III.3.4. Calibration Curve, LOD and LOQ	64
III.4. Carbaryl	66
III.4.1. Fluorescence Experimentation	67
III.4.2. Fluorescence Enhancement by CD Inclusion	67
III.4.3. Investigations into the Enhancement of Fluorescence	68
III.4.4. Calibration Curve	69
III.5. Atrazine	70
III.5.1. Absorption and Fluorescence Measurements	71
III.5.2. Enhancement of Fluorescence by CD Inclusion	72
III.6. Metalochlor	73
III.6.1. Absorbance and Fluorescence Measurements	74
III.7. Imidacloprid	75
III.7.1. Absorption and Fluorescence Measurements	75
III.8. Azoxystrobin	76
III.8.1. Absorption and Fluorescence Measurements	77
III.9. Simultaneous Detection of Pesticides in a Sample	78
III.10. Synchronous Scanning Fluorescence	81
III.10.1. Calibration Curves, LOD and LOQ	83
III.10.2. Simultaneous Detection of Pesticide Using Synchronous Scanning	88
III.10.3. Spiked Sample Detection Using Synchronous Scanning	92
III.10.3.1. Carbofuran Spiked Sample Detection	92
III.10.3.2. Carbaryl Spiked Sample Detection	94

III.11. Conclusions	95
IV. RESULTS AND DISCUSSIONS-	Photochemically Induced Fluorescence
	of Pesticides
	97
IV.1. Imidacloprid	97
IV.1.1. Photochemically Induced Fluorescence	98
IV.1.2. Fluorescence Enhancement by CD Inclusion	100
IV.2. Azoxystrobin	100
IV.2.1. Photochemically Induced Fluorescence	101
IV.2.2. Fluorescence Enhancement by CD Inclusion	103
IV.2.3. Determination of Binding Constants	106
IV.2.4. Limit of Detection and Quantification	108
V. RESULTS AND DISCUSSIONS-	UV-A Photochemistry of the Pesticide
	Azinphos-Methyl
	111
V.1. Calibration Curve, LOD and LOQ of AZM with HP-β-CD	112
V.2. Fluorescence Based Studies of the UV-A Photolysis of AZM	113
V.2.1. Previous Work	
V.2.2. Goal of this Work	114
V.3. Decay Rates of the Formation and Photolysis of the Highly Fluorescent Intermediate	116
V.3.1. Quantum Yields and Extinction Coefficients	117
V.3.2. ^1H NMR Studies of the UV-A Photolysis of AZM	120
V.3.3. HPLC Studies of the UV-A Photolysis of AZM	121
V.4. Conclusions	122
VI. CONCLUSIONS	124

Acknowledgements

During my time at UPEI, I have had the chance to meet and work with people that will remain a part of my life for long after I have finished. These people have done so much for me over the past 2+ years that I am forever thankful.

Dawna Lund and Jill MacDonald were my saviours when it came to faulty instruments and the daunting task of being lab supervisor. Without their guidance and reassurance I never would have been able to get through the past years as smoothly as I did.

My friends are also to thank, for because of them, on days when nothing seemed to go right and my nerves were shot, they were there to cheer me up and encourage me to keep my head up and stay calm.

My supervisory committee also shares a part of this with me for Dr. Linkletter assisted me in the use of HPLC and allowed me to use his instrument on very short notice (and didn't get mad when it broke down and the entire building smelled like fish). Dr. Russ Kerr, I thank so much for allowing me the opportunity to go on the trip of a lifetime for one of my graduate courses. It's something I'll never ever forget.

My dear friend Carrie Snow, who I can't possibly thank enough, for without Carrie, the lab just wouldn't have been the same. From all your help with topics I didn't quite understand to the jokes we shared. I will never be able to thank you enough.

I also wish to thank my parents for all their support, emotionally AND financially as I made my way through this section of my life. I am so grateful to have such understanding, supportive parents.

Finally, I would like to thank Dr. Brian Wagner, who took a chance on me when one day I showed up in his office, looking for some advice on what to do with my life. He offered a guy, who had no previous lab experience, a spot in his lab to work and learn and because of that opportunity, I am where I am. I will never forget this chance you have given me. Thank you so much.

List of Figures

Figure 1. A simplified version of the Jablonski diagram.

Figure 2. An illustration of a 1:1 host:guest inclusion complex being formed.

Figure 3. The three types of cyclodextrins with the various cavity sizes

Figure 4. Chemical structure of β -cyclodextrin and hydroxypropyl- β -cyclodextrin.

Figure 5. Increased energy gap due to change in polarity of environment.

Figure 6. The two fungicides used in this project. a) Chlorothalonil, CHT b) Acoxystrobin, AZY

Figure 7. The insecticides used in this project. a) Carbofuran, CAF b) Carbaryl, CAB c) Azinphos-Methyl, AZM d) Imidacloprid, IMI.

Figure 8. The herbicides used in this project. a) Atrazine, ATR b) Metolachlor, MET

Figure 9. Chemical structures of a) N-methyl anthranilic acid (NMA) and b) 9,10-Diphenylanthracene (DPA)

Figure 10. Chemical structures of a) Benzazimide (BA) and b) Anthranilic Acid (AA).

Figure 11. Absorption spectrum of 3mL of 1.75×10^{-4} M Carbofuran solution in the absence (and in the presence of β -CD).

Figure 12. Fluorescence spectra of 1.75×10^{-4} M CAF without CD with the addition of β -CD and with the addition of HP- β -CD.

Figure 13. Comparison of 1.75×10^{-4} M CAF in ethanol to 1.75×10^{-4} M CAF in water.

Figure 14. Fluorescence titration of CAF with HP- β -CD.

Figure 15. The double reciprocal plot of the fluorescence titration of CAF with HP- β -CD.

Figure 16.a. Fluorescence spectra of the CAF calibration solutions with 10mM Hp-b-CD.

Figure 16.b. Calibration curve of 10mM HP- β -CD with various concentrations of Carbofuran.

Figure 17. The fluorescence emission of CHT with/without α -CD

Figure 18. A fluorescence titration of CHT with α -CD.

Figure 19. Calibration curve of CHT. Various concentrations of CHT with α -CD (10mM).

Figure 20. The fluorescence spectra of 10 mM α -CD with CHT.

Figure 21. Calibration curve of CAB with HP- β -CD (10mM).

Figure 22. The fluorescence spectra of 3.00×10^{-5} M ATR in the absence of CD and in the presence of HP- β -CD.

Figure 23. Fluorescence spectrum of the mixed pesticide solution containing CAF, CAB, CHT and AZM.

Figure 24. Synchronous scanning fluorescence spectrum vs. Steady state fluorescence spectrum of a CAF solution.

Figure 25. Synchronous scanning fluorescence spectrum vs. Steady state fluorescence spectrum of a CAB solution.

Figure 26. A calibration curve for CAF using SSF using the scanning wavelengths optimized for the pesticide CAF.

Figure 27. A calibration curve for CAB using SSF with the scanning wavelengths optimized for the pesticide CAB.

Figure 28. The fluorescence spectra of the calibration curve solutions of CAF.

Figure 29. The fluorescence spectra of the calibration curve solutions of CAB.

Figure 30. Synchronous scan of 100 ppb CAF, 100 ppb CAB and a mixture of 100 ppb of each CAF, CAB, CHT, and AZM.

Figure 31. The synchronous scanning spectra of 100 ppb CAB and a mixture of 100 ppb of each CAF, CHT, CAB and AZM.

Figure 32. Fluorescence of Imidacloprid before UV exposure, after approx. 5 minutes and 35 minutes of UV-A exposure.

Figure 33. The fluorescence spectrum of AZO with/without UV exposure

Figure 34. The absorption spectrum of unphotolyzed (—) and photolyzed (---) AZO.

Figure 35. The fluorescence spectra of a photolyzed solution of AZO

Figure 36. Fluorescence titration of photolyzed AZO with HP- γ -CD.

Figure 37. The proposed mechanism of AZM with both major and minor pathways.

Figure 38. The fluorescence intensity of NMA vs. UV exposure time.

Figure 39. The portable fluorimeter.

List of Tables

Table 1. Chemicals used during this project and their sources.

Table 2. Pesticide stock solution preparation details.

Table 3. Different fluorimeter settings and CDs used for each pesticide.

Table 4. Results from CAF spiked sample trial using steady state fluorescence

Table 5. Results from fluorescence trials of CHT with various CDs.

Table 6. Results from spiked sample test using SSF for CAF

Table 7. Results from spiked sample test using SSF for CAB

List of Abbreviations

PEI	Prince Edward Island
HPLC	High performance liquid chromatography
GC-MS	Gas chromatography-mass spectrometry
NMR	Nuclear magnetic resonance
S_0	Ground electronic state
S_n	Excited electronic state
CD	Cyclodextrin
H	Host
G	Guest
UV-Vis	Ultraviolet-Visible
PIF	Photochemically induced fluorescence
LOD	Limit of detection
LOQ	Limit of quantification

SD	Standard deviation
λ_f , Max	Wavelength of maximum fluorescence
PSF	Polarity sensitivity factor
Cps	Counts per second
K	Binding/equilibrium constant
SSF	Synchronous scanning fluorescence
Φ	Quantum yield
ϵ	Extinction coefficient
LC ₅₀	Lethal concentration
CHT	Chlorothalonil
AZY	Azoxystrobin
CAF	Carbofuran
CAB	Carbaryl
AZM	Azinphos-methyl
IMI	Imidacloprid
ATR	Atrazine
MET	Metolachlor
DPA	9,10-diphenyl anthracene
BA	Benzazimide
NMA	N-methylanthranilic acid
AA	Anthranilic acid

Abstract

Traditional methods of pesticide detection used on Prince Edward Island (PEI) are very expensive and time consuming. These methods are typically only useful after harm has been done to the environment, and cannot be used in prevention. A new method for rapid, on-site detection of these pesticides would not only be of value financially, it could also prove to be essential in preventative measures, for example by monitoring streams. Fluorescence, the light emitted by electronically excited molecules, is a highly sensitive technique for detecting and measuring the concentration of molecules in solution. Most pesticides used on Prince Edward Island show only weak native fluorescence in water. However by forming a supramolecular host:guest inclusion complex, in which the pesticide "guest" becomes included within the internal cavity of an organic host molecule, this fluorescence is increased for many guest molecules. In some cases, this enhancement of the fluorescence might be sufficiently large enough to allow for the development of a fluorescence-based trace analysis technique with sensitivity in the required ppb level. In this project, native and modified cyclodextrins and their effect on the fluorescence of a series of pesticides used on PEI, specifically carbofuran, carbaryl and chlorothalonil along with five others, is measured with results varying from 670 parts per trillion for carbaryl to 69 ppb for Chlorothalonil. In addition, UV photolysis of certain pesticides can also lead to enhanced fluorescence such as azoxystrobin and imidacloprid, and thus also be a technique used in the trace detection of pesticides. This occurs via creation of a more highly fluorescent molecule from a previously non-fluorescent or weakly fluorescent pesticide. Synchronous scanning, a method of measuring fluorescence by scanning both excitation and emission wavelengths simultaneously, which results in narrower measured emission bands is also examined in detail to separate fluorescent bands of similar emission wavelengths, and thus simultaneously measure a set of two or more pesticides in solution. Overall, the main goal of this work is to develop a sensitive, enhanced fluorescence based trace analysis

technique for pesticides, which could eventually be carried out using a portable fluorimeter, so that samples could be analyzed on site, in a matter of minutes, rather than in a lab over a period of days.

I. ***INTRODUCTION***

While the heated debate on banning domestic pesticides for cosmetic use on Prince Edward Island (PEI) carries on in the media, farmers continue to apply copious amounts of agricultural pesticides to their crops with much less media attention. With the goals of producing healthier crops with higher yields, farmers on PEI continue with the practice of industrialized farming with emphasis on production. This involves larger and larger farms, with highly sophisticated machinery, huge volumes of pesticides, and an ever growing strain on the local and global environments. PEI continually relies on agriculture as one of its primary industries. PEI is known worldwide for its main crop, the potato, and local farmers are determined to live up to that reputation by producing a premium product each growing season. With this reliance on production in order to make a living, farmers find themselves turning to agricultural pesticides in order to prevent any pests or disease from destroying their valuable crops. It is estimated that a single field can have as many as 19 pesticide applications in a single year.¹

PEI, being the smallest Canadian province, cultivates over 44% of its total land area; 660,000 acres out of a total of 1.4 million acres.² This area of land is farmed on an annual basis and considering the fact that PEI is surrounded by water, there are clear implications from having such an extensive amount of agricultural area in such a close proximity to waterways. Another of PEI's major industries is golf. As of 2009, PEI boasts 30 beautiful courses scattered throughout the province. This land area is not accounted for in the previous statistic regarding

total cultivated land on PEI. Each golf course can be and usually is another source of pesticides entering the environment, although not as significant a source as the farming sector.

Agricultural contamination of Prince Edward Island's water table is always a major concern to the residents living on PEI. Many rural residents depend on water from wells for their drinking water. With all of these pesticides being deposited into the waterways, testing of water continues to be an issue for local residents. Whether it is the misuse of pesticides during application or by unexpected extreme weather events, pesticides have been showing up in water and air tests as far back as when testing of local waters and air began in 1994. In 2006, a study was done on the air quality of Prince Edward Island, in order to see if all these pesticide applications were having any negative effects. The study showed that in every single air sample taken, the pesticide chlorothalonil, which has proven cancer causing effects³, was present. Even in samples taken from villages where chlorothalonil had not been applied, trace amounts were detected. Because of spray drift, a typical cause of the contamination of water, pesticides had actually spread from fields to villages where no farming took place.³ This was a major wakeup call for the Government of Prince Edward Island.

In the last 15 years, over 26 fish kills have been reported on PEI⁴, with the possibility of many more kills having gone unreported or unnoticed. Two of the more recent fish kills reported on PEI happened at the Dunk and Tryon rivers in the summer of 2006. In each case, it was two and three days respectively, after the fish kill occurred that the incidents were reported and water samples from those rivers sent to the Environment Canada research lab in Moncton, New Brunswick. These samples were then analyzed, showing amounts of

chlorothalonil five times greater than the acceptable level for this pesticide in water. It is believed that at the time of the fish kills, the concentration would have been much higher but due to the time spent in water and exposure to UV light from the sun, it is expected that much of the chlorothalonil was photolyzed into bi-products.⁵ Strict regulations on pesticide usage have been put in place by the Government of Prince Edward Island to help with a reduction of these fish kill events. The Pesticide Control Act was written in 1988 but without much enforcement prior to the late 1990s. The occurrence and frequency of fish kills is a devastating fact to all residents of PEI.

Application of pesticides is restricted by the Pesticide Control Act so that farmers may not apply pesticides in winds less than four kilometres per hour or higher than fifteen kilometres per hour. The province has also created strict buffer zone regions- the area of land between cultivated fields and natural water bodies- which is at least 25 metres wide.⁶ The government of Prince Edward Island has also placed strict buying regulations on farmers and require them to have an extensive amount of training in handling, moving and application of pesticides.

Pesticide sales on Prince Edward Island have been on the decline in recent years with the popularity of “organic” farming practices drawing many new proponents. In 2007, 630 282 kg of active ingredients (AI) were purchased according to the non-domestic pesticide retail sales report of 2007 down from 718 410 kg of AI during the previous year.⁷ In the year 2000, pesticide application reached an all-time high at 1.62 kg per acre of land on PEI.⁶ The trend since then has been decreasing due to more enforcement of the Pesticide Act and a steep rise

in fines in 2003.⁶ In more recent years, new, more efficient pesticides have been and continue to be developed. The “new generation” pesticides target a wider range of pests. These broad spectrum pesticides, which can kill more than one species of pests per application, are being applied less often than single target organism pesticides that require many applications. Insecticide sales on Prince Edward Island have been decreasing since 1993, down 72% according to Statistics Canada. Even with this enormous drop in sales, the rate of fish kills remains equal with previous years dating back as far as any pesticide related fish kills have been recorded.⁴ This illustrates the importance of a reliable method of pesticide detection in natural waters that is fast and cost effective as current methods tend to be expensive and often time consuming. Also, it shows an even greater value for a detection method that could be potentially used as a method to monitor water systems, for prevention of contamination of natural water bodies from pesticide runoff and drifts.

I.1. *Standard Methods of Pesticide Detection on Prince Edward Island*

Currently on Prince Edward Island, there is no accredited water testing laboratory in use by either the Government of Prince Edward Island or Environment Canada. All water samples that are taken from areas of suspected pesticide related fish kills are sent away to Moncton, New Brunswick where an Environment Canada research laboratory carries out the required testing. This lab usually performs a sample extraction and then High Performance Liquid Chromatography (HPLC) or gas chromatography-mass spectrometry (GC-MS) on the sample. The required time for the completion of experiments and reporting of results can take

anywhere from a few days to several weeks depending on the availability of the Environment Canada employees and lab space. The cost of these tests can run the province of Prince Edward Island substantial amount of money.

In order to perform these types of experiments for the trace detection of pesticides in natural waters, extraction must be done on the samples to separate the pesticides present. Carbon tetrachloride (CCl₄) is often used to perform this task. CCl₄ is a known agent in ozone depletion in the stratosphere. It also accumulates in tissues in aquatic species and is a known human carcinogen.⁸ Along with the drawbacks of using these methods of detection mentioned, neither method (HPLC or GC-MS) of testing can be performed on site. All samples must be collected, stored properly for transporting and then taken to the laboratory for analysis.

Using HPLC or GC-MS as a means of trace detection of pesticides in natural waters has the benefit of high accuracy and sensitivity. In most cases, depending on the type of pesticide, levels as low as 1 part per billion (ppb) and in some cases, in the parts per trillion (ppt) range can be detected and quantified.^{9,10} Although it is not a requirement for a detection limit to be that low, it is helpful in cases where time has passed between the fish kill occurring and the discovery of the polluted water body for most pesticides have a lifetime of only a few days when present in water. In these cases, only small amounts of pesticide may remain in the water.¹¹

With these considerations in mind, it is easy to see why the development of a rapid, on-site method for detection of pesticides in water would be of such a value to the province of PEI.

In this project, the application of fluorescence-based trace detection techniques for pesticides will be investigated.

1.2. *Enhancement of Natural Fluorescence*

Molecular fluorescence is a process that occurs when a molecule absorbs UV or visible radiation at a particular wavelength, known as the excitation wavelength, and is promoted from its ground electronic state (S_0) to an excited electronic state of the same multiplicity (S_n , $n=1,2,3,\dots$) (denoted by A in Figure 1). Once excited, the molecule can then return to its ground state in a number of different ways. Two possible ways of releasing this excitation energy are by heat (non-radiative decay) or by releasing a photon (radiative decay). There are two distinct non-radiative pathways. Internal conversion (IC) occurs when an excited molecule transfers from the lowest vibrational energy level of the excited electronic state to a high vibrational energy level of a lower state of the same multiplicity, typically the ground electronic state (an isoenergetic process) followed by rapid vibrational relaxation (VR) to the lowest vibrational level of the ground state. Thus, the excess energy is released as heat. Intersystem crossing (ISC) differs in that the excited singlet molecule transfers to a vibrational level of a triplet state (e.g. T_1). The excited triplet molecule can then relax back to the original ground state radiatively by a process known as phosphorescence (P). The radiative decay of the excited S_1 state back to the singlet S_0 ground state is the process referred to as fluorescence. Fluorescence is a radiative decay between states with the same multiplicity, whereas phosphorescence involves a change in spin. The intensity of the emitted fluorescent photons is measured in a fluorescence

experiment. A plot of the intensity of the emitted light as a function of a wavelength is referred to as the fluorescence spectrum. The two pathways, radiative and non-radiative, compete with one another. It is when the non-radiative pathway is minimal that fluorescence is at a maximum. These various pathways are illustrated in the Jablonski diagram shown in Figure 1.

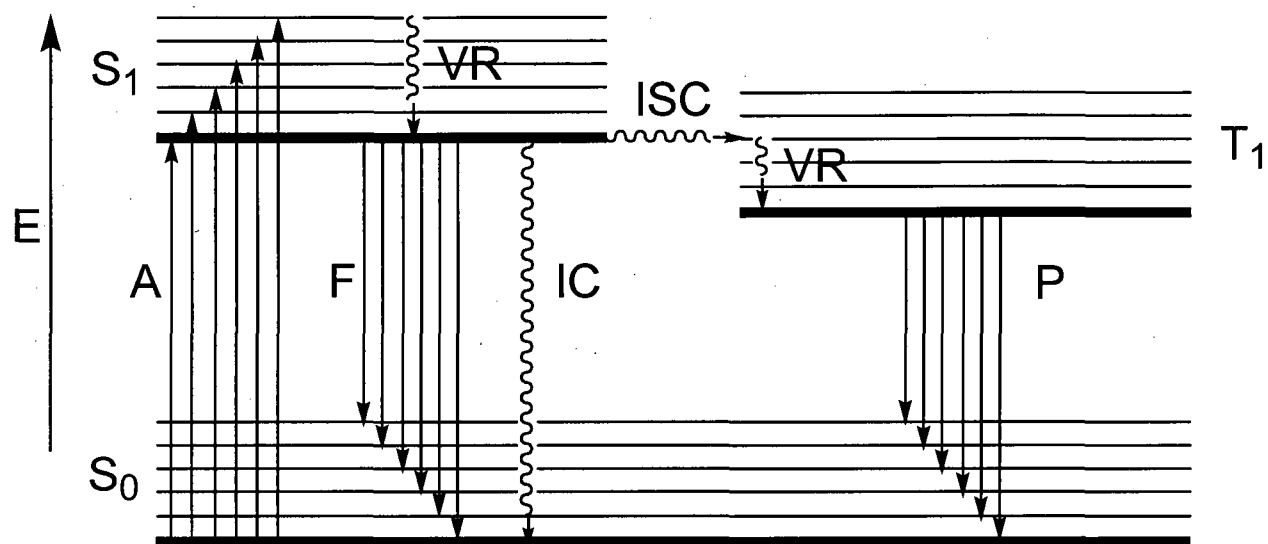


Figure 1. A simplified version of the Jablonski diagram.^{12, 13}

There are many different types of experimental fluorescence techniques. These include steady state, time-resolved, synchronous scanning and fluorescence depolarization.^{12, 13} This project however, only deals with steady state and synchronous scanning fluorescence spectroscopy. The most common and easily understood fluorescence technique is steady state fluorescence, in which a fluorescent species, present in a solution, is exposed to an excitation source that is stable and constant. As long as the excitation source remains stable, there exists a steady state concentration of excited molecules in the S_1 state, as the rate of S_0 to S_1

excitation will equal the rate of S_1 to S_0 decay. For a given population of S_1 molecules, since the fluorescence intensity is directly proportional to the concentration of excited S_1 molecules, it can be deduced that the fluorescence intensity is also constant, and directly proportional to the concentration.^{12, 13} A steady state fluorescence spectrum can then be obtained by measuring that intensity as a function of the emission wavelength, using an emission monochrometer which will select and scan the wavelength.¹²

From steady state fluorescence spectroscopy, two important pieces of data are obtained quantitatively: both the fluorescence intensity at a given wavelength ($I_{F,\lambda}$) and the wavelength of the maximum intensity ($\lambda_{F,max}$, can be more than one) can be determined from the fluorescence spectrum.¹² In addition, the total fluorescence emission (F) can be determined as the area of the measured fluorescence spectrum.

Fluorescence quantum yield (Φ_F) is defined as the fraction of the number of photons emitted by an excited state molecule during its relaxation to the ground state relative to the number of photons that are absorbed.¹² Quantum yield is defined by Eq 1.1

$$\Phi_F = \frac{k_F}{k_F + k_{NR}}$$
 Eq. 1.1

The fluorescence quantum yield is determined from the rate of total fluorescence (k_F) divided by the sum of the rate of total fluorescence and the rate of non-radiative decay pathways (k_{NR}).

Those non-radiative pathways include the rate of internal conversion (k_{IC}) and the rate of intersystem crossing (k_{ISC}).

Fluorescence is a process that requires certain criteria in a molecule that allows it to fluoresce significantly. Aromatic molecules are ideal for molecular fluorescence because of their delocalized π -electrons, due to the conjugated double bond system. These electrons can be efficiently excited from their ground π energy level (S_0) to an excited π^* energy level (S_1) in the UV-A to visible region. The energy gap between the S_0 and S_1 states are relatively large for such aromatic compounds, making competing internal conversion relatively low, resulting in significant fluorescence. Pesticides have a wide variety of shapes and configurations and many are aromatic, making them of potential interest in fluorescence experiments.

In synchronous scanning fluorescence spectroscopy, scanning of both the excitation wavelength and emission wavelength occurs simultaneously. Through this synchronized scanning, a constant wavelength interval between the two wavelengths is maintained.¹⁴ If this interval is equal to the Stokes' shift, the difference between maxima of the absorption and emission spectra, then the resulting fluorescence spectrum will have a much narrower band without any loss in sensitivity.¹⁴ This becomes ideal when working with two or more fluorophores present in one solution, to reduce or even eliminate spectral overlap.

There exists large numbers of different pesticides that exhibit natural fluorescence that are used in farming practises today.¹⁵ In most cases however, the fluorescent signal is too weak to be of any interest in trace detection. To be a worthwhile technique, detection levels would ideally be in the low ppb range. A major goal of this project is to use various methods to

enhance this fluorescence signal to a level where it would be of use in the trace detection of pesticides and in particular, those of interest on PEI, in natural waters.

There are several studies reported in the literature that discusses the use of cyclodextrins, a common molecular host (see later) to enhance the fluorescence emission of some pesticides.¹⁵⁻¹⁸ Pesticides coumatetralyl, chlorpyriphos, deltametrin, and fenvalerate have all shown promising results from the addition of cyclodextrin to enhance the natural fluorescence of the pesticide molecules. These pesticides are not specifically relevant to PEI for they are currently not applied here. Cyclodextrin addition with a goal to enhance the natural fluorescence will be explored further for a wide range of pesticides used on PEI. Furthermore, most previous studies used native cyclodextrins only; better results can be obtained using chemically modified cyclodextrins.¹⁶⁻¹⁹

I.2.1 Supramolecular Host-Guest Inclusion Complexes

Supramolecular chemistry, in particular, host-guest supramolecular chemistry is one of the possible methods of increasing the natural fluorescence of a pesticide. In his Nobel lecture, J.M. Lehn described supramolecular chemistry as “chemistry beyond the molecule”.²⁰ It involves two or more molecules that are held together, not by an ionic or covalent bond(s), but by intermolecular forces such as van der Waals forces and/or hydrogen bonding. Host-guest supramolecular chemistry occurs when a smaller molecule, the guest, becomes included within a hollow, usually larger, host molecule. There are many types of host-guest complexes that can form but the most common and simplest is a 1:1 host:guest complex. An example of 1:1

host:guest complexation is illustrated in Figure 2. Other possible complexes include 2:1, 2:2, and 1:2 but in this project, only 1:1 complexes were found.

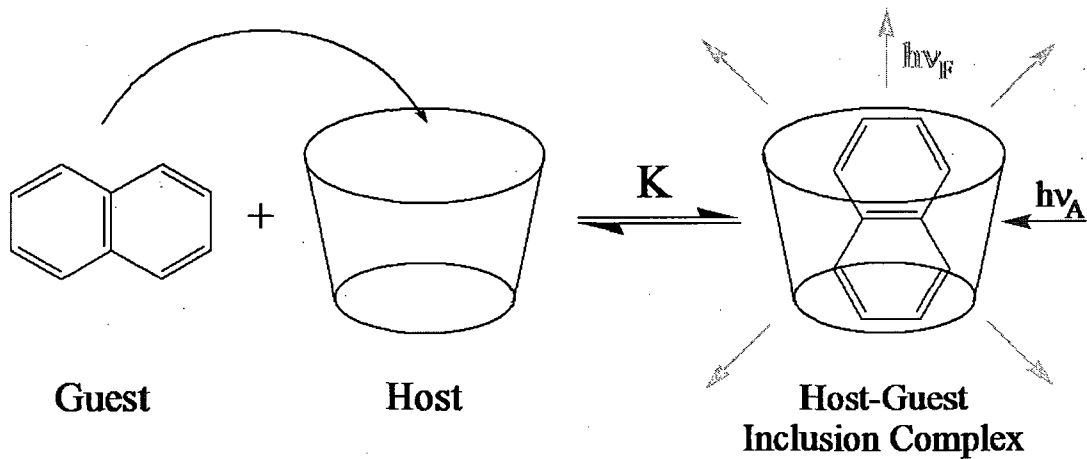


Figure 2. An illustration of a 1:1 host:guest inclusion complex being formed. $h\nu_A$ represents the light being absorbed by the complex. $h\nu_F$ is the fluorescence being emitted.

The inclusion of a guest within a host can be well studied using guest fluorescence.^{12, 21}

²² For example; the fluorescence of a polarity-sensitive guest in aqueous solution is often increased, or enhanced, upon inclusion into a molecular host. Fluorescence enhancement, F/F_0 , is measured by first determining the fluorescence of a pesticide molecule without the presence of a host, (F_0), and then determining the fluorescence of the pesticide in the presence of a host, (F), and dividing the two. The enhancement as a function of host concentration can be determined by a fluorescence titration. Essentially, a fluorescence titration is a measure of the F/F_0 at a fixed guest concentration as a function of varying host concentrations. For a 1:1 host:guest complex, the data collected from the fluorescence titration can be fit using eq. 1.2 as shown,^{21, 22} to extract the binding constant, K .

$$\frac{F}{F_0} = 1 + \left(\frac{F_{\max}}{F_0} - 1 \right) \times \frac{[Host]_0 K}{1 + [Host]_0 K} \quad \text{Eq.1.2}$$

The quality of the data and the goodness of the fit can then be determined by comparing the experimental data with a plot of Eq. 1.2 with the recovered values of F_{\max}/F_0 and K . Furthermore, a simple double reciprocal plot of $1/(F/F_0 - 1)$ vs. $1/[Host]$ will show if it is indeed a 1:1 complex. A linear plot will be obtained in the case of a simple 1:1 complexation but will be curved if higher order complexes form.¹⁹ There are more complicated equations for other complexes but for the sake of this project, only 1:1 host:guest complexes will be discussed.

Although there are many different types of organic and inorganic hosts, only one type of host molecule was used for this project, namely cyclodextrins.²³⁻²⁶

Cyclodextrins (CDs) are of vast importance in supramolecular host-guest chemistry for a number of reasons. CDs are made from starch and are non-toxic. They are relatively easy and environmentally friendly to make. CDs are made in large quantities and are reasonably inexpensive to purchase, they can be consumed safely by humans and finally, by using them as hosts, the physical and spectroscopic properties of guest molecules can be altered, in some cases significantly, to obtain desired information.^{19, 20} They are also easily chemically modified in order to improve upon their properties.^{24,26}

Cyclodextrins come in a variety of sizes ranging from six, seven or eight glycopyranose units. α -cyclodextrin denotes the six unit CD, β -cyclodextrin denotes the seven unit CD and γ -cyclodextrin, the eight glycopyranose unit CD. These native CDs each have a distinct cavity size

which makes choosing the right sized CD an important part of host-guest inclusion chemistry.²³

Figure 3 shows a cartoon depiction of α -, β - and γ -CD when dissolved in an aqueous solution.

These hosts take on a truncated cone shape or “molecular bucket”, due to the hydrogen

bonding that takes place within the molecule.¹⁹

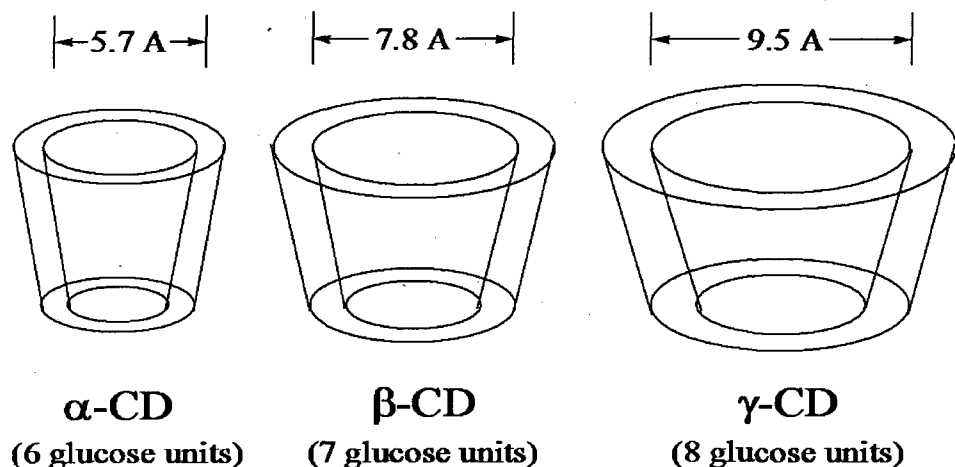


Figure 3. The three types of cyclodextrins with the various cavity sizes.

The CD molecule has twice the number of secondary hydroxyls as it does primary hydroxyls, which make up the larger and smaller rims of the “molecular bucket” respectively. In each CD, there are three hydroxyl groups attached to one glycopyranose unit, as shown in Figure 4. These hydroxyl groups allow, through fairly simple techniques, for substitution and modification of the CD. These modifications are usually done in efforts to improve the effects of the host molecule. Properties such as cavity size, solubility and polarity of the cavity can all be affected by a modification to a native parent cyclodextrin.^{23, 26}

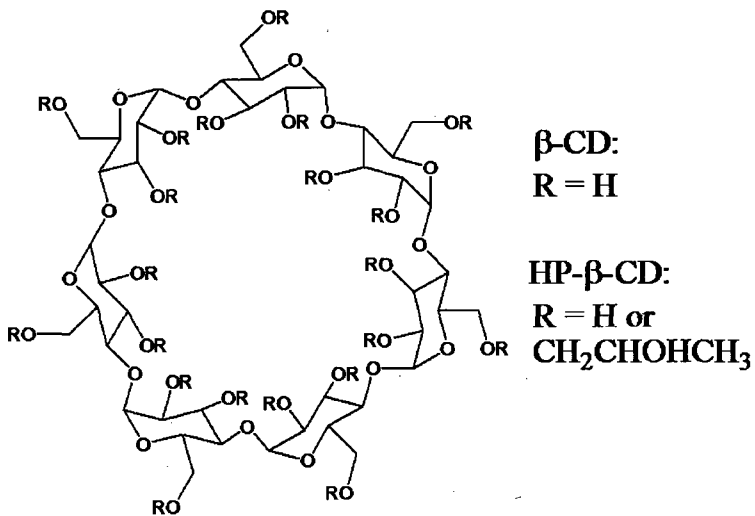
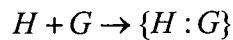


Figure 4. Chemical structure of β -cyclodextrin and hydroxypropyl- β -cyclodextrin.

As previously discussed, cyclodextrins are important as hosts because of their hollow internal cavities. When dissolved in aqueous solutions, the inner cavity fills with water molecules. This tends to be an energetically unfavourable situation and thus any presence of a less polar molecule in solution, usually displaces the water molecules and enters the cavity itself. The less polar molecule, in this case, the pesticide molecule, becomes included within the cavity of the CD and forms an inclusion complex. Inclusion occurs until equilibrium is reached.²³

The equilibrium formation of the complex {H:G} for the free host (H) and guest (G) molecules is expressed as shown in Eq. 1.3.¹² The important parameter is K, the binding constant. The magnitude of K is a reflection of how strongly the host binds the guest. The equation for K is shown in Eq. 1.4.



Eq. 1.3

$$K = \frac{[\{H : G\}]}{[H][G]}$$

Eq. 1.4

In host-guest inclusion, the included guest often experiences changes in some of its characteristics. In this case, the sought after change is the enhancement of the fluorescence signal of the guest. When the guest pesticide molecule enters the hollow cavity of the host, fluorescence property changes such as a shift in emission maxima, a change in the fluorescence lifetime and the quantum yield of the pesticide can all occur.^{12, 19} There are several possible reasons for the alteration of these fluorescence properties.^{12, 19} The most important is the difference in polarity inside the cavity as opposed to that of the aqueous solution, which can result in a change in the relative spacing of energy levels. If the excited state, S_1 , is more polar than the ground state, S_0 , then it is more destabilized in the less polar cavity. This results in a larger S_1 - S_0 energy gap, as illustrated in Figure 5. This increase in energy gap means that fluorescence is occurring at a higher energy. If this is the case, a blueshift (emission shifts to lower wavelength, i.e. to the left on an emission spectrum) will result.

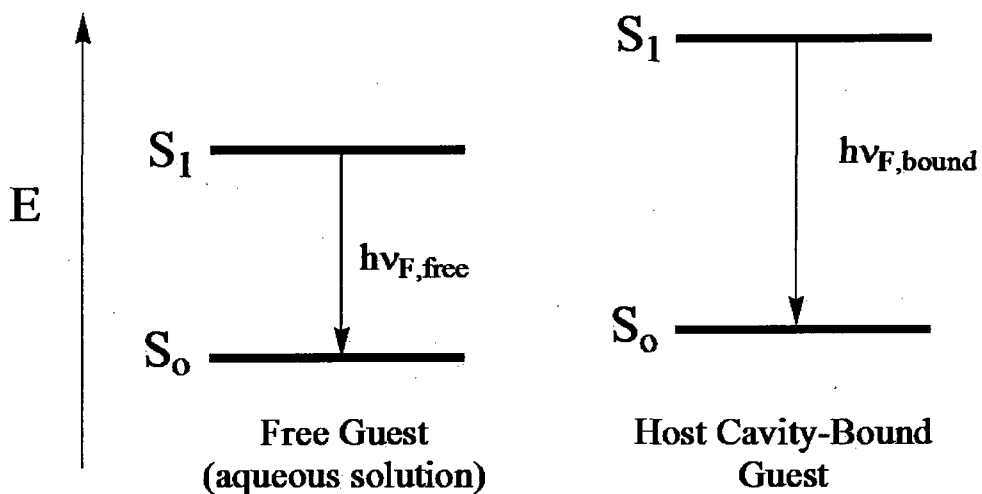


Figure 5. Increased energy gap due to change in polarity of environment.

Another important effect of the polarity-induced increased energy gap is the resulting decrease in the rate of internal conversion. According to the energy gap law,²⁷ the rate of internal conversion (k_{IC}) decreases as the difference in energy between S_1 and S_0 increases; $k_{IC} \propto \exp \{-(E_1 - E_0) / k_b T\}^{27}$ where k_b is the Boltzmann constant. This reduction in k_{IC} upon inclusion results in an increase in the fraction of excited state molecules that relax via fluorescence; *i.e.* the fluorescence quantum yield increases (see Eq. 1.1), and so does the measured fluorescence intensity. This can result in a significant fluorescence enhancement.

A second possible effect of inclusion on guest fluorescence results from the constrictive nature of the host cavity. When a fluorophore is free in aqueous solution, it can undergo relatively unrestricted intramolecular rotations. This can lead to the formation of a Twisted Intramolecular Charge Transfer (TICT) excited state, especially in aqueous solution, as such a charge transfer state represents a relaxation in energy compared to the initially formed, locally excited state S_1 .²⁸ This results in red-shifted, lower intensity emission for such fluorophores in

aqueous solution. When included inside a host cavity, the intramolecular rotation or “twisting” motion required by the molecule to form the TICT state can be significantly restricted, to a point where this rotation can no longer occur, thus eliminating the formation of the TICT state, resulting in a blue-shifted, enhanced fluorescence relative to aqueous solution.

Finally, a third possible reason for the enhancement of fluorescence due to inclusion is that the cavity of the host can protect the pesticide fluorophore from quenchers. O₂, the most common quencher, is very efficient at quenching the excited state of many fluorophores and is present at a significant concentration in water at room temperature. With the addition of the host molecule, the pesticide fluorophore can become included within the cavity and thus returning its natural fluorescence to that similar to an oxygen-purged solution.^{12, 19}

I.2.3. Photochemically Induced Fluorescence (PIF)

Many farms are not located near major water bodies but rather, small branches of a larger body. Streams and smaller ponds are more common around farms and that is a major source of where the contamination begins. This contaminated water then flows to larger bodies and if this occurs before breakdown of that pesticide occurs, contamination of a much larger body of water can occur. These water bodies are generally shallower and for the most part, sunlight can penetrate through to the bottom. Photochemical degradation, the process in which a harmful pesticide molecule breaks down into smaller molecules that may or may not be as harmful to the environment, can occur faster in these more shallow water bodies due to more direct exposure to UV light from the sun.

However, the breaking of bonds in a molecule from the direct exposure to UV radiation can sometimes yield a product with completely different photocharacteristics than the parent pesticide molecule. Previous studies in our and other labs on the pesticides azinphos-methyl,^{16,29} azoxystrobin,³⁰ and imidacloprid³¹ have shown that, although the parent pesticide molecules are weakly or non-fluorescent, exposure to UV irradiation can create new molecules that have significantly greater fluorescent signals. This is referred to as photochemically induced fluorescence (PIF) and is known to be a rapid, inexpensive, and simple method to transform non- or weakly fluorescent molecules into much stronger fluorescent photoproducts.³² This method of combining UV photolysis with fluorescence based trace detection could potentially be a useful technique for obtaining fast, accurate results, with minimal sample preparation and experimental wastes. It can also be combined with inclusion into CDs, to increase the fluorescence signal even further; this will be attempted on azoxystrobin and imidacloprid for the first time in this project.

I.3. *Pesticides of Interest*

The application of the different types of pesticides on Prince Edward Island is vast.^{7,33} Various amounts of herbicides, insecticides and fungicides are used on agricultural fields. The most abundant type of pesticide applied on Prince Edward Island is fungicides, and of those the most used is chlorothalonil (2,4,5,6-tetrachloroisophthalonitrile, CHT, in Fig. 6.a). This fact makes studying this pesticide a major priority. Chlorothalonil is a fully substituted benzene ring, containing four chlorine atoms and two nitrile groups. In Prince Edward Island in 2007, CHT was

considered to be a class A pesticide, with sales greater than 50 000 Kg.⁷ It is a broad spectrum fungicide that is used on vegetables, turf, and some fruits. It is primarily used to combat grey mold, early and late potato blights, fruit rot and some types of mildews.³⁴ CHT is highly toxic to fish and in particular, rainbow trout, one of Prince Edward Island's main fresh water fish.

Extremely low levels of CHT in fresh water seem to affect the natural lives of this species of trout, with amounts as low as 1 µg/L causing irreversible effects. LC₅₀, a toxicology term, is the lethal concentration of a pesticide dissolved in water in this case, that would kill fifty percent of the population of a specific species.³⁵ CHT has an LC₅₀ value of between 10 µg/L and 76 µg/L in rainbow trout.³⁴

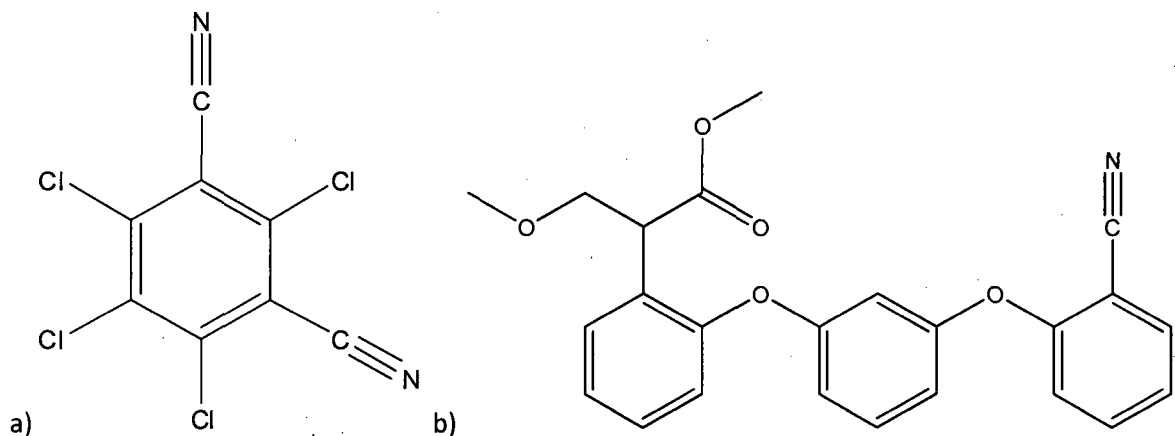


Figure 6. The two fungicides used in this project. a) Chlorothalonil, CHT b) Azoxystrobin, AZO

Azoxystrobin (AZO, in Fig. 6.b) is a fungicide that belongs in the class C pesticides as reported by the non-domestic annual pesticide sales report of 2007.⁷ AZO is a natural product found in certain wood decaying mushrooms which inhibit the growth of other fungi. AZO comes

from the family of strobilurins and is considered highly toxic with a LC₅₀ value of 0.47 mg/L in rainbow trout.³⁶

Carbofuran (2,3-dihydro-2,2-dimethylbenzofuran-7-ol methylcarbamate, CAF, **Fig 7.a**) and carbaryl (1-Naphthyl-N-methylcarbamate, CAB, **Fig 7.b**) are considered old in the pesticide world, with evidence of use dating back to 1969 and 1956 respectively.^{37,38} They are both insecticides of the carbamate pesticide family and work by disrupting the normal nerve functions of an organism. Carbaryl and carbofuran are both class C pesticides on Prince Edward Island, with sales in the range of 1000 to 10,000 Kg. They are applied mainly to crops such as potatoes, sugar beets, corn, and a range of smaller vegetables. Salmon, trout and perch are the most sensitive aquatic species to these pesticides, and levels between 250 ppb and 970 ppb will result in death.^{37,38}

Azinphos-methyl (AZM, **Fig. 7.c**) was another commonly used insecticide and acaricide on Prince Edward Island until recently, when the province of PEI put in place a very strict regulation on its use. AZM is highly toxic to fish and other non-target species and is responsible for several of the more recent fish kills on Prince Edward Island.³⁹ The United States Environmental Protection Agency recently banned all use of AZM due to a large number of applicators developing illnesses. AZM was used primarily on potatoes, but was also used on many other fruits and vegetables.⁴⁰

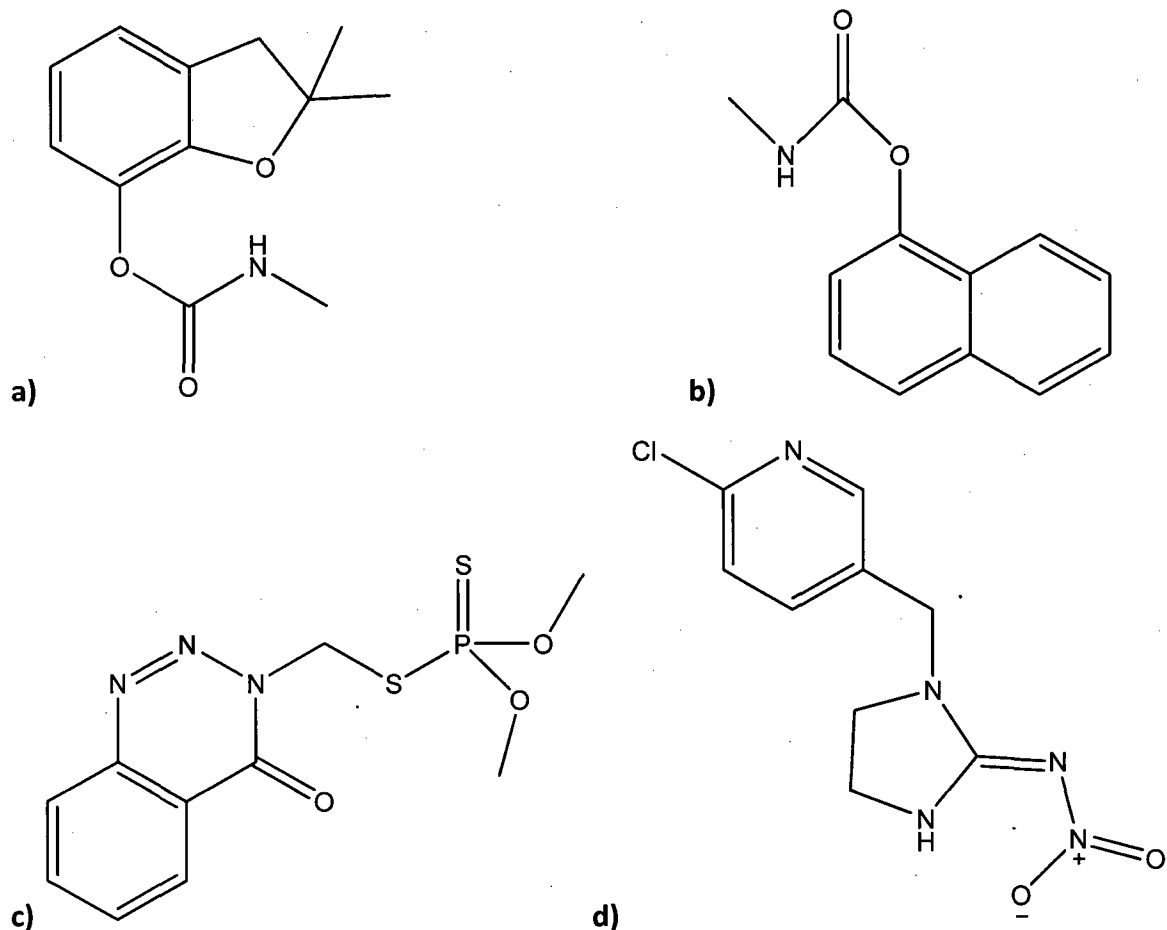


Figure 7. The insecticides used in this project. a) Carbofuran, CAF b) Carbaryl, CAB c) Azinphos-Methyl, AZM d) Imidacloprid, IMI.

Imidacloprid ([1-(6-chloro-3-pyridylmethyl)-N-nitroimidazolidin-2-ylideneamine], IMI, Fig. 7.d) is a class C insecticide used mostly for termite and flea control. It is taken up readily by the roots and leaves of plants and works to block the nerve transmissions in insects. It is considered to be an environmentally friendly pesticide due to its relatively low persistence in soil and water. It also shows above average activity, even in very small amounts.³¹

One of only two herbicides of interest that was studied in this project was atrazine [(2-chloro-4-(ethylamino)-6-isopropylamino-s-triazine), ATR, Fig. 8.a]. Atrazine is another class C

pesticide with sales between 1000 and 10 000 Kg on Prince Edward Island.⁷ It is considered to be one of the most widely used and persistent pesticides on the market today. The issue that arises with atrazine is its ability to bind with humic substances in soil and water, which allows it to exist in the environment for extended periods of time.⁴¹ It is a member of the triazine family of pesticides and usually targets broadleaf or can be used as a non-target herbicide on plowed lands. Atrazine is considered to be only slightly toxic to aquatic life,⁴² although in some laboratory experiments, low part-per-billion aliquots have shown endocrine disruption in certain species of frogs.⁴³

The second of the two herbicides that were studied is metolachlor (MET, Fig. 8.b). It is a class C herbicide⁷ with suspected carcinogenic activity as well as a possible endocrine inhibitor. It has a relatively high solubility in water which makes this pesticide a contamination risk. Metolachlor is only moderately toxic to fish when contaminations occur.⁴⁴

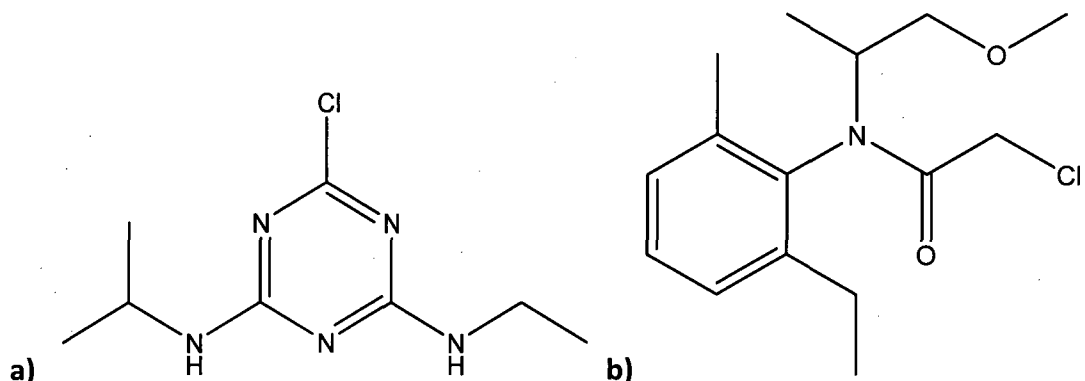


Figure 8. The herbicides used in this project. a) Atrazine, ATR b) Metolachlor, MET

1.4. *Overall Project Goals*

The main focus of this project from beginning to end was to survey a list of pesticides from the non-domestic annual pesticide sales reports of Prince Edward Island from recent years and to see which pesticides would be possible candidates for detection by fluorescence. This required measurement of the UV-Visible absorption spectrum of each pesticide, followed by measurement of the fluorescence spectrum. Once fluorescence data was collected on each pesticide, a systemic method of approach was used to determine whether or not this fluorescence could be enhanced by either supramolecular host-guest inclusion using native and modified cyclodextrins, or by UV photolysis. If successful in enhancing the fluorescence signal of a particular pesticide, analytical information was then gathered in various ways. Firstly, the proper fit of the host was determined. Choosing which host molecule to use is an intricate part of trace detection of pesticides by fluorescence. The best host was chosen as that which gave the largest overall enhancement of the pesticide fluorescence. After the proper host was determined, a fluorescence titration was then performed, a measure of enhanced fluorescence as a function of host concentration. This provided information on the magnitude of the binding constant of the pesticide in the cyclodextrin. The host enhanced fluorescence was then used to obtain a calibration curve of fluorescence signal versus concentration of the particular pesticide in the presence of the preferred cyclodextrin. With a precise calibration curve, a limit of detection (LOD) and limit of quantification (LOQ) could be determined.

After finding out which pesticides can be detected in the required part per billion levels, pesticide “cocktails” were then analyzed in an attempt to detect multiple pesticides at the same

time from the same solutions. Oftentimes, with heavy rains and soil runoff, more than one pesticide is involved in contamination of a water body.⁵ If this fluorescence-based method of trace detection of pesticides in water is to be useful, it will have to be able to detect more than one pesticide in a water sample. These homemade cocktails are designed to replicate real world situations where more than one pesticide is present and responsible for environmental disasters such as fish kills.

The overall focus of this project is to compile a list of pesticides that are commonly used on PEI that can be detected in the low ppb range using CDs or UV photolysis to enhance the fluorescence signal of the pesticide while present in water. Once this is achieved, it is a goal to use the enhancement of the fluorescence from either UV photolysis or CD inclusion and to incorporate synchronous scanning fluorescence, to detect different pesticides simultaneously and accurately from one mixed solution. The resulting methods and protocols developed in this project using a desk fluorimeter will then be applied by a future research student in this lab to use a portable fluorimeter run by a laptop computer, to develop a field-use fluorescence-based trace analysis technique.

II. **EXPERIMENTAL**

II.1. *Materials Used*

Table 1 lists the chemicals that were used in this project; all were used as received.

Special safety precautions were taken while working with pesticides. A properly fitted respirator with cartridges, vinyl gloves and eye goggles were all used while handling these toxic compounds and all solution preparation took place in a fumehood.

Materials Used	Manufacturer, Stated Purity
Anthranilic Acid	Aldrich, 98%
N-Methylantranilic Acid	Aldrich, 98%
Atrazine	Fluka, 97.2%
Azinphos-methyl	Riedel-de Haen, 98.6%
Azoxystrobin	Fluka, 99.9%
Benzazimide	Aldrich, 98%
Carbaryl	Riedel-de Haen, 99.7%
Carbofuran	Aldrich
Chlorothalonil	Riedel-de Haen, 99.2%
α -Cyclodextrin	Sigma, 98%
β -Cyclodextrin	Cerestar

Materials Used	Manufacturer, Stated Purity
γ -Cyclodextrin	Cerestar
Hydroxypropyl- α -Cyclodextrin	Aldrich
Hydroxypropyl- β -Cyclodextrin	Aldrich
Hydroxypropyl- γ -Cyclodextrin	Aldrich
Imidacloprid	Riedel-de Haen, 99.9%
Metolachlor	Riedel-de Haen, 98.0%
9,10-Diphenylanthracene	Aldrich, 97%
Methanol	Sigma-Aldrich, 99.9%
Water	UPEI Chemistry Lab, Nanopure De-ionized

Table 1. Chemicals used during this project and their sources.

II.2. *Instrumentation*

II.2.1. UV-Vis Absorbance Spectroscopy

A Cary 50 Bio UV-Vis spectrophotometer was used to perform all absorbance measurements.

A 3 mL aliquot of solution was added to a 1 cm² quartz cuvette and placed in the sample holder of the spectrophotometer. An absorbance scan of each solution was measured from 600 nm to 250 nm using the medium scan rate speed. An absorption spectrum was collected for each of the eight different pesticide solutions and analyzed to determine the wavelength of

maximum absorbance of each solution and to help in determining the optimum excitation wavelength for fluorescence measurements.

II.2.2. Steady-State Fluorescence

For the steady state fluorescence experiments, 3 mL aliquots of solution were placed in the same 1 cm² quartz cuvettes as used in the absorbance experiments. Samples were run on a PTI luminescence fluorimeter equipped with Felix software and on a Perkin-Elmer LS 55 Luminescence Spectrometer. Some solutions required dilution in order to have the optimal absorbance between 0.25 and 0.30, this absorbance range is considered ideal for obtaining fluorescence spectra.¹² Other solutions did not absorb enough to fall in this range so the experiments were run at the highest possible concentration that the solubility properties of the pesticides would allow.

The cuvette was placed in the sample compartment of the fluorimeter and each excitation and emission slit was opened to allow for the proper amount of light to come in contact with the sample and the photomultiplier tube. The slit widths used were varied for each individual sample. The excitation wavelengths were typically chosen based on the maximum absorbance previously determined from the UV-Vis spectra. In the case of chlorothalonil, the fluorescence was measured at increasing increments of 10 nm to see if any excitation wavelengths would produce fluorescence. Once the excitation wavelengths were chosen for each pesticide solution, the emission wavelength range was selected in relation to the selected

excitation wavelength. It was usually set at 10 nm past the excitation wavelength and scanned for 200 nm.

Fluorescence spectra were then obtained and studied in order to determine several valuable pieces of data. The maximum fluorescence intensity (I_F), the wavelength of maximum fluorescence intensity ($\lambda_{F,max}$), and the integrated area of the fluorescence spectrum (F) were all determined, to be used to give information on specific properties of the solutions being analyzed. Solvent blanks were also scanned and subtracted from the original spectra to ensure that there were no solvent effects or contributions to the fluorescence information.

II.2.3. UV Photochemistry

All photochemical reactions were performed in 1cm^2 quartz cuvettes in one of two photochemical reactors. For the UV-A photochemistry of azinphos-methyl and imidacloprid, reactions were performed in a Rayonet Photochemical Reactor, consisting of 16 UV-A Xenon lamps (maximum emission wavelength of 350 nm) arranged in a circle with equal spacing between each lamp. A cuvette holder was designed in house that allows for replicable positioning of the sample cuvettes at the centre of the lamps. A cooling fan was also used to ensure temperature change effects were minimal.

For the UV-C photochemistry of azoxystrobin, a photochemical reactor was built in-lab which consisted of a fastened Pyrex beaker on the inside of a cardboard box that had been lined with aluminum foil. A small portion of the top of the cardboard box was removed in order

to allow a handheld UV-C lamp (maximum emission wavelength of 254 nm) to fit properly in place. On one side of the box, a door was added to allow access to the inside of the box where the sample was placed. The entire box was then covered with a black cloth to ensure that no additional light got in or out.

II.3. *Pesticide Stock Solution Preparation*

All solutions were made up to volume accordingly with nanopure de-ionized water that was collected from a Sybron Ultrapure water filter connected to a de-ionized water line in the lab. Further dilutions of these stock solutions will be discussed in more detail later on in the experimental section as appropriate. Table 2 lists each pesticide, how much of the pesticide was dissolved and the total amount of water used to make up to volume. Each pesticide solution required a minimum of 5 minutes sonication in order to fully dissolve. Each solution was stored in a dark cupboard at room temperature for the duration of the fluorescence trials. Solutions were stable under these conditions for up to three weeks and then new solutions would be made if trials went longer than that time period.

Pesticide	Mass (g)	Volume of Water (ml)	Concentration (M)
Chlorothalonil	0.0011	1000	4.1×10^{-6}
Azoxystrobin	0.0031	500	1.5×10^{-5}
Carbaryl	0.0025	250	5.0×10^{-5}
Carbofuran	0.0039	100	1.75×10^{-4}
Azinphos-Methyl	0.0079	250	7.6×10^{-6}
Imidacloprid	0.0052	100	2.0×10^{-4}
Atrazine	0.0016	250	3.0×10^{-5}
Metolachlor	0.0057	100	7.0×10^{-4}

Table 2. Pesticide stock solution preparation details.

II.4 *Determination of the Percent Water in the Cavity of Various Cyclodextrins*

The determination of the amount of water that is present in the cavity of a particular cyclodextrin is important for determining the actual mass of the CD being used in order to accurately calculate the CD concentration in solution for the experiments described in Section II.7.1.

For this project, new bottles of HP- γ -CD, HP- β -CD and β -CD were used and thus the percent water present in the cavity of each had to be determined. For γ -CD, HP- α -CD and α -CD, the percent water had previously been determined in our lab.

To determine the percent water present in the cavity of the CD, a vacuum oven was used for drying and a weigh by difference method was used for determination of water lost from each sample. To begin, the masses of six previously dried vials were recorded and approximately 0.1 g of CD was placed into each individual vial. Each vial was then weighed with the CD present, and the mass of each vial was recorded again. By subtracting the mass of the vials with CD by the mass of the vials without CD, the precise amount of CD in each vial was found to an accuracy of 0.1 mg. The vials were then placed in the vacuum oven for one hour to dry. After each hour, the vials were taken out of the oven and weighed. This was repeated for a total of four hours. The samples were dried until three consecutive measurements had consistent masses to ensure that all the water that was present in the cavity had been removed. The new mass was then determined by subtracting the mass of the vial with CD after four hours of vacuum drying by the mass of the vial with CD that had not been dried. By dividing the lost mass by the “wet” CD mass and multiplying by 100, the percent mass of water lost is determined.

II.5. *Fluorescence Quantum Yields and Extinction Coefficients*

Fluorescence quantum yield measurements were carried out using the relative technique,^{12,45} in which the fluorescence emission of the fluorophore of interest is compared to that of a fluorophore with a well known quantum yield. A fluorescence quantum yield experiment was done for azinphos-methyl and for its highly fluorescent photochemical intermediate, N-methylantranilic acid (NMA, see Fig. 9.a). This experiment was carried out by

making three solutions; 4.0×10^{-4} M N-methylanthranilic acid, 9.13×10^{-5} M AZM and 2.66×10^{-4} M 9,10-diphenylanthracene (DPA, the quantum yield standard, see Fig. 9.b). A solution of DPA is commonly used as a standard in fluorescence quantum yield measurements because of its high fluorescence efficiency, and well determined quantum yield ($\phi_F = 0.90$).^{12,45} Figure 9 shows the molecular structures of NMA and 9,10-DPA.

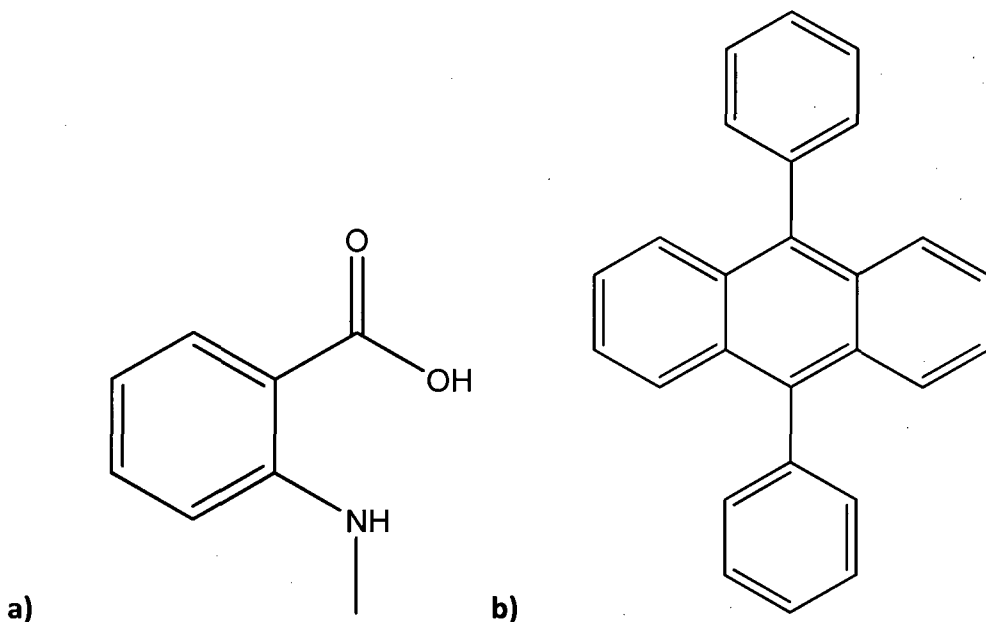


Figure 9. Chemical structures of a) N-methyl anthranilic acid (NMA) and b) 9,10-Diphenylanthracene (DPA)

II.5.1. Quantum Yield and Extinction Coefficient Solution Preparation

The solution of NMA was made by dissolving 0.0030 g of NMA (98%) into 50.00 ml of nanopure water. The solution of AZM was made by dissolving 0.0029 g into 100.00 ml of nanopure water. It required one hour of sonication to dissolve. The solution of DPA was made

by dissolving 0.0022 g of the DPA into 25.00 ml of cyclohexane. All solutions were prepared in volumetric flasks.

II.5.2. Quantum Yield and Extinction Cofficient Procedure

Purging the 9,10-DPA solution of O₂ was necessary in this experiment due to oxygen's efficiency as a fluorescence quencher. To purge this solution, an airtight septum was placed on the top of a quartz cuvette containing the DPA solution. A needle tip was then inserted to release pressure of the sealed cuvette and to allow oxygen to de-gas. A gas line with a long needle tip was connected to allow Argon gas to be passed through the solution. The sample was left to purge for approximately five minutes to ensure all oxygen had been flushed from the solution.

The absorbance spectrum was measured for each solution with a Cary 50 Bio UV-Vis spectrophotometer between 600 nm and 250 nm at medium scan speed and the absorbance at 315 nm was recorded. The fluorimeter was set up to have an excitation wavelength of 315 nm with emission wavelengths from 325-550 nm and 0.25 mm slit widths. The fluorescence spectra were obtained from the PTI luminescence fluorimeter with those same solutions from the absorbance experiments.

The fluorescence spectrum of each solution was recorded and the area under the spectrum, integrated. With this absorbance (A) and the integrated fluorescence data (area), the refractive indices (n) and the fluorescence quantum yield of the standard solution of DPA ($\phi_{F,S}$),

which has been reported in literature to be 0.90,⁴⁵ the fluorescence quantum yields of AZM and NMA were determined using Eq. 2.5. The subscript S refers to the standard, DPA.

$$\Phi_F = \Phi_{F,S} \times \frac{Area}{Area_s} \times \frac{A_s}{A} \times \frac{n^2}{n_s^2} \quad \text{Eq. 2.5}$$

The extinction coefficient, ϵ , is a measurement of how strong a molecule absorbs at a particular wavelength. The extinction coefficients of AZM and NMA were determined by using the Beer-Lambert Law (Eq. 2.6).

$$A = \epsilon c l \quad \text{Eq. 2.6}$$

The absorbance, A, at 315 nm was previously determined from the absorbance spectra and the concentration, c, is the concentration of the AZM and NMA solutions that were made. The path length, l, of the quartz cuvette was 1.0 cm.

II.6. *Photochemically Induced Fluorescence*

II.6.1. Imidacloprid Photolysis and Steady State Fluorescence

A 3 mL aliquot of the imidacloprid stock solution was placed in a 1 cm² quartz cuvette and the fluorescence intensity measured. The excitation wavelength was set at 337 nm and the emission wavelength range was measured from 365 nm to 550 nm with a 1 mm slit width. After measuring the fluorescence of the unphotolyzed imidacloprid solution, it was placed in the Rayonet photochemical reactor and irradiated under UV-A (max. emission, 350 nm) light for 15 minutes. The fluorescence was measured again with the fluorimeter set to the same settings. This process was repeated every 15 minutes, for one hour, until the fluorescence intensity had stopped increasing.

II.6.2. Azoxystrobin Photolysis and Steady State Fluorescence

Azoxystrobin photolysis was performed in a home-made photochemical reactor under UV-C exposure. 3 mL of 1.5×10^{-5} M AZO solution in a 1cm² quartz cuvette was placed in the photochemical reactor for 30 minute increments and the fluorescence intensity measured, once with no exposure time, and then again after each 30 minute interval until fluorescence intensity ceased to increase. The fluorescence experiments were run at an excitation wavelength of 369 nm and the emission wavelength was measured between 400 and 600 nm. The excitation and emission slit widths were set at 1 mm.

II.7. *Host:Guest Enhanced Fluorescence*

The procedure for determining enhancement by CD is a rather simple one. 3 mL of a stock solution of pesticide was added to the proper mass of each of the three native cyclodextrins along with each of the three modified cyclodextrins to obtain a CD concentration of 10 mM. The solutions were then placed in the fluorimeter and run at the excitation and emission wavelengths and slit widths along with the stock solution with no CD. The fluorescence enhancement, F/F_0 , was then calculated as the ratio of the integrated area of the fluorescence spectrum of the stock solution with CD relative to the stock solution with no CD. CDs that produced an enhanced fluorescence signal were then studied further by performing fluorescence titrations.

II.7.1 Determination of the Binding Constant, K

The pesticide solutions that showed enhancement of fluorescence by CD inclusion were studied further to extract the binding constant, K, by performing a fluorescence titration. This is a measurement of the fluorescence enhancement, F/F_0 , as a function of CD host concentration. It was done for each pesticide by adding 3mL of the pesticide solution to 1 mM increments of CD, varying the amount of CD to give solutions with CD concentrations from 1 mM to 10 mM, and then determining F/F_0 for each concentration. A solvent blank was also measured and subtracted from each solution. The measured data was then fitted by the program CDEQWIN (written in the Wagner research lab) which performs a non-linear least squares fit of the data to equation 1.2.¹²

Eq 1.2 is used when a 1:1 host:guest inclusion complex is formed to extract the value of K. It is then plotted using the commercial graphing program, *Fig.P.* as a function of F/F_0 vs host concentration. If a 1:1 host:guest complex is formed then a double reciprocal plot of $1/[F/F_0 - 1]$ vs. $1/[CD]$ will result in a linear plot.

Each pesticide required different settings on the fluorimeter and different CDs (due to size and shape) to optimize the enhancement of the natural fluorescence signal. The optimized settings are listed in Table 3.

Pesticide	Concentration	λ_{EX}	λ_{EM}	Slit Widths
Chlorothalonil	4.1×10^{-6} M	290 nm	310-500 nm	2 mm
Carbofuran	1.75×10^{-4} M	280 nm	290-400 nm	1 mm
Carbaryl	5.0×10^{-5} M	280 nm	300-425 nm	1 mm
Azoxystrobin	1.5×10^{-5} M	369 nm	400-600nm	1 mm
Imidacloprid	3.0×10^{-5} M	290 nm	350-550 nm	1 mm
Azinphos-methyl	9.1×10^{-6} M	315 nm	325-525 nm	2 mm

Table 3. Different fluorimeter settings and CDs used for each pesticide.

II.7.2. Calibration Curves

Calibration curves were created by making five solutions of known pesticide concentration (ranging from 20 ppb to 100ppb by increments of 20) by dilution of the stock

pesticide solution. 3 mL of each concentration of pesticide solution was then added to the appropriate mass of CD to obtain a 10 mM CD concentration and dissolved by five minutes of sonication. Each sample was run in the fluorimeter at set excitation and emission wavelengths and proper slit widths. The spectra were all corrected by running a solvent blank with CD and subtracting it from the pesticide spectra. The fluorescence intensity value was recorded from the maximum intensity wavelength and plotted using the graphing program *Fig.P* as a function of pesticide concentration. Calibration curves in this project were deemed satisfactory with a linear correlation coefficient, *r*, between 0.999 and 1.000.

II.7.3. Limit of Detection and Quantification

The slope of the line was found from the regression statistics in the graphing program, *Fig. P*. A nanopure water blank was measured 10 times and the intensity was recorded from each spectrum at the maximum intensity wavelength of the pesticide solution and the standard deviation was calculated from those values. Using Eq. 2.7 and 2.8, the limit of detection (LOD)⁴⁶ and limit of quantification (LOQ)⁴⁶ were found, where S_0 represents the standard deviation of the water blanks and *m* is the slope of the calibration curve.

$$LOD = \frac{3 \times S_0}{m} \quad \text{Eq. 2.7}$$

$$LOQ = \frac{10 \times S_0}{m} \quad \text{Eq. 2.8}$$

II.8. HPLC Experiments

For the HPLC experiments, solutions of azinphos-methyl, benzazimide (1,2,3,-benzotriazin-4(3H)-one, BA, **Fig. 10.a**), N-methylantranilic acid and anthranilic acid (AA, **Fig. 10.b**) were all studied. The structures of BA and AA are shown in Figure 10.

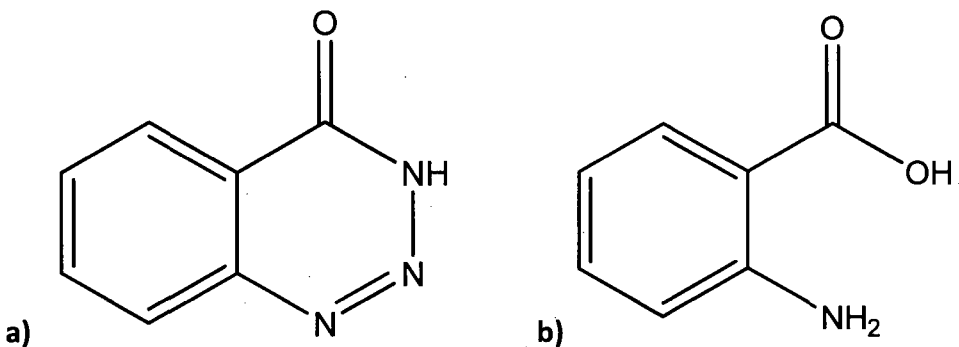


Figure 10. Chemical structures of a) Benzazimide (BA) and b) Anthranilic Acid (AA).

II.8.1. HPLC Solutions Preparations

A 2.5×10^{-4} M solution of AZM and a 2.5×10^{-4} M solution of benzazimide were prepared in order to be studied via HPLC analysis. 0.0079 g of AZM was dissolved in to a 60:40 mix of water:methanol in a 100 mL volumetric flask and was sonicated for 30 minutes. 0.0018 g of BA was dissolved in a 60:40 mix of water:methanol in a 50 mL volumetric flask and sonicated for 30 minutes.

Eight 3 mL aliquots of the 2.5×10^{-4} M AZM solution were irradiated in the photochemical reactor for varying amounts of time. Solution 1 was irradiated for one hour, solution 2, for two hours and so forth until solution 8 was irradiated for 8 hours, the time when photolysis of AZM had been deemed complete.

Another 3 mL solution consisted of a mixture of 1.5 mL of the 2.5×10^{-4} M AZM and 1.5 mL of the 2.5×10^{-4} M BA solution was left unphotolyzed and run as a standard.

Finally, 2.5×10^{-4} M solutions of N-methylantranilic acid (NMA) and anthranilic acid (AA) were prepared in order to determine the retention times of these two solutions, as they were possible intermediates of the photolysis reactions. 0.0038 g of NMA was dissolved into a 60:40 mix of water:methanol in a 100 mL volumetric flask. 0.0034 g of AA was dissolved into a 60:40 mix of water:methanol in a 100 mL volumetric flask. Both solutions required 5 minutes of sonocation in order to dissolve.

II.8.2. HPLC Analysis

All HPLC experiments were run on a Varian HPLC machine that consisted of a Varian Autosampler Prostar 410, Varian PDA Detector Prostar 330, and a Varian Solvent Delivery Module Prostart 240. A Pursuit C18 reversed-phase column and a UV wavelength detector set at 285 nm were used.

A total of thirteen solutions were analyzed in the HPLC. A 20 μ L sample of the 2.5×10^{-4} M AZM solution and a 20 μ L sample of the 2.5×10^{-4} M BA solution were measured as standards, along with 2.5×10^{-4} M solutions of NMA and AA. 20 μ L of each of the eight solutions of varied UV exposure and 20 μ L of a 50:50 AZM:BA mixture were measured as well. A 20 minute run time was sufficient to show optimal separation of peaks.

II.9. *¹H NMR Solution Preparation and Analysis*

Four different solutions were prepared for the ¹H NMR experiments. A 300 mHz Bruker UltraShield NMR was used for all ¹H NMR experiments. A 3.0×10^{-3} M solution of AZM in methanol-d4 was prepared as the solution to be studied. Reference solutions of aniline, N-methylantranilic acid, and benzazimide were prepared to the same concentration as the AZM solution, all in methanol-d4. The ¹H NMR spectrum of AZM was obtained, firstly without any exposure to UV-A light and then again after being photolyzed in the Rayonet photochemical reactor for 6 hours and then again after 36 hours of exposure.

II.10. *Synchronous Scanning Fluorescence Experiments*

II.10.1 Sample Preparation

For the first part of the synchronous scanning experiments, pesticide mixtures, along with standard pesticide solutions were measured to determine if an individual pesticide could be detected in the presence of other pesticides in a solution.

In the first set of experiments, seven solutions were prepared; 100 ppb carbofuran, carbaryl, azinphos-methyl and chlorothalonil were all made by adding the appropriate amount of pesticide to water and dissolving. Using those solutions, three pesticide mixtures were created.

Mixture one contained equal parts of carbofuran, chlorothalonil and azinphos-methyl. Mixture two contained equal parts carbaryl, chlorothalonil, and azinphos-methyl and mixture three contained equal parts of each of the four pesticides used in this experiment.

In the second set of experiments, calibration curves of both carbofuran and carbaryl were prepared by proper dilutions of their respected stock solutions to make five new solutions for each pesticide. The concentrations increased by intervals of 20 ppb starting at 20 ppb and going to 100 ppb. Once the calibration curves were prepared, six spiked sample solutions were prepared by Carrie Snow, a fellow graduate student. These solutions contained known (only to her) equal concentrations of CHT and AZM and known differing amounts of CAF and CAB. This was done to ensure the testing be a blind testing procedure which would replicate field testing whereby the tester is unaware of the concentrations present until after the experiment is completed.

II.9.2. Synchronous Scanning Procedure

The synchronous scanning option on the fluorimeter was selected and the emission and excitation wavelengths were chosen depending on which pesticide would be looked at first. Since carbofuran and carbaryl are much more fluorescent pesticides than CHT or AZM, they were the only two that were studied. The excitation wavelength interval for carbofuran was 266 nm to 416 nm and the emission wavelength interval was 290 nm to 440 nm. This maintained a constant difference of emission wavelength to excitation wavelength of 24 nm. The excitation and emission wavelength intervals for carbaryl were 256 nm to 406 nm and 300

nm to 450 nm respectively. This maintained a constant difference of 44 nm between the excitation wavelength and emission wavelengths. The slit widths were set at 1 mm for all synchronous scanning experiments.

The spiked sample procedure using synchronous scanning fluorescence was slightly different. Once the calibration curves were created in the fluorimeter using the same specifics as used in the first set of experiments, the six solutions of unknown amounts of carbofuran and carbaryl were measured. The peak intensities at the maximum fluorescence intensity for each of the two pesticides being observed were recorded. Those intensity values were then substituted in to the equation of the line, calculated from their respected calibration curve, and the concentration of the unknown solution was calculated. Only then were the actual values revealed and a percent error calculated.

III. RESULTS AND DISCUSSION: Enhanced Fluorescence of Pesticides in Water by Cyclodextrin Inclusion

Each pesticide was extensively studied to determine whether it would be a candidate for fluorescence enhancement via UV photolysis or supramolecular host:guest inclusion using native or modified cyclodextrins. This chapter is focused on the details of how the fluorescence of each pesticide responded to cyclodextrin addition, and whether a large enough fluorescence enhancement is obtained to allow for its trace detection at the ppb level. This chapter also examines the possibility of more than one pesticide being detected accurately in a mixture of pesticides using fluorescence.

III.1. Determination of the Percent Water in the Cavity of Various Cyclodextrins

Cyclodextrins, in their natural form, contain water molecules inside the cavity of the CD itself. In order to accurately determine the concentration of a prepared CD solution, it was necessary to determine the amount of water present inside the cavity of the solid CD prior to dissolving it in the pesticide solution using a vacuum oven. The resulting water contents (average of two samples) were: HP- γ -CD: 5.1%, HP- β -CD: 3.9%, and β -CD: 11.8%. The percent water content for α -CD, HP- α -CD and γ -CD were previously determined by the Wagner group and were found to be 8.8%, 3.3%, and 6.7% respectively. These percent water contents were taken into account in calculating the concentrations of the pesticide-CD solutions.

III.2. *Carbofuran*

The pesticide Carbofuran (see structure, Fig. 7.2) was selected as a pesticide of interest for this project due its high sales volume and application rates on PEI according to the Prince Edward Island Non-Domestic Pesticide Sales Report of 2007.⁷ The aromatic structure of the CAF molecule makes it an ideal starting point for the fluorimetric based trace analysis of pesticides in water.

III.2.1. Absorption and Fluorescence Measurements

A solution of 1.75×10^{-4} M carbofuran in water was chosen as the concentration of the stock pesticide solution because absorbance measurements of this solution showed that this pesticide absorbed in the UV-B region with an absorbance peak from 290 nm to 270 nm. The maximum absorbance at 280 nm is 0.35 and this is an ideal absorbance for fluorescence experiments. At any wavelengths lower than this, there exists a risk of the cyclodextrin host absorbing some of the light. The absorption spectrum of 1.75×10^{-4} M carbofuran in water is shown in Figure 11.

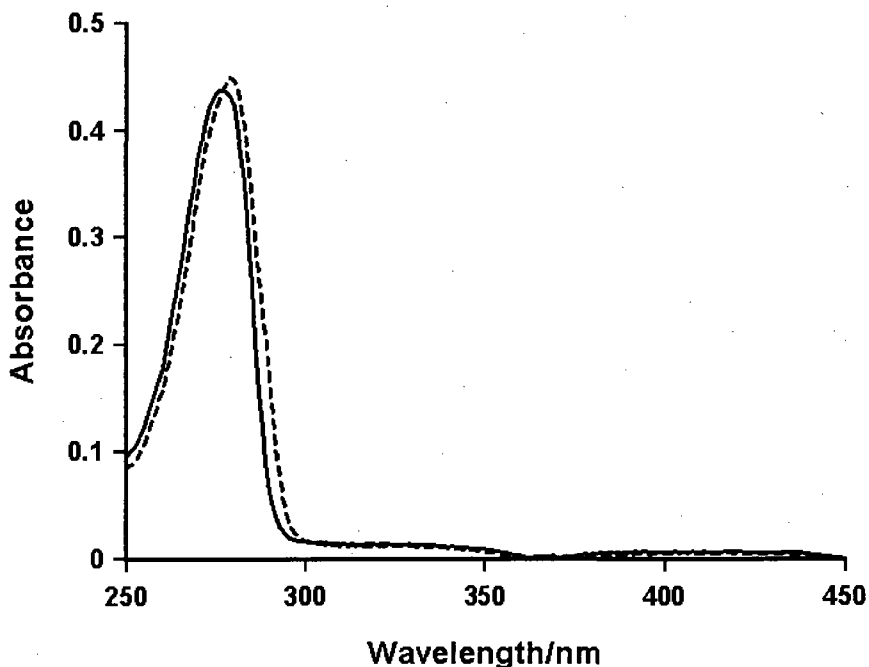


Figure 11. Absorption spectrum of 3mL of 1.75×10^{-4} M carbofuran solution in the absence (—) and in the presence (---) of β -CD.

For the fluorescence experiments, an excitation wavelength of 280 nm was chosen based upon the absorption results. The emission wavelengths were chosen in relation to the excitation wavelength. The emission wavelengths were measured from 290 nm to 500 nm. A 10 nm buffer region from the excitation wavelength to the emission wavelength was used to ensure that no scattered excitation light was detected. The emission range was 210 nm to ensure that none of the fluorescence band was cut off. The actual slit widths (both excitation and emission) were set to 1 mm in order to provide the best possible signal with minimal background noise. This was done by measuring a solution of carbofuran in the fluorimeter and adjusting the slits and re-running until the optimum slit width was found, based on the total fluorescence to noise ratio.

III.2.2. Fluorescence Enhancement by CD Inclusion

Since carbofuran was found to be fluorescent in water, it made it worthwhile for the purposes of this project to test various CDs in order to possibly enhance that fluorescence signal by way of forming host:guest inclusion complexes between the CDs and the pesticide molecules.

β -CD and HP- β -CD were tested with the carbofuran pesticide solution as per the experimental procedure in Chapter 2. In both cases, significant enhancements of the fluorescence were found, indicating that host:guest inclusion complexes are likely being formed. In Figure 12, the natural fluorescence of CAF, the enhanced fluorescence of CAF with β -CD and the enhanced fluorescence of CAF with HP- β -CD are shown.

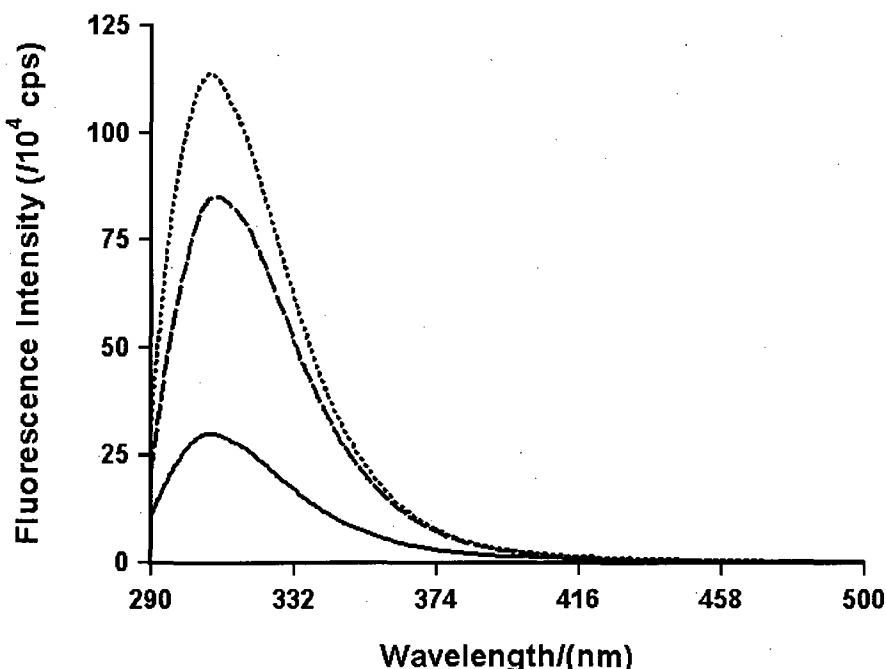


Figure 12. Fluorescence spectra of 1.75×10^{-4} M CAF without CD (—) with the addition of β -CD (---) and with the addition of HP- β -CD (···).

The natural fluorescence of the pesticide was enhanced by a factor 2.8 in the presence of β -CD and 3.5 in HP- β -CD. This additional enhancement is attributed to the fact that modified CDs are usually more effective at forming host:guest inclusion complexes and provide a less polar environment.¹² The modified CD has a slightly less polar environment inside the cavity relative to the inside cavity of a native CD, therefore increasing the binding of the hydrophobic pesticide molecule. In addition, HP- β -CDs, with the substituted hydroxypropyl groups, have a slightly larger cavity than the un-substituted cavity of the β -CD. The hydroxypropyl groups act like arms, extending the cavity further than in the case of an unsubstituted cavity. This allows for more of the molecule to be included within the cavity and therefore bind more strongly and experience more of the effects of the CD.

III.2.3. Investigation into the Mechanism for the Enhancement of CAF Fluorescence

There are various reasons why enhancement of fluorescence can occur when a weakly- or non fluorescent molecule becomes included within the cavity of a host molecule. There are several tests that can be performed in order to gain a better understanding of why this enhancement occurs for a specific fluorescent guest. Quenching of fluorescence can cause a fluorescence signal to be drastically reduced or even eliminated if there is the presence of a quencher in the solution. The host molecule can often offer protection from quenchers such as oxygen. While the CAF molecule is included within the cavity, it is safe from collisions with oxygen molecules that are present in the sample that will increase the rate of internal conversion. With this protection, k_{IC} is decreased and thus fluorescence is increased. To test this

idea, the fluorescence of a sample of unpurged 1.75×10^{-4} M CAF solution was measured. The same solution was then purged for five minutes with Argon gas to flush out any oxygen present in the sample and the spectrum was measured again. Purging the sample resulted in only a 7% increase in fluorescence, compared to 350% in HP- β -CD. The difference in spectra showed that oxygen did play a part in quenching some of the fluorescence but it was a very minimal effect compared to the large enhancement shown from CD inclusion. This indicates there are still other factors contributing to the enhancement that need to be investigated.

As was briefly discussed in Chapter 1, the less polar environment of the substituted CD can result in an increase in the energy gap between the S_1 and S_0 energy levels of the molecule and thus fluorescence of this molecule is occurring at a higher energy than fluorescence of an un-bound molecule. It also increases the likelihood that fluorescence will occur rather than by relaxation, by the non-radiative decay pathway of internal conversion. Looking at the fluorescence spectra of the CAF: β -CD and CAF:HP- β -CD however, there is no measurable blueshift in the maximum intensity wavelength (304 nm) which would be observed if there was an increase in the energy gap. Therefore it is not expected that this is the reason behind the enhanced fluorescence.

Further experimentation by testing the fluorescence of the molecule in a less polar medium was done. Ethanol was used as a solvent because it is less polar than water and because the polarity of cavity of the HP- β -CD was measured to be very similar to ethanol.^{12, 47, 48}

A 1.75×10^{-4} M CAF solution in ethanol was prepared in order to test the effect of a less polar solvent on the fluorescence by comparing maximum emission intensities. Figure 13 shows the comparison of the fluorescence of CAF in ethanol to the fluorescence of CAF in water.

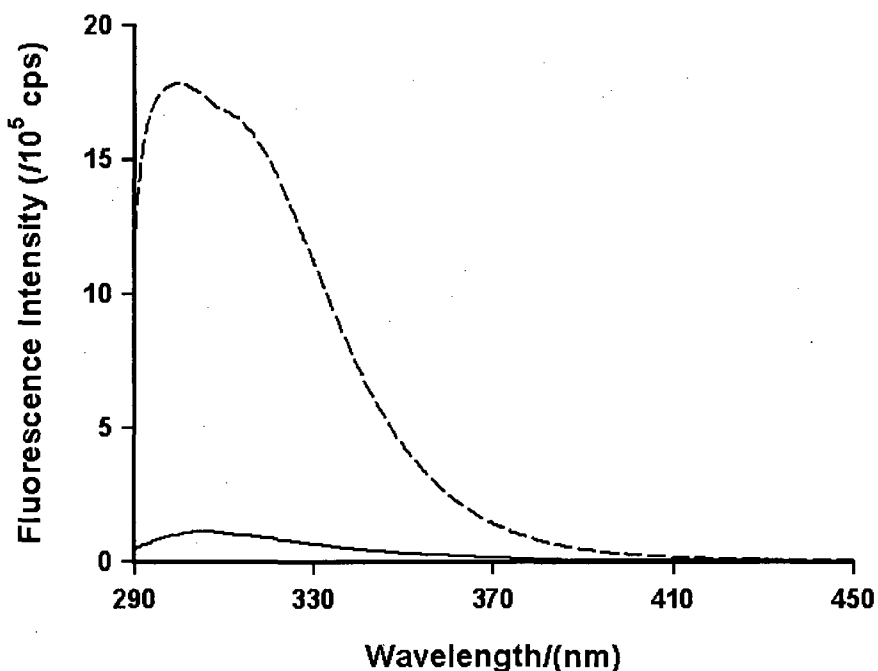


Figure 13. Comparison of 1.75×10^{-4} M CAF in ethanol (---) to 1.75×10^{-4} M CAF in water (—).

This experiment showed that the pesticide molecule, CAF, had an enhancement in ethanol as compared to water, thus proving that the enhanced fluorescence is due largely to the change in polarity of its environment. This experiment also showed that there is in fact, a very small change in the maximum intensity wavelength that could not be seen in the fluorescence spectrum of CAF in water with CD most likely due to the enhancement not being as substantial. The $\lambda_{F,\max}$ shifted from 304 nm in water to 302 nm in ethanol.

The polarity sensitivity factor (PSF), which is the ratio of fluorescence of a fluorophore in ethanol, F_{EtOH} , to fluorescence of a fluorophore in water, F_{water} , corrected by the difference in absorption of each solution, gives an idea of how sensitive the fluorescence of that particular molecule is to the polarity of its local environment.^{19,49} The PSF equation is shown Eq. 3.6.

$$PSF = \frac{F_{EtOH}}{F_{water}} \times \frac{A_{water}}{A_{EtOH}}$$
 Eq. 3.6

The PSF for CAF was determined from Eq. 3.6 to be 19.0 which illustrates exactly how sensitive the CAF molecule is to the change in polarity. The high sensitivity from the change in polarity is most likely the reason for the substantial enhancement of the fluorescence of CAF. However, the observed enhancement of 3.5 in CD is much lower than the PSF, indicating that the pesticide is not experiencing the full possible polarity effect. This suggests that the pesticide is only partially included within the cavity, or perhaps that there are still water molecules associated within.

Since fluorescence was shown to enhance by such a large factor in changing the solvent from water to ethanol, much like the change of local environment in going from water to the cavity of a CD, it is unlikely that the restriction of rotational motion of the molecule would be a major cause of the increased fluorescence. It is possible that some restriction could lead to enhancement of the fluorescence, but in this case, the most probable reason is the sensitivity of the molecule to polarity.

III.2.4. Fluorescence Titrations

Fluorescence titrations were performed using the 1.75×10^{-4} M CAF solution and the correct masses of β -CD and HP- β -CD. By performing this titration, F/F_0 can be determined by dividing the integrated fluorescence spectrum of the CD:Pesticide solution, F , by the integrated fluorescence spectrum of the pesticide solution without the presence of the CD, F_0 . By fitting F/F_0 vs. the concentration of the β -CD to Eq. 1.2 using CDEQWIN, the binding constant, K , of the host β -CD and the guest, CAF was found to be $177 \text{ M}^{-1} \pm 60 \text{ M}^{-1}$ (average of three trials).

For HP- β -CD, using the data from the titration, F/F_0 vs. concentration of HP- β -CD was fitted to Eq. 1.2 and K was found to be $204 \text{ M}^{-1} \pm 9.0 \text{ M}^{-1}$ (average of three trials). The slightly higher value of K for CAF:HP- β -CD shows that the pesticide molecule binds better to the cavity of the modified CD as compared to the native CD (although the two binding constants are not significantly different when the error limit for K in β -CD is taken into account). Although it is not a large difference, when combined with the slightly larger enhancement by HP- β -CD, it is considered to be the more favourable host. It is postulated that the hydroxypropyl groups on the CD are acting like arms, creating a cavity that is more protected, more non-polar and slightly larger which provides a better environment for the pesticide guest molecule.¹² The fluorescence titration of CAF with HP- β -CD is shown in Figure 14.

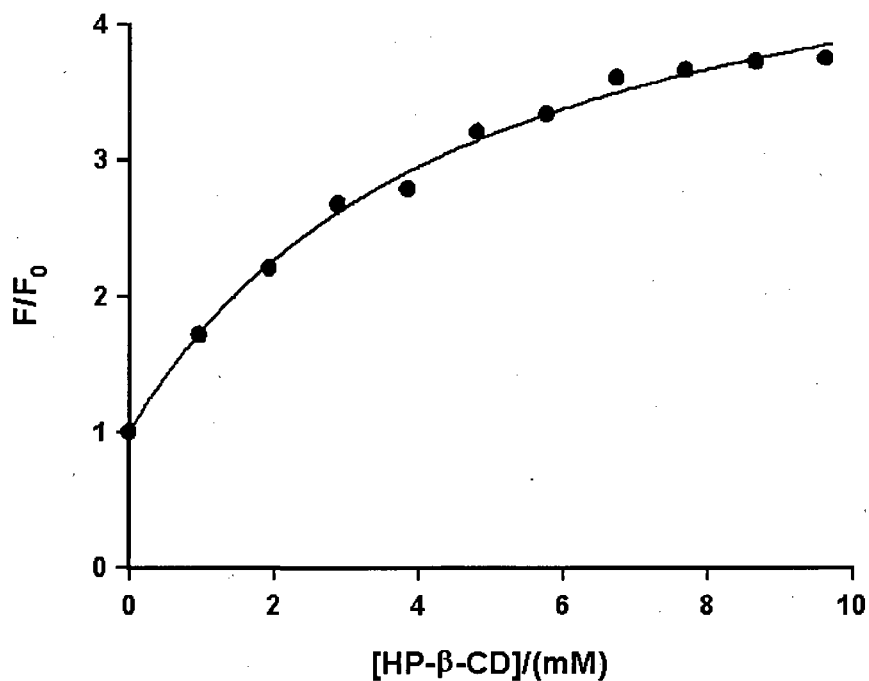


Figure 14. Fluorescence titration of CAF with HP- β -CD. A binding constant average (3 trials) of $204\text{ M}^{-1} \pm 9.0$ was calculated from the data F/F_0 vs [HP- β -CD].

Fluorescence titrations are also very useful for determining the stoichiometry of the host:guest complex that it is being formed between the pesticide molecule and the host CD. This is done by generating a double reciprocal plot of the titration data; if this plot is linear, it is indicative of a 1:1 complex. If it is not linear then a more complex host:guest complex is being formed. In the case of both β -CD and HP- β -CD, the double reciprocal plot showed that it is indeed a 1:1 complex being formed between the host CD and the guest CAF molecule. Figure 15 shows the double reciprocal plot of the fluorescence titration of CAF with HP- β -CD. The linearity (0.999) of this plot confirms that a 1:1 host:guest complex is being formed.

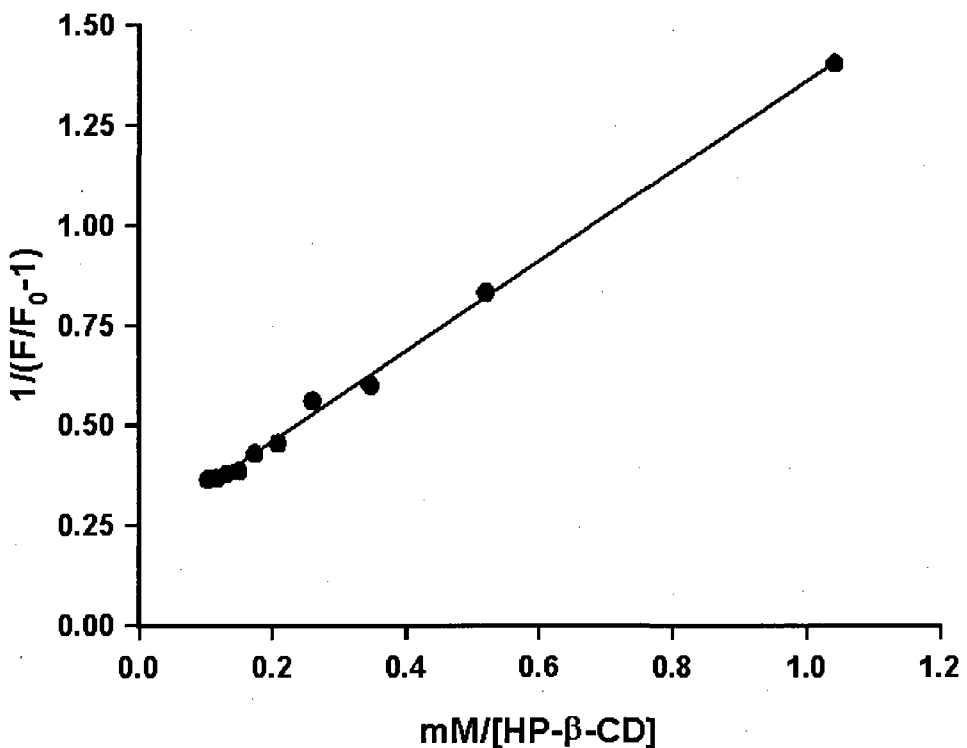


Figure 15. The double reciprocal plot of the fluorescence titration of CAF with HP- β -CD.

III.2.5. Calibration Curve, LOD and LOQ

Once the binding constants were found and HP- β -CD was clearly established as the best host for CAF for inclusion complexes, work with β -CD ceased. Calibration curves of carbofuran in water with the addition of 10 mM HP- β -CD were then determined. The first calibration curve was from 10 ppm to 2 ppm in order to see if it is possible using fluorescence to detect the pesticide at this level. The 2 ppm solution still has a very strong fluorescent signal so the concentration was decreased and a new calibration curve was made from 500 ppb to 100 ppb. At 100 ppb, the fluorescence signal was still distinguishable so a third and final calibration curve was created. The concentrations of the solutions for this calibration curve decreased from 100

ppb down to 20 ppb. The calibration curve required a linear correlation coefficient, r , of at least 0.999 to be deemed satisfactory, which at this small of a concentration took several attempts. The fluorescence spectra of the calibration solutions are shown in Figure 16.a and the plotted calibration curve data are shown in Figure 16.b

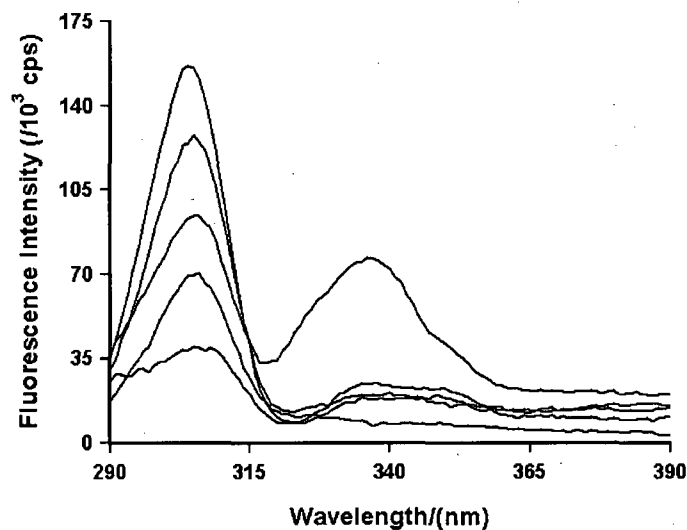


Figure 16.a. Fluorescence spectra of the CAF calibration solutions with 10mM HP- β -CD. The solutions range from 100 ppb (top) in equal decreasing concentrations to 20 ppb (bottom).

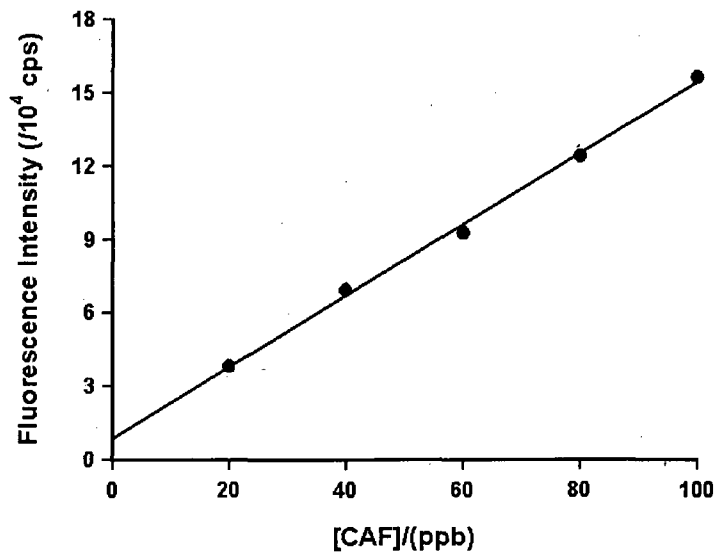


Figure 16.b Calibration curve of 10mM HP- β -CD with various concentrations of Carbofuran. The calibration curve has a linearity of 0.9993.

Once the calibration curve met acceptable linear limits, the slope of the line, m , of the calibration curve was found from the graphing program, *Fig.P*. The slope from the calibration curve of CAF with HP- β -CD was 533.8 cps/ppb. A solvent blank of nanopure water was measured ten separate times in the fluorimeter. The intensities at 304 nm were recorded from each and the standard deviation was calculated. The standard deviation of the water blanks was found to be 745.46 counts per second (cps). Using Eq. 2.7 and Eq. 2.8 from Chapter 2, the limit of detection and the limit of quantification of CAF in water with the addition of HP- β -CD for enhancement of the fluorescence were determined. The limit of detection by using supramolecular host:guest chemistry to enhance the natural fluorescence of CAF in water was found to be 4.2 ppb. The limit of quantification was found to be 14.0 ppb. In terms of detection levels, this is well below required detection levels to make this method of detection worthwhile.

The non-zero value of the y -intercept is attributed to the relatively high baseline of this particular fluorimeter, and the very low concentration and thus low fluorescent signals involved for this calibration curve. The solvent blank could be subtracted from the calibration solutions but it was decided against for it adds an extra unnecessary step to the procedure.

It was discovered during calibration curve trials of this pesticide, that there was one previous literature report on the fluorescence enhancement of carbofuran, along with carbaryl by CD addition in the journal *Analytica Chimica Acta*.¹⁵ Pacioni et al. had looked at the determination of carbofuran and carbaryl in certain fruits and tap water. Since it was discovered so late in the experimental process, it was decided that work would be completed

on this pesticide and results would be compared. Also, because one of the goals of this project was to compile a list of pesticides used in PEI that are naturally fluorescent, and that the fluorescence be enhanced by CD, literature work would provide useful information. The limit of detection that was reported in this journal article was 15.9 ppb. The LOD in this current work thus represents an improvement of a factor of approximately 4. The work done on CAF was completed for comparison but also, more importantly, to possibly investigate further the fluorescence of this pesticide in a mixture and also by another fluorescence method, synchronous scanning fluorescence, which was not used in the Pacioni paper.

Pacioni et al. also reported binding constants for β -CD and HP- β -CD as $190 \pm 10 \text{ M}^{-1}$ and $123 \pm 7 \text{ M}^{-1}$, respectively.¹⁵ The β -CD values is fairly similar to the current results however the binding constant for HP- β -CD iss much lower than that found in this project. This is attributed to the lower degree of substitution of the HP- β -CD that was used by Pacioni et al.¹⁵ The HP- β -CD that was used in the literature report had a degree of substitution of 5.5 hydroxypropyl groups per CD. The HP- β -CD that was used for this project had a degree of substitution of 7.0 hydroxypropyl groups per CD. The additional hydroxypropyl groups would most likely be the reason behind the higher binding constants and lower LOD found in this work.

III.2.6. Spiked Samples

It was determined that using fluorescence with supramolecular host:guest inclusion to detect trace levels of carbofuran in water was possible in the ppb range. To build upon this, the next logical step was to determine how accurately one could determine the concentration of

this pesticide in water test samples. Several unknown spiked water samples were prepared in order to mimic real-world situations, whereby the user is unaware of the concentration present in the sample being tested. In this experiment, three unknown solutions were prepared and measured under identical conditions to previous fluorescence trials performed on CAF in this project.

By firstly creating a calibration curve ($r = 0.999$), an equation for the line can be calculated by plotting the intensities of the fluorescence band at 304 nm for each of the concentrations, 20 ppb to 100 ppb. The line equation in this experiment was $y = (1000.6\text{cps}/\text{ppb})x + 83281 \text{ cps}$ where y is the intensity of the peak of the unknown spiked sample and x is the concentration in ppb. By recording the intensities of each of the unknown solutions at the same maximum intensity wavelength, in this case 304 nm, the user can then substitute in those values for y and then solve the equation for x which will give the concentration of the unknown solution. Table 4 shows the results of the unknown spiked water sample trials.

Sample	Calculated Concentration (ppb)	Actual Concentration (ppb)	Percent Error (%)
A	39	37	5
B	65	96	32
C	44	57	23

Table 4. Results from CAF spiked sample trial using steady state fluorescence.

There is a fairly large percent error present in the spiked sample trials that were done. Only one trial of unknown spiked sample detection was performed on this pesticide. However, this work does demonstrate that this method for detection of an unknown concentration in water is feasible.

III.3. *Chlorothalonil (CHT)*

Chlorothalonil (see structure, Fig 6.a) is a relatively small pesticide molecule in comparison to the other molecules of interest in this project. It has a fully substituted benzene ring involving four chlorine atoms and two nitrile groups. It continues to be the most used pesticide on PEI and has been so for the last several years.^{7,33} Due to this fact, this pesticide was at the top of the list of pesticides to be extensively studied in this project.

III.3.1. Absorption and Fluorescence Measurements

CHT has a low solubility in water and required the stock solution to be made at the maximum solubility in order to observe any absorbance from the absorbance measurements of this relatively small pesticide molecule. In these studies, a 1.1 ppm stock solution was prepared which was the maximum concentration of CHT which would dissolve. For fluorescence measurements, a pesticide solution will ideally absorb at the excitation wavelength between 0.2 and 0.3. In this case, the pesticide showed very little absorbance due to the small concentration of chlorothalonil present in the solution. The absorbance spectrum showed a

very minimal peak in the high UV-B, low UV-A region around 320 nm. This made finding an ideal excitation wavelength for fluorescence a trial and error process.

Fluorescence experiments were performed on the chlorothalonil solution by changing the excitation wavelengths by 10 nm increments from 340 nm down to 280 nm and changing the emission wavelengths in relation to the excitation wavelengths. Each spectrum was collected and compared in order to determine if any further fluorescence trials would be done. After comparing all the spectra, the excitation wavelength of 290 nm was chosen as it produced the highest fluorescent peak. The emission range of 300 nm to 475 nm was found to be optimal in viewing the entire fluorescence band. Chlorothalonil, in water, was found to be only weakly fluorescent with a maximum fluorescence intensity measured at 340 nm.

III.3.2. Fluorescence Enhancement by CD Inclusion

Due to the relatively small size of the CHT molecule, α -CD and HP- α -CD were first selected to be the trial host molecule for experimentation. The fluorescence of each 10 mM solution of CHT with CD was measured and with each CD, substantial fluorescence occurred. For α -CD, fluorescence enhanced by a factor of 9.0 and for HP- α -CD, fluorescence enhanced by a factor of 8.2. Since such a large enhancement of the natural fluorescence occurred with the addition of the native and modified α -CDs, solutions of β -CD, HP- β -CD, γ -CD and HP- γ -CD were prepared using the same method and testing at identical conditions. In each case, varying degrees of fluorescence enhancement occurred, as described in the next section. Figure 17 shows the enhancement of the natural fluorescence of CHT with the addition of α -CD.

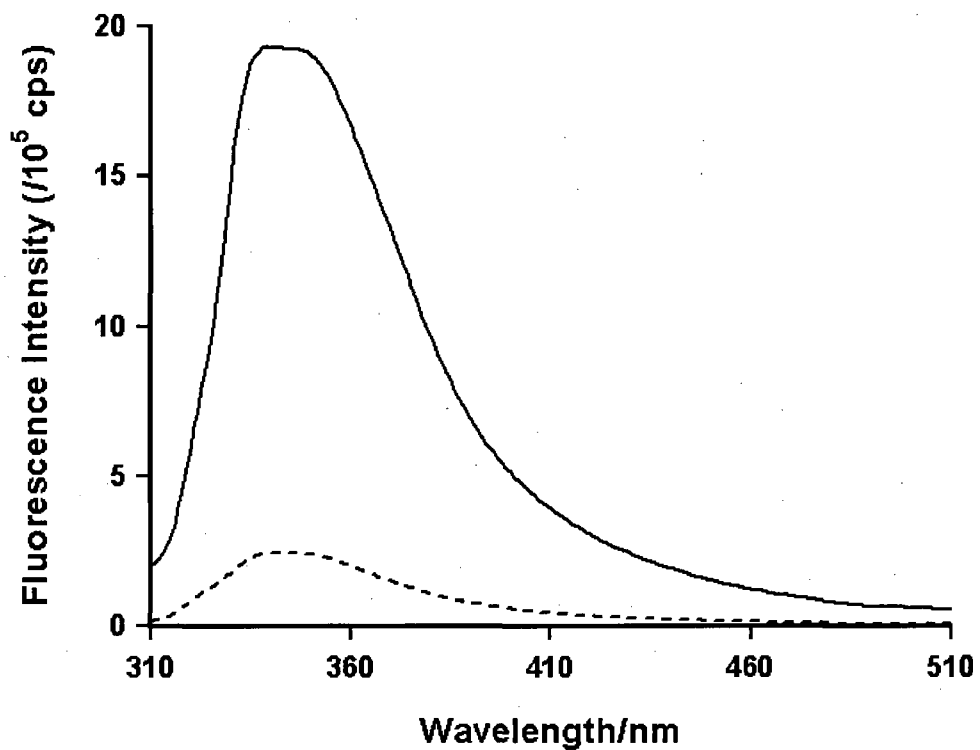


Figure 17. The fluorescence emission of CHT without α -CD (---) and with (—)10 mM α -CD.

III.3.3. Fluorescence Titrations

Once it was determined that each CD produced an enhancement of fluorescence, fluorescence titrations were done with each of the CDs to find the binding constants and host:guest complexes. The results of the various CDs on the total enhancement of the CHT fluorescence along with binding constants are shown in Table 5.

Cyclodextrin	Total Enhancement, F/F_0	Binding Constant, $K (M^{-1})$
α -CD	9.0	280
HP- α -CD	8.2	78
β -CD	5.4	110
HP- β -CD	11.0	20
γ -CD	9.8	73
HP- γ -CD	10.0	250

Table 5. Results from the fluorescence trials of CHT with various CDs.

Table 5 illustrates that all CDs gave somewhat similar results in terms of enhancement, ranging from approximately 5.5 to 11. HP- β -CD gave the largest enhancement of all the CDs but when a fluorescence titration was done using this CD, it was found that it had a very low binding constant, most likely due to the very small size of the molecule resulting in a poor fit inside the relatively large cavity size. α -CD had the highest binding constant of all the CDs and a relatively large enhancement so it was chosen as the CD that would be used for calibration curves and to find the LOD and LOQ.

In a comparison of the K values found with the addition of the un-substituted α -, β - and γ - CD to the pesticide solution, α -CD clearly showed the most favourable fit. The K value decreased as the size of the cavity of the host CD was increased. For the modified CDs, HP- α -CD did not have as high a binding constant as the un-substituted α -CD and K decreased even more for HP- β -CD. It has the lowest binding constant out of any CF that was tested. The K value of HP- γ -CD is higher than the other substituted CDs but not quite as high as α -CD. This is the

reasoning behind the choice of α -CD as the host to be used. Figure 18 shows the fluorescence titration of CHT with α -CD

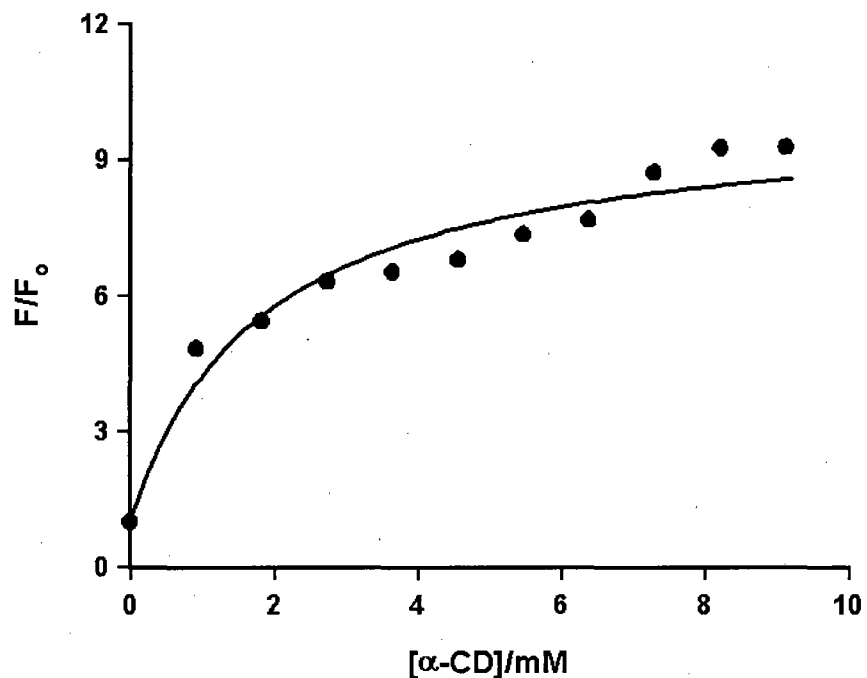


Figure 18. A fluorescence titration of CHT with 10 mM α -CD.

Only one trial was done for each of the CDs so there are no error values to report. It is hypothesized that since the size of the α -CD cavity is so small, the hydroxypropyl arms of the HP- α -CD are interfering with the pesticide molecule entering. The opposite is thought to be happening with HP- γ -CD, where the arms are going inside the cavity resulting in a tight, optimal fit for the pesticide, thus preventing the CHT molecule from leaving once it enters. This was hypothesized by comparing the binding constants that were found as α -CD had the best binding constant and HP- γ -CD was second highest.

III.3.4. Calibration Curve, LOD and LOQ

Since all fluorescence experiments with CHT were done on a 1 ppm solution, and a reasonable detection level is required to be in the part per billion levels to make this a worthwhile detection technique, the concentrations for the calibration curve were chosen to be from 500 down to 100 ppb. A linear calibration curve was obtained with a linear correlation coefficient value of 0.993.

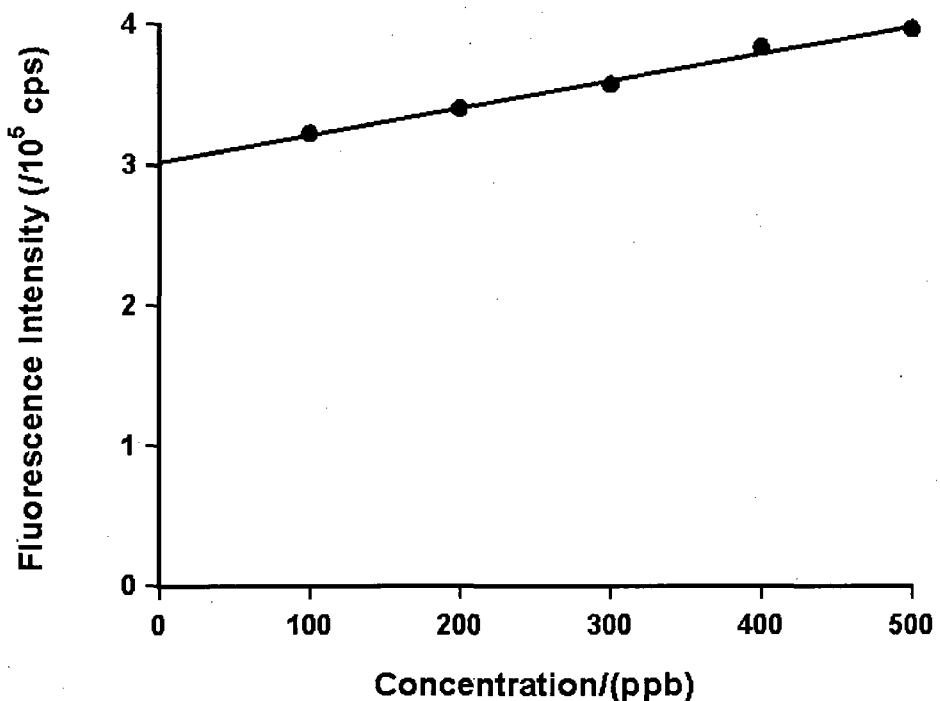


Figure 19. Calibration Curve of CHT. Various concentrations of CHT with α -CD (10mM). The curve has a linearity of 0.993

Several attempts were made at obtaining a calibration curve with a linear correlation coefficient of 0.999 but these attempts were unsuccessful. The fluorescence at these concentrations was very small, although still distinguishable, as shown in Fig. 20.

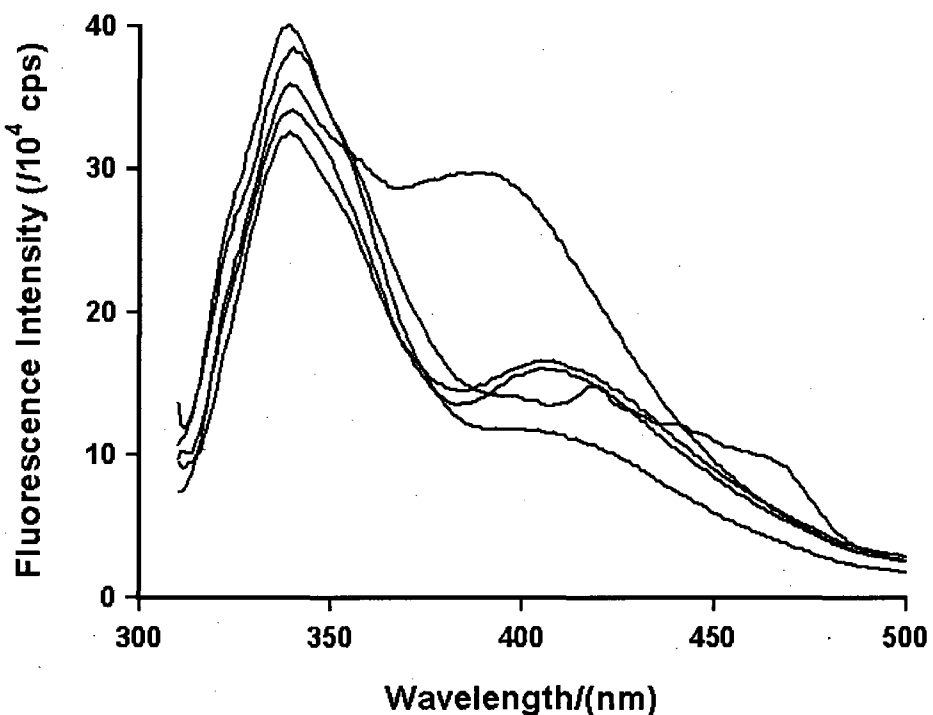


Figure 20. The fluorescence spectra of 10 mM α -CD with CHT. Concentrations range from 500 ppb (top) to 100 ppb (bottom).

A calibration curve with lower concentrations was not attempted due to the small fluorescence signal of 100 ppb, any lower peak intensity would have been too difficult to distinguish between the peaks of the different concentrations. Once the calibration curve intensities were plotted, the slope of the calibration curve was found to be 191.30 cps/ppb. The standard deviation was calculated as per the experimental procedure to be 4423.6 cps. Using

this data, the LOD and LOQ were calculated. The limit of detection for CHT using host:guest inclusion with α -CD as the host, for the enhancement of natural fluorescence in water was found to be 69 ppb. The limit of quantification using the same method of enhancement was found to be 230 ppb. This method of detection would be border line effective in trace detection of pesticides in natural waters. Oftentimes only traces of contamination remain in water bodies due to the time between actual contamination and the discovery of that particular contamination. Although peaks would be distinguishable in the higher ppb range, lower ppb concentrations would be difficult to calculate due to the overall weak fluorescence of this pesticide molecule even when included within the cavity of a CD. Without the addition of CD, a LOD would have been impossible to find due to the weak fluorescence signal.

III.4. *Carbaryl (CAB)*

Carbaryl (see structure, Fig 7.b) belongs to the carbamate family of insecticides along with carbofuran and is primarily used on PEI to control mosquitoes, ticks, ants and beetles.⁵⁰ Results on the fluorescence of carbaryl have been reported by the Pacioni group¹⁴ in the same paper that discussed the enhancement of carbofuran. Since one of the main goals of this project was to compile a list of pesticides that could be detected in ppb concentration range using the CD enhanced fluorescence technique, it was decided that this pesticide would be studied as it would be also included as one of the pesticides used in pesticide cocktails and synchronous scanning experiments (again, both of which were not studied in the Pacioni Paper).

III.4.1. Fluorescence Experimentation

Since the fluorescence properties of this pesticide molecule are well known,^{15,51} it was reasonable to omit the primary fluorescence trials that involve determining optimal excitation and emission wavelengths, as was previously done for carbofuran and chlorothalonil. A 10 ppm carbaryl stock solution was prepared for the initial fluorescence trial. The concentration was chosen because at this concentration there is an excellent fluorescence band at the reported excitation and emission wavelengths.

III.4.2. Fluorescence Enhancement by CD Inclusion

The fluorescence measurements of 10 mM β -CD- and HP- β -CD- carbaryl solutions were obtained to determine the F/F_0 of carbaryl with the excitation wavelength set at 290 nm and an emission wavelength from 300 nm to 400 nm. Carbaryl is a very fluorescent molecule even without the addition of CD and the slit widths had to be adjusted accordingly to keep the fluorescence signal from going too high on the fluorimeter, thus the reasoning behind such narrow slits (0.5 nm) for this experiment in relation to the other fluorescence trials. With the addition of β -CD, a fluorescence enhancement of a factor of 1.6 was obtained. With the addition of HP- β -CD, a total fluorescence enhancement of a factor of 1.9 was obtained. Like carbofuran, this pesticide gives better results with the modified CD cavity as compared to the native CD. Investigations into the reasoning behind the enhancement showed very similar results to that of carbofuran, as discussed in the next section.

III.4.3. Investigations into the Enhancement of Fluorescence

Purging of the carbaryl solution with argon gas to rid the solution of any oxygen molecules showed no increase in the fluorescence intensity, indicating that no quenching of the fluorescence was taking place by the presence of oxygen in the solutions. Also by examining and comparing the spectra of the fluorescence of CAB with the fluorescence of CAB in the presence of the host CDs, there appeared to be no shifting of the wavelength of the maximum emission. The fluorescence spectrum of the carbaryl solution in water was also compared to a fluorescence spectrum of a carbaryl solution in ethanol to see if any shift in maximum intensity would occur due to the change in polarity. In both fluorescence spectra, the maximum intensity wavelengths is at 334 nm, however interestingly enough, the molecule is actually less fluorescent in the less polar medium by a factor of 1.9. A polarity sensitivity factor was calculated for this molecule to be 0.41. This experiment disproves that the change in polarity causes the increase in fluorescence: In fact this molecule shows an opposite polarity dependence then the many usual cases of fluorescence enhancement (explained earlier in terms of S_1 - S_0 energy gaps). A possibility is the internal rotation of the side arm off the naphthalene group becomes restricted once it becomes included within the cavity, thus reducing the efficiency of a non-radiative decay pathway. In fact, such an increase in the fluorescence would have to be substantial in the HP- β -CD, to overcome the decrease in fluorescence due to polarity. There is no evidence for this, it is strictly hypothesized and could only be confirmed by further investigations, possibly by substituting water with a high viscosity solvent, such as glycol. Furthermore, the mechanism for the observed polarity-induced reduction in fluorescence would also need to be investigated by future photo-physical studies.

III.4.4. Calibration Curve

Once it was determined that the fluorescence of this pesticide could be detected with ease at the ppb level, a calibration curve of CAB was prepared in order to get the necessary data to calculate the limit of detection and limit of quantification. The calibration curve of CAB is shown in Figure 21.

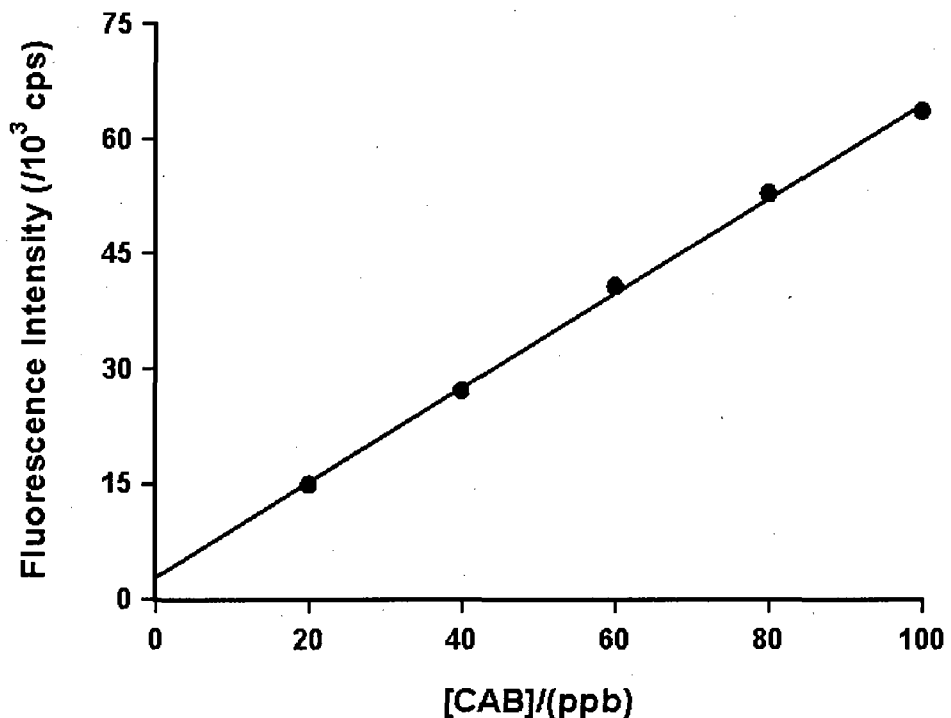


Figure 21. Calibration curve of CAB with HP- β -CD (10mM). Concentrations of CAB ranged from 100 ppb to 20 ppb and the curve had a linearity of 0.999.

From the calibration curve ($r = 0.999$), the slope is found to be 7700 cps/ppb and the standard deviation is 1800 cps. Using Eq. 2.7 and Eq. 2.8, the LOD and LOQ for the pesticide carbaryl with the presence of HP- β -CD, were determined to be 300 ppt and 2.30 ppb

respectively. The limit of detection for CAB is considered to be excellent as it can be detected in the ppt range. In comparison, Pacioni et al¹⁵ had reported a LOD value of 1.9 ppb while another literature report, using HPLC/MS/MS, had a limit of detection of 1 ppb⁵² so this result is extremely promising.

Because work on the binding constants of this pesticide with β -CD and HP- β -CD had been done by the Pacioni group previous to these experiments,¹⁵ fluorescence titrations with CAB were not determined in this project in order to focus time on the simultaneous detection of pesticides present in a sample. The binding constant for HP- β -CD with carbaryl was 640 ± 53 M⁻¹ as reported by Pacioni et al.¹⁵

III.5. *Atrazine (ATR)*

Atrazine (see structure, Fig. 8.a), a common herbicide used frequently on Prince Edward Island, was another pesticide of interest in this project due to its application rates and environmental concern.³³ Atrazine has been linked to significant decrease in birth weight of babies where traces have been discovered in drinking water.³⁹ It is even more commonly used in the United States where it is ranked second most applied pesticide. It causes numerous irreversible health effects to fish and amphibians.⁵³

III.5.1. Absorption and Fluorescence Measurements

A stock solution of atrazine was prepared according to the experimental procedure to give a concentration of 3.00×10^{-5} M. 3 ml of the solution was placed in a quartz cuvette and the absorbance of the solution was measured. This pesticide absorbed strongly in the UV-C range and moderately in the UV-B range and very minimally in the UV-A. At 290 nm, the solution had an absorbance of 0.024. This was chosen as the excitation wavelength to be tried initially in order to determine if atrazine is fluorescent. Again, due to the absorbance of CDs in the lower UV-B range and higher UV-C, the absorbance at wavelengths less than 270 nm by the molecule was ignored to avoid CD absorbance during fluorescence trials.

Fluorescence trials were performed by a trial and error method as used before with chlorothalonil to see if any fluorescence would occur despite the low absorbance by ATR. The first trial was at an excitation wavelength of 270 nm and emission from 280 nm to 600 nm. The rest of the trials went in increments of 10 nm up until an excitation wavelength of 330 nm with an emission of 340 nm to 600 nm.

The results from the fluorescence trials showed that there is a very small fluorescence peak around 348 nm. The excitation wavelengths each produced a slightly different intensity with 290 nm producing the largest intensity peak out of all the wavelengths measured.

III.5.2. Enhancement of Fluorescence by CD Inclusion

Atrazine was then tested to see if the weak fluorescence signal in water could be enhanced by the addition of native or modified CDs. Similar to the previous experiments, 6 solutions were prepared, each with a different CD, and were tested to see if any enhancement occurs from the addition of these modified and native CDs. Fluorescence measurements on all six solutions were obtained with excitation wavelength of 290 nm and an emission wavelength range of 305 nm to 575 nm.

For each of the solutions, there is only a slight enhancement of the fluorescent signal. Without a substantially large enhancement of the very weak fluorescent signal of the pesticide, using fluorescence to detect this pesticide in low ppb levels in water would be impossible, therefore it is concluded that this method would not be practical for detection of atrazine in water. Figure 22 shows the weak fluorescent band of Atrazine along with the minor enhancement from the addition of HP- β -CD.

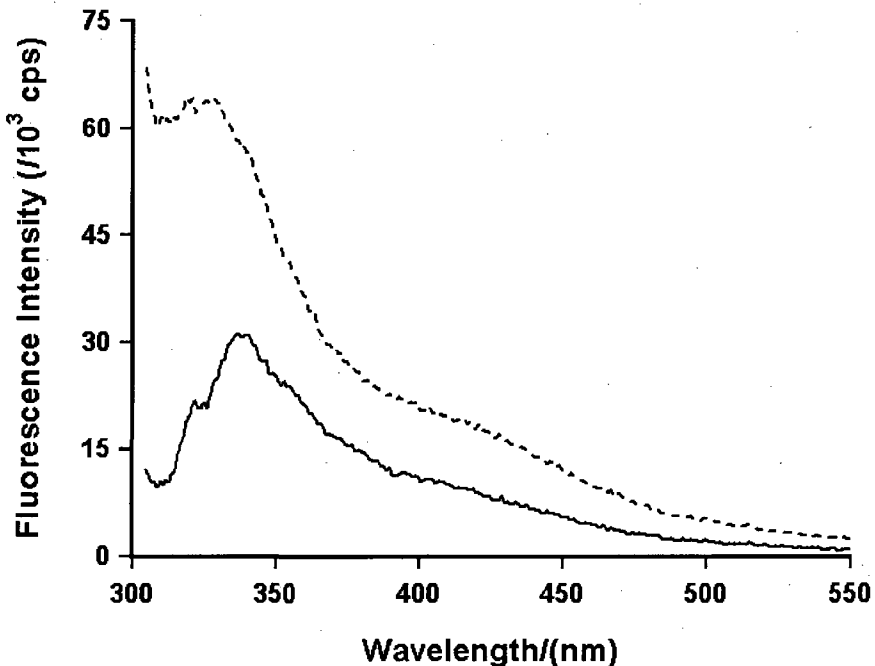


Figure 22. The fluorescence spectra of 3.00×10^{-5} M ATR in the absence of CD (—) and in the presence of HP- β -CD (---).

The enhancement of fluorescence by CD addition was observed. The weak fluorescence of ATR at 7 ppm was enhanced by a factor of approximately 2, but was still too low for trace detection of this pesticide to be possible in the low ppb levels. Scattered light or background noise from the CD is significant in this case, due to the low intensity of the fluorescence of ATR and is a problem for the accurate detection of this pesticide at low concentrations.

III.6. Metolachlor (MET)

Used to control outbreaks of broadleaf species, metolachlor (see structure, Fig. 8.b) became one of the more prominent herbicides that are predominately applied on potatoes for

protection against a wide range of broadleaf species. It is also commonly sprayed on golf courses to combat crab grass. Metolachlor is a member of the chloroacetanilide family of herbicides that contain well over twelve other equally as harmful herbicides.⁵⁴

III.6.1. Absorption and Fluorescence Measurements

The absorbance of an aliquot of 7.0×10^{-4} M stock solution of metolachlor in water was measured. The pesticide solution absorbs fairly well at 275 nm. It has an absorbance of 0.289 which is a strong absorbance compared to the other pesticides in this project. This strong absorbance would most likely be related to the large concentration of the solution due to the high solubility of metolachlor in water. Unfortunately, 275 nm is in the region where most CDs will start to absorb. Solutions of metolachlor with β -CD and HP- β -CD were measured in the UV-Vis spectrophotometer and there was no change on the absorbance, it remained at 0.289. It was therefore decided fluorescence experiments with CDs could be carried out.

For the initial fluorescence experiment, an excitation wavelength of 275 nm was chosen as this was the maximum of the absorption band. The emission wavelength was from 285 nm to 550 nm. Unfortunately, there was no sign of fluorescence from this molecule. Similar to the other pesticides in this project, several excitation wavelengths were chosen above and below the 275 nm peak and to ensure that this molecule is not fluorescent. There was still no evidence of fluorescence.

Two solutions of metolachlor with β -CD and HP- β -CD were made and measured in the fluorimeter under identical conditions and produced similar disappointing results. The lack of measureable fluorescence from this molecule indicates that it cannot be determined using fluorescence based detection in water.

III.7. *Imidacloprid (IMI)*

Imidacloprid (see structure, **Fig. 7.d**) is an insecticide that is used fairly extensively on Prince Edward Island. It is a member of the controversial neonicotinoid family of insecticides that have very strong toxicity to insects but very low toxicity to mammals. Since IMI has a high toxicity to insects, it has a very low application rate. This, in addition to its non-persistence in aqueous habitats, has resulted in IMI being considered to be a more “environmentally friendly” insecticide.³¹

III.7.1. Absorption and Fluorescence Measurements

A broad absorbance peak was present at approximately 278 nm. At 290 nm, the absorbance was 0.281, which was previously discussed as in the ideal absorbance range (0.2 to 0.4) for fluorescence experiments. In comparison to other pesticides used in this project, imidacloprid has a considerably strong absorbance, even at this low concentration. A wavelength of 290 nm was chosen because as discussed previously, the lower the excitation wavelength, the greater the possibility of the CD absorbing some of the light.

The solution of IMI was measured in the fluorimeter as described in the experimental section. The results from the fluorescence experiment showed no traces of fluorescence, even at large slit widths. The excitation wavelength was adjusted in increments of 10 nm from 270 nm to 320 nm in hopes of seeing some fluorescence at a different excitation wavelength but unfortunately there was none. With no evidence of natural fluorescence, IMI is not a candidate for direct fluorescence based trace detection.

During each of these fluorescence scans, the same solution was used and it remained in the fluorimeter between each scan. The light source remained on and the sample was present under constant exposure to UV light from the xenon lamp. Slowly, over the course of several scans, a fluorescent band started to appear, using an excitation wavelength of 300 nm with an emission band from about 375 nm to 500 nm. This indicated that there exists a potential for using UV radiation to photolyze IMI, to produce a more fluorescent photoproduct, which will be explored in Chapter 4.

III.8. *Azoxystrobin (AZO)*

There are presently nine different fungicides used on Prince Edward Island and only three of those nine are candidates for fluorescence based trace detection. Chlorothalonil is presently the most used fungicide on PEI and was studied in detail yielding favourable results. Azoxystrobin (see structure, **Fig 6.b**) and propiconazole are the other fungicides that are possible candidates.

Azoystrobin has unique properties that set it apart from other pesticides in this project.

The sheer size of the molecule is unique to the project as well as the fact that this fungicide is relatively new and derived from a natural product found in mushrooms.^{55, 56}

IV.2.1. Absorption and Fluorescence Measurements

A 1.5×10^{-5} M azoxystrobin solution was prepared as described in the experimental section. The absorbance spectrum shows two small broad peaks at approximately 370 nm and 310 nm, each with an absorbance around 0.025. Despite the low absorbance at this concentration, fluorescence trials were performed because the structure of AZO contains three aromatic rings; it has the potential to be fluorescent.

Fluorescence trials were performed on the same stock solution as used in the absorbance measurements and in the same quartz cuvette. The excitation wavelength was chosen as the peak of the absorbance band and the emission wavelengths were chosen in relation to the excitation wavelength. Identical to previous fluorescence experiments in this project where the pesticide did not absorb well, the excitation wavelength was chosen by trial and error. The first excitation wavelength was 290 nm and then increased by 10 nm to 340 nm. There was no evidence of fluorescence at these excitation wavelengths thus it was concluded that AZO was not a candidate for direct fluorescence based trace detection.

Interestingly enough, in a very similar manner to that in which the photoproduct of imidacloprid was found, a fluorescent band gradually appeared as the amount of time under

exposure to UV light increased while the solution was in the sample compartment of the fluorimeter. The generation of a highly fluorescent photoproduct by UV radiation will be examined in detail in Chapter 4.

III.9. *Simultaneous Detection of Pesticides in a Sample*

The ultimate real-world setting that would be faced in a contamination of a water system would typically involve multiple pesticides being washed down into a body of water at the same time. To be a replacement method of detection for HPLC, it would be necessary to have the ability to detect multiple pesticides in a sample simultaneously or at the very least, through several runs of the same sample in the fluorimeter with changes to the excitation and emission wavelengths.

In this project, four of the pesticides that have been studied in the Wagner lab (including three in this project) were mixed together in a single sample for fluorescence experiments. Equal 100 ppb concentrations of carbofuran and carbaryl, which showed very promising results along with chlorothalonil which also showed promise, and azinphos-methyl, a pesticide that has undergone previous extensive study by Wagner et al.²⁹ were added together in a volumetric flask.

The major issue that can arise from multiple pesticides in one solution is the similarity of excitation and emission wavelengths. Since CAF is excited best at 280 nm and both CHT and CAB are best excited at 290 nm, one of three possible events can occur. With the additional

pesticides present in the solution, they could all absorb at the excitation wavelength and reduce a particular pesticide's fluorescence. This is unlikely because of the very low levels of pesticides present and small absorbance of each pesticide at 100 ppb. Another possible result is that the emission of two or more pesticides will overlap, increasing the signal for each pesticides and thus indicating a higher concentration than is actually present. A third outcome, the one which would be necessary to use this technique on mixed solutions, would be that each pesticide has a unique maximum emission wavelength, separated enough that the fluorescence signal from each pesticide is unaffected by the presence of the others. This would be the ideal outcome. Unfortunately, because of the additional pesticide molecules all absorbing in the same region and the broad fluorescence spectra involved, the fluorescence bands were strongly overlapped and could not be resolved. This is shown in Figure 23. Since the fluorescence of AZM and CHT at 100 ppb is very weak relative to CAB and CAF, neither could be detected in the spectrum. There is a slight shoulder on the left side of the fluorescence spectrum that was originally thought to be the CAF fluorescence. It was later proven to be CAF by measuring a 100 ppb CAF solution without the other pesticides present and comparing the maximum fluorescence intensities of each (304nm).

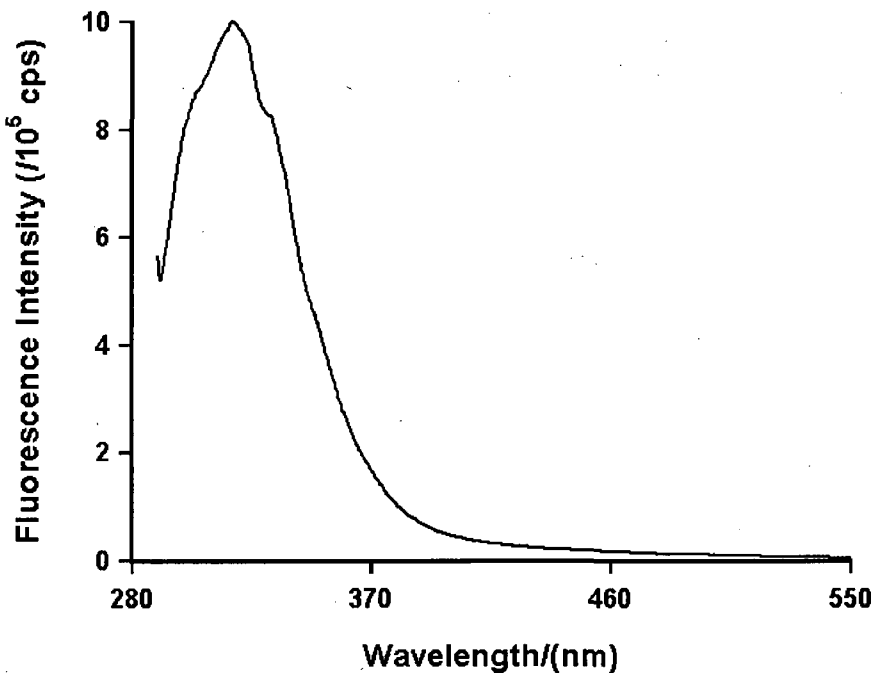


Figure 23. Fluorescence spectrum of the mixed pesticide solution containing CAF, CAB, CHT and AZM.

In Figure 23, one broad peak is shown. The broadness of each of the fluorescence bands makes it difficult to distinguish between individual peaks. The CAF peak on its own matches the peak from the mixed solution perfectly but the CAB peak from the mixture is skewed and doesn't look the same as the CAB peak from the CAB solution without the presence of the other pesticides. The excitation and emission wavelengths were also shifted 10 nm lower and 10 nm higher to see the effects on the fluorescence. By shifting lower, the peaks all looked very similar but they were slightly lower in intensity because the pesticides don't absorb as well at 270 nm. When the excitation wavelength was changed to 290 nm, the CAF peak disappeared completely. This is to be expected because the previous work on CAF showed that using an excitation wavelength of 290 nm produced no fluorescence band. This change of excitation

wavelength brought the fluorescence intensity of the mixed solution down to a much lower intensity, similar to the standard 100 ppb CAB solution.

It was decided that due to the broadness of the fluorescence peaks, this method would not be of much use for the detection of various pesticides simultaneously. Band overlaps causes too much interference so the detection would be very difficult and inaccurate.

III.10. *Synchronous Scanning Fluorescence (SSF)*

Synchronous scanning fluorimetry was used to possibly narrow the broad fluorescence peaks that are obtained from steady state fluorescence. By maintaining a constant separation between excitation and emission wavelengths, both are scanned synchronously and simultaneously in order to maximize signal at the maximum intensity wavelength and minimize the broad "shoulders" of the fluorescence bands. The separation between the excitation and emission wavelengths is determined from the range between the maximum excitation of a pesticide molecule and maximum intensity wavelength of the fluorescence. To elaborate, the carbofuran absorption maximum is at 280 nm and its peak fluorescence intensity occurs at a wavelength of 304 nm, therefore the spacing is fixed at 24 nm. This allows the molecule to be excited at the maximum excitation wavelength only when the emission is being measured at the peak emission spectrum, thus reducing or eliminating the "shoulders". Spectra for both carbofuran and carbaryl were obtained by both steady state fluorescence and synchronous scanning fluorescence to see if the broadness of the fluorescence bands could be reduced in efforts to separate the peaks enough that they did not interfere with one another when both

are present in a sample. It was also hoped that that intensity of the peaks would not be affected by this or at worse, any decrease in intensity would be minimal. The spectra are shown in Figures 24 and 25.

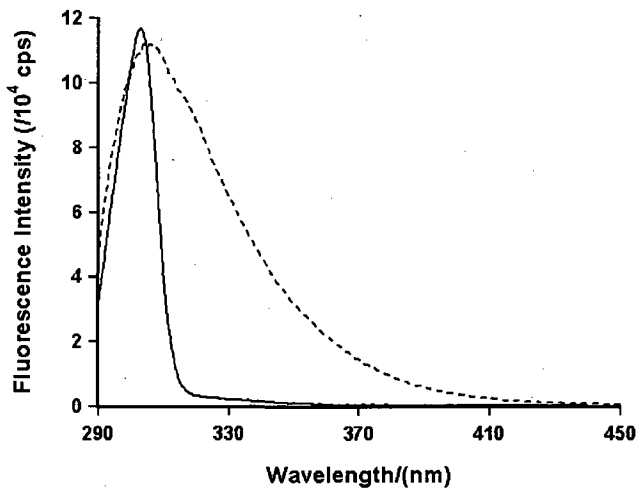


Figure 24. Synchronous scanning fluorescence spectrum (—) vs. Steady state fluorescence spectrum (---) of a CAF solution. The synchronous scanning wavelengths are optimal for the pesticide CAF.

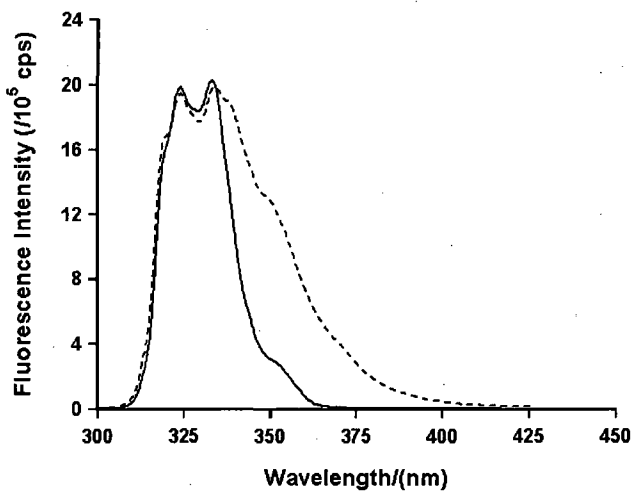


Figure 25. Synchronous scanning fluorescence spectrum (—) vs. Steady state fluorescence spectrum (---) of a CAB solution. The synchronous scanning wavelengths are optimal for the pesticide CAB.

It is clear from the comparison of the two spectra that the broadness of the peaks was substantially reduced and the intensity was only minimally affected by the change in fluorescence technique. In CAB, there was no change in the intensity at all. This is a positive step in being able to determine two or more pesticides in a solution due to the distinguishable nature of the separation of peaks.

III.10.1. Calibration Curves, LOD and LOQ Using SSF

Early fluorescence trials using SSF indicated that there was a slight reduction in the maximum intensity of the fluorescence bands. If this is to be a worthwhile addition to the enhancement of fluorescence by host:guest inclusion, the loss of sensitivity can only be minimal. Therefore, two calibration curves were prepared to get the LOD and LOQ of each pesticide using synchronous scanning fluorescence and those values would be compared to previously determined LOD and LOQ of steady state fluorescence to see if there is a loss in sensitivity.

Since CAF and CAB are the only two pesticides that have been studied that can be used to illustrate multiple pesticides visible in one solution, they were the two that were used to see if the calibration curves, limits of detection and limits of quantification could still be found and to determine the cost of using SSF.

Five solutions of CAF and five solutions of CAB were made with concentrations from 20 ppb to 100 ppb were prepared identically to the previous calibration curve solutions. Again,

solutions of CAF and CAB in 10mM HP- β -CD were then made and the fluorescence measured in the fluorimeter. The excitation wavelength region for CAF was 266 nm to 416 nm and the emission wavelength region was 290 nm to 440 nm. The spacing for CAF was chosen to be 24 nm because that is the difference between the maximum excitation and maximum emission wavelengths. The excitation wavelength region for CAB was 256 nm to 406 nm and the emission wavelength region was 300 nm to 450 nm. This was chosen because the difference in the maximum excitation wavelength and maximum emission wavelength (Stokes' shift) is 44 nm. The two calibration curves are shown in Figures 26 and 27.

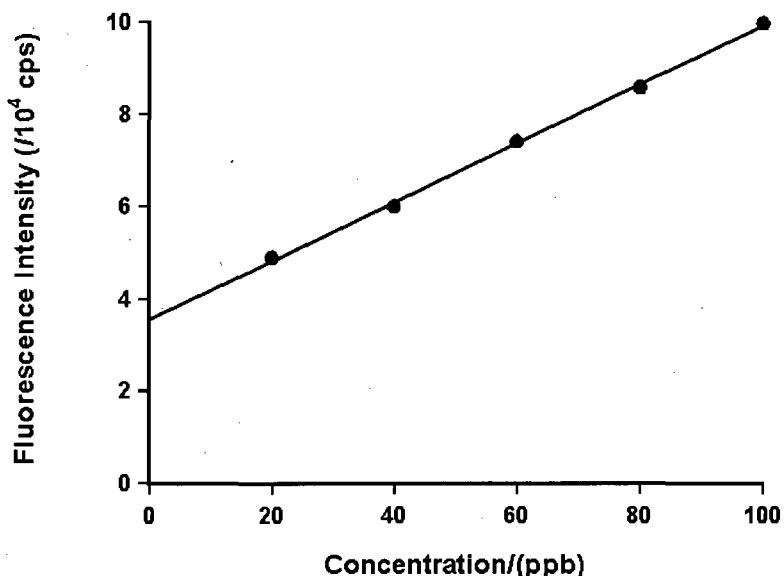


Figure 26. A calibration curve for CAF using SSF using the scanning wavelengths optimized for the pesticide CAF. The line has an r value of 0.999.

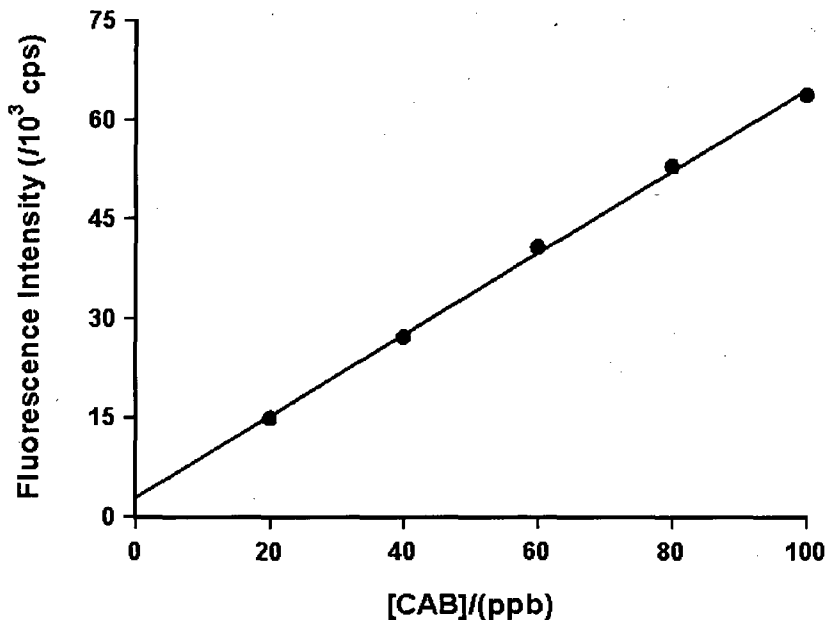


Figure 27. A calibration curve for CAB using SSF with the scanning wavelengths optimized for the pesticide CAB. The line has an r value of 0.999.

Calibration curves for both pesticide:HP- β -CD solutions were successfully obtained by using SSF and each had the required 0.999 linear correlation that was deemed satisfactory. Figures 28 and 29 show the synchronous scanning fluorescence spectra obtained from the PTI fluorimeter when the fluorescence of the calibration solutions of both CAF and CAB (100 ppb to 20 ppb) were measured.

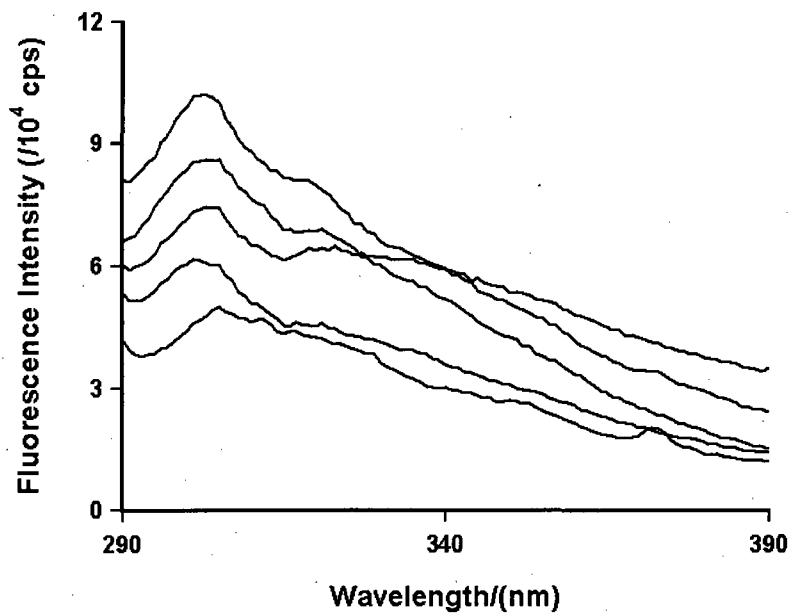


Figure 28. The fluorescence spectra of the calibration curve solutions of CAF. 100 ppb solution is highest and followed in decreasing order down to 20 ppb by increments of 20 ppb.

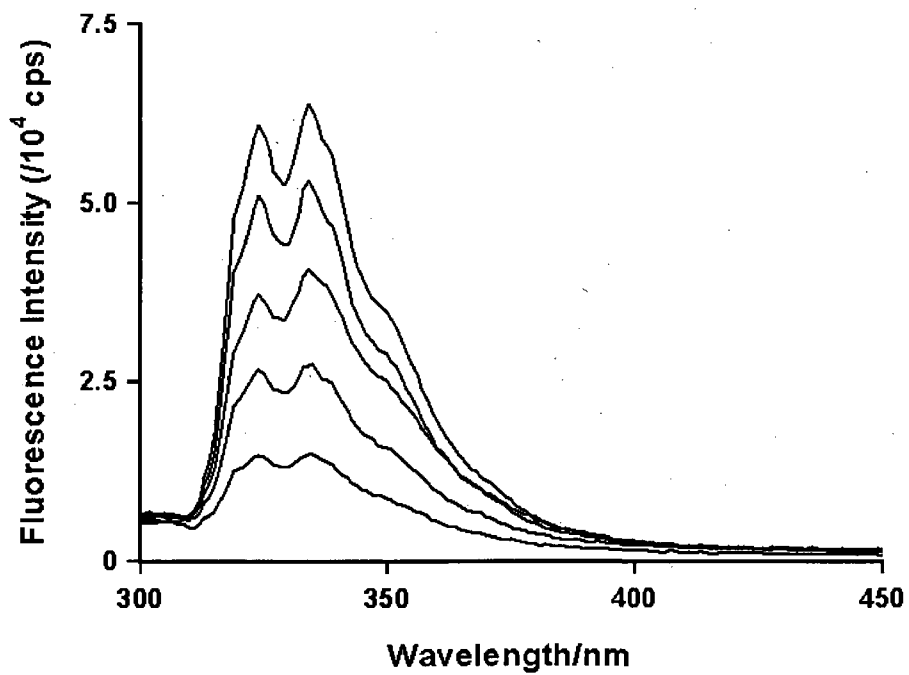


Figure 29. The fluorescence spectra of the calibration curve solutions of CAB. 100 ppb solution is highest and followed in decreasing order down to 20 ppb by increments of 20 ppb.

After obtaining these calibration curves, it was then necessary to find the slope of the line which was calculated by *Fig. P.* and the standard deviation by measuring the water blank ten times and collecting the intensities from each of the maximum intensity wavelengths. The maximum intensity wavelengths did not change from steady state fluorescence and were used in this experiment as well. A wavelength of 334 nm was chosen for the CAB solution and 304 nm was chosen for the CAF solution. The standard deviation was calculated to be 1760.92 for CAB and 2550.40 for CAF. The slopes were calculated to be 7668.76 cps/ppb for the CAB curve and 1455.55 cps/ppb for the CAF curve. By entering this data into Eq. 2.7 and 2.8, the limit of detection for CAB was found to be 690 ppt and 5.3 ppb for CAF. The limit of quantification for CAB was 2.3 ppb and for CAF it was calculated to be 17 ppb.

The effect of switching from steady state fluorescence to synchronous scanning fluorescence on the limit of detection was determined to be minimal. The LOD for CAF using steady state fluorescence was 4.2 while synchronous scanning fluorescence gave an LOD of 5.3. This was not considered a significant loss of sensitivity and is a major step in the right direction towards achieving the goal of detecting multiple pesticides in one solution. The limit of detection using steady state fluorescence on the PTI fluorimeter was 300 ppt. The LOD reported by the Pacioni group for CAB using steady state fluorescence was 1.9 ppb.

In theory, synchronous scanning fluorescence shouldn't produce any less of a fluorescence signal than steady state fluorescence because at the maximum intensity wavelength, it is absorbing at the maximum excitation wavelength. This method should also reduce the effect of contaminants that are present in the sample, especially with tests on

natural waters. More likely than not, even after filtration, natural water samples will have trace contaminants that could possibly affect the fluorescence of a particular pesticide. Since synchronous scanning fluorescence is fine tuned to a particular molecule, it has the potential to help reduce these effects.

III.10.2. Simultaneous Detection of Pesticides Using Synchronous Scanning

The idea of using synchronous scanning fluorescence to distinguish between carbamate pesticides is a fairly new idea. Ni and Cao did work on carbamate pesticides where they worked with synchronous scanning for detection in vegetables.⁵⁷ In that paper, the authors were focused on separating three pesticides (carbofuran, carbaryl and propoxur) in vegetable samples. However, they did not use CDs to enhance the fluorescence. In fact, the use of CDs to enhance the fluorescence of any pesticides using SSF to separate the spectra has never been attempted previous to this thesis project. With each pesticide responding differently to the inclusion into a cavity of a CD, each enhancing by different factors, it becomes difficult to detect some weaker fluorescent molecules in the presence of more fluorescent molecules. Early findings in this project have determined that, despite an overlap of fluorescent bands in a mixture of pesticides, it is possible through the use of synchronous scanning fluorescence to eliminate the unwanted “shoulders” of a fluorescent band and therefore it may be also possible to eliminate overlap between other fluorescent molecules with similar emission wavelengths and thus distinguish between many fluorescent molecules at the same time.

A solution of four different pesticides mixed together was prepared as explained in the experimental section. Proper aliquots of CHT, CAB, CAF, and AZM were put into a 100 mL volumetric flask and diluted to mark to give equal concentrations of 100 ppb for each of the pesticides. A synchronous scan of this solution was performed by scanning excitation wavelengths from 266 nm to 416 nm and scanning emission wavelengths from 290 nm to 440 nm. Due to the low concentrations of pesticides present in the solution, the actual slit widths were opened up to 1.25 mm. A 100 ppb solution of CAF was run by itself to act as a reference to the pesticide cocktail solution in order to determine if the fluorescence is affected. After both solutions were measured, it was noticed that distinguishable peaks for CAB were also present so a third solution of 100 ppb CAB without the presence of other pesticides was measured. These fluorescence spectra are shown in Figure 30.

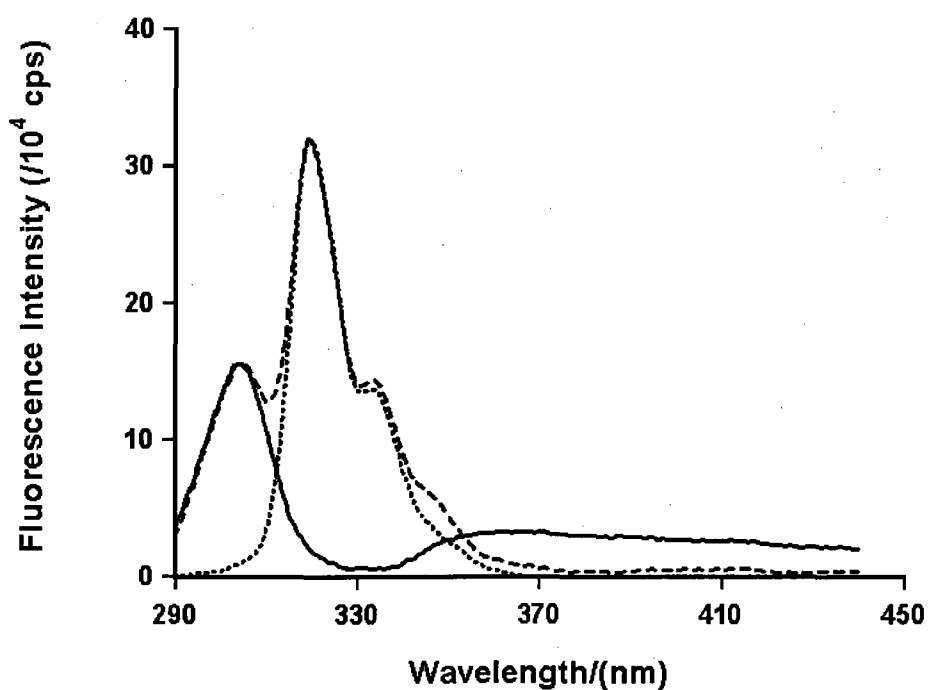


Figure 30. Synchronous Scan of 100 ppb CAF(—), 100 ppb CAB(···) and a Mixture of 100 ppb of each CAF, CAB, CHT, and AZM (---). The scanning wavelengths are optimized for CAF detection.

This scan was done at the optimum wavelength ranges for CAF to see if it could be detected in a mixture. The results from this experiment were promising in terms of peak separation. There was no effect on the intensity of fluorescence of CAF and very little effect on the intensity of fluorescence of CAB from the presence of CHT and AZM. The carbofuran peak was virtually unaffected by the additional pesticides attributable to the finely tuned settings of synchronous scanning fluorimetry. It was surprising that at these wavelength settings, carbaryl was so distinguishable but did not seem to hinder or enhance the fluorescence peak of the carbofuran.

A solution of 100 ppb carbaryl was measured using synchronous scanning with the excitation and emission wavelength ranges set for optimal fluorescence of this particular pesticide. The excitation wavelength range was from 256 nm to 406 nm and the excitation wavelength range was from 300 nm to 450 nm. The actual slit widths were the same as the previous experiment in order to maintain consistency and to be able to compare the loss of fluorescence displayed from the change in excitation and emission wavelength ranges. Figure 31 shows the fluorescence spectrum of 100 ppb CAB and the pesticide mixture using synchronous scanning fluorimetry.

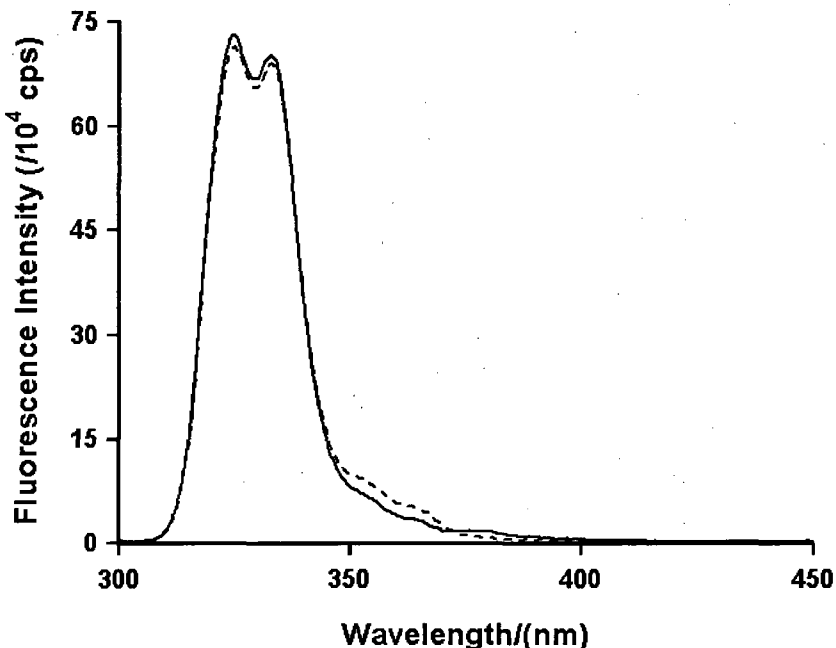


Figure 31. The Synchronous Scanning Spectra of 100 ppb CAB and a Mixture of 100 ppb of each CAF, CHT, CAB and AZM. The scanning wavelengths are optimized for the detection of CAB.

The wavelength regions were set at the optimum range for CAB fluorescence for this fluorescence measurement. This eliminated the CAF peak entirely without affecting the intensity of the CAB peak.

As was the case with the carbofuran solution under optimal conditions, carbaryl does not seem to suffer from loss of intensity due to the presence of other pesticide molecules in solution at these wavelength ranges. The difference in the two spectra shown is very minimal in relation to the intensity of the peaks. It is interesting to note that the base of the fluorescence peak of the pesticide mixture is slightly broader than the CAB solution on its own. This broadening could be a result of the fluorescence of the CHT present in the solution. Looking at the emission wavelengths, it seems the shoulder is approximately where CHT fluorescence

would be occurring. If this is due to CHT it does not seem to have any effect on the peak intensity, which is the main goal of this section.

III.10.3. Spiked Samples Using Synchronous Scanning Fluorescence

Synchronous scanning fluorescence is a valuable tool for eliminating the broadness of fluorescence peaks which in turn can allow for peak separation between overlapping fluorescent bands of two separate molecules. Previously, it has been determined that no loss of signal from a target pesticide molecule is reported from the presence of other fluorescent molecules in a solution. The focus now shifts to determine whether or not spiked samples of a target pesticide can be accurately measured while in the presence of other fluorescent pesticides using SSF.

Carbofuran and carbaryl were both examined in order to see if the concentration of an unknown spiked water sample could be accurately determined while in the presence of each other. CHT and AZM spiked sample trials were not performed due to their very weak fluorescence in solutions of low ppb concentrations.

III.10.3.1. Carbofuran Spiked Sample Detection

A new calibration curve of CAF was prepared for these spiked sample trials as explained in Chapter 2. Again, like the previous spiked sample trials, the solution concentrations were unknown to the tester until after the experiments were completed. Two of the four solutions

contained only unknown amounts of CAF. The other two contained unknown amounts of CAF, plus 100 ppb CHT, 100 ppb AZM and 100 ppb CAB. The reasoning for the differences in solutions with addition of 100 ppb of each of the different pesticides is to see if the concentration can be accurately determined not only on its own, but in the presence of other fluorescent pesticides. The results from the spiked sample trial are shown in Table 5. The actual slit widths for the experiment were adjusted to 1 mm as this proved to be the ideal width for these concentrations and the excitation and emission wavelength regions were set at the optimum regions for CAF as determined in the previous section. The equation of the line derived from the calibration curve is $y = (1748.2 \text{ cps/ppb})x + 3108.3 \text{ cps}$.

Solution	Calculated Conc. (ppb)	Actual Conc. (ppb)	Error (%)
A	89	88	1.1
B	52	52	0
C	66	65	1.5
D	89	98	9.2

Table 6. Results from spiked sample test using SSF for the detection of CAF in the presence of three other pesticides and 10 mM HP- β -CD.

Solutions A and C contained the additional 100 ppb of CAB, AZM and CHT, but did not affect the accuracy of the CAF detection. The results from the spiked sample tests using SSF are very accurate, with only minor percent errors ranging from 0% to 9%. In fact, for all four

samples these spiked sample tests for CAF using SSF were more accurate than those discussed previously for CAF using steady state fluorescence (Section III.2.7.)

III.10.3.2. Carbaryl Spiked Sample Detection

A series of spiked sample detections for carbaryl were performed using the same procedure as the previous spiked sample experiment for carbofuran. A new calibration curve was made using proper dilutions and the addition of 10 mM HP- β -CD. For this experiment, a total of four solutions of unknown concentrations were again blindly prepared. Two of the four solutions contained unknown amounts of CAB with the presence of CAF and two of the four solutions did not have CAF present. The excitation and emission wavelength regions were changed to the optimum settings for CAF as determined previously. The slit widths remained unchanged at 1 mm for they were ideal for these trials. The results of this experiment are reported in Table 6. The equation of the line derived from the calibration curve was $y = (3284.949 \text{ cps/ppb})x + 33744.08 \text{ cps}$ with an r value of 0.992.

Solution	Calculated Conc. (ppb)	Actual Conc. (ppb)	Error (%)
A	35	44	20
B	99	96	3
C	79	69	13
D	91	96	5

Table 7. Results from spiked sample tests using SSF for the detection of CAB in the presence of three other pesticides and 10 mM HP- β -CD.

The results from the spiked sample test for carbaryl were not quite as accurate as for the carbofuran trial. It is not fully understood what caused the greater inaccuracy, whether it was user errors, such as improper dilutions or loss of solution from transferring the solution from a vial to a quartz cuvette or just inaccuracy from the calibration curve not being sufficiently linear as the calibration curve prepared for this trial had an r value of 0.992.

Overall, the spiked sample trials were considered successful as it was possible to detect, with accuracy ranging from 0% to 9% for CAF and 3% to 20% for CAB, each pesticide in the low ppb range even in the presence of the other highly fluorescent pesticide, which is necessary to be considered a worthwhile method of trace detection of pesticides.

III.11. Conclusions

In this chapter, a total of seven different pesticides, presently used in varying amounts on Prince Edward Island, were studied in detail. Each pesticide was examined to see if firstly, the pesticide showed any natural fluorescence in water, and secondly, if that natural fluorescence could be enhanced by forming an inclusion complex with a host cyclodextrin molecule, native or modified, to a point where it could be detected in trace amounts in water.

Out of the seven pesticides tested, CAF and CAB showed excellent results with LOD values in low part per billion levels (4 ppb, 0.3 ppb, respectively), CHT showed promising results and could be detected at 70 ppb. Binding constants and host:guest complexes between the

guest pesticide molecules and the host cyclodextrin molecules were also determined and reported.

Spiked samples were done on two of the pesticides (CAF and CAB) and showed accuracy in the detection of these pesticides from 0% to 9% for CAF and 3% to 20% for CAB. Mixtures of different pesticides were tested to determine if each could be detected simultaneously and by use of synchronous scanning fluorescence, this was possible for two of the four. Due to the weak fluorescence band of CHT and AZM relative to CAB and CAF, it was only possible to identify CAF and CAB in the mixtures.

Atrazine and Metolachlor were not successfully detected in water due to the very weak fluorescence of atrazine and absence of measureable fluorescence of metolachlor. Azoxystrobin and imidacloprid also showed signs of fluorescence but only after exposure to UV light. These pesticides will be examined more closely in Chapter 4, using photochemically induced fluorescence.

IV. RESULTS AND DISCUSSION- Photochemically Induced Fluorescence of Pesticides

Many aromatic pesticides are fluorescent and make for good candidates for supramolecular host:guest inclusion in order to enhance the natural fluorescence of the molecule. However, there are some aromatic pesticides which contaminate natural water systems nearby to the application sites, which are non-fluorescent, and thus not directly detectable using fluorescence based methods. There are numerous cases in the literature that have dealt with certain pesticides such as α -cypermethrin and fenvaletrate, in which the pesticide showed no measureable fluorescence in water but when photolysed by UV light, produced a strongly fluorescent photoproduct.^{17, 18} Previous work on the photolysis of AZM also shows the generation of a highly fluorescent intermediate by UV photolysis and will be further discussed in Chapter 5. This chapter will describe two non-fluorescent pesticides used on PEI which were exposed to ultraviolet light in an effort to create a fluorescent photoproduct, and attempts at further enhancement by host:guest inclusion using CDs.

IV.1. *Imidacloprid (IMI)*

As was shown in Chapter 3, IMI does not directly exhibit any natural fluorescence in water. It was discovered however, that under the exposure to UV radiation, IMI is photolyzed and a strongly fluorescent photoproduct is generated. It was this generation of a fluorophore from previously non-fluorescent IMI that allowed for the possibility of further enhancing this fluorescence via the formation of host:guest inclusion complexes.

IV.1.1. Photochemically Induced Fluorescence

At this point, a detailed and precise literature search was conducted to see if there were any reports on the photochemistry of IMI. This revealed a very recent (2007) paper from Flores *et al.*³¹ discussing imidacloprid and the photochemical degradation reaction that takes place when IMI is under constant UV exposure. In that paper, it was discussed how imidacloprid is photolyzed into a highly fluorescent molecule when irradiated with UV light and could be detected in trace amounts in water and certain peppers.^{31, 58} Flores *et al.* were also able to elucidate the highly fluorescent intermediate in their work. The highly fluorescent photoproduct of IMI was found to be 1-(6-chloro-3-pyridyl-methyl)-2-(hydroxyimino)-3,4-didehydroimidazolidine.

The ability to detect this fluorescent product of IMI was a promising lead into the addition of CDs in efforts to further enhance the fluorescence of the photoproduct, which to our knowledge, had previously never been done. The Flores paper did not specify the wavelength region that was used for the UV exposure to the IMI sample. In the present work, the exposure wavelength of 350 nm in the photochemical reactor was used.

An initial fluorescence measurement was taken for imidacloprid without any exposure to UV light. The solution was then photolyzed for 5 minute intervals with the fluorescence measured after each interval. After 35 minutes of exposure, the fluorescence signal stopped increasing and remained at a constant intensity. It was decided that the solution would be measured for an additional 15 minutes to ensure that the newly formed photoproduct was stable. The fluorescence intensity remained unchanged for those additional three 5-minute

intervals, thus proving that the newly formed fluorophore was stable under these conditions. Figure 32 shows the fluorescence signal of the IMI solution before any UV exposure, after 5 minutes in the photochemical reactor and the same solution after 35 minutes in the photochemical reactor.

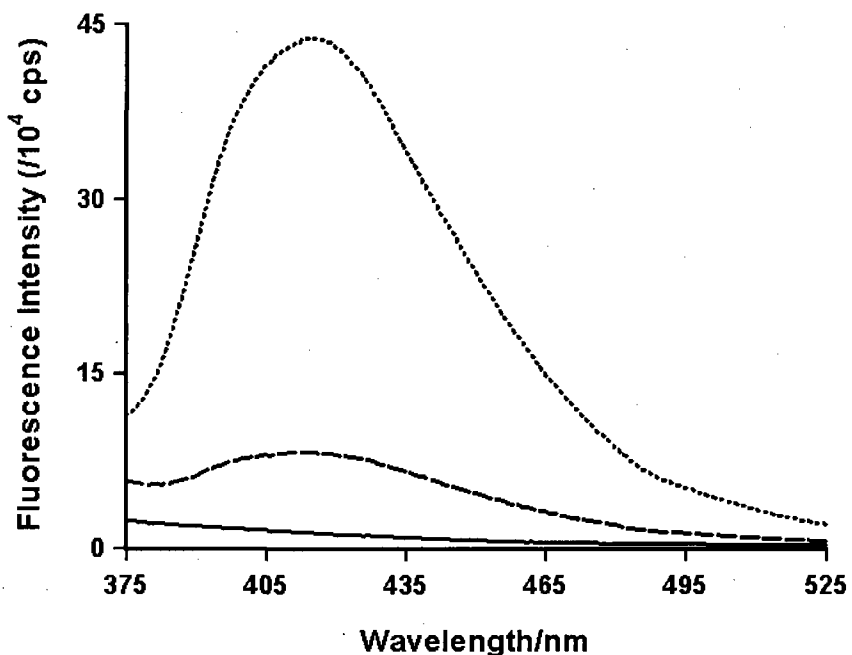


Figure 32. Fluorescence of imidacloprid before UV exposure (—), after approx. 5 minutes (---) and 35 minutes (···) of UV-A exposure.

A limit of detection for this new fluorophore was not determined in this project for it had previously been done by the Flores group.³¹ They reported a LOD of 2 ppb. However, the possibility of improving upon this reported PIF trace detection method by the addition of CD had not been previously explored.

IV.1.2. Fluorescence Enhancement by Cyclodextrin Inclusion

The LOD reported by Flores *et al.*³¹ was a very promising result for the detection of an originally non-fluorescent pesticide in water. It was decided that, since this newly formed fluorophore had been detected in the low ppb range and the structure of the photoproduct had been elucidated, some further experiments on the effects of CD addition on the fluorescence of this molecule would be studied.

Five solutions of photolyzed imidacloprid were prepared as per the experimental section. Four of those solutions were then added to one of four CDs; β -CD, HP- β -CD, γ -CD and HP- γ -CD. The size of the cavity of α -CD was assumed to be too small to enclose the relatively large IMI photoproduct and depending on the resulting data would be examined later on if any enhancement occurred with the addition of other CDs.

The fluorescence spectra were obtained for each of the solutions to determine if any further fluorescence enhancement occurred from the addition of CD. Unfortunately, there was no further enhancement of the fluorescence of the already highly fluorescent photoproduct of imidacloprid. It was decided that α - and HP- α -CD would not be revisited based on the results from the other host molecules.

IV.2. *Azoxystrobin (AZO)*

Azoxystrobin, like imidacloprid, did not show any native fluorescence in water. During fluorescence trials, exposure to UV light while in the sample compartment of the fluorimeter caused photolysis of the AZO to occur. During photolysis of AZO, the generation of a strongly fluorescent photoproduct took place. This made AZO a candidate for the fluorescence-based trace detection in water by PIF coupled with enhanced fluorescence by CD addition. A precise literature search for the photochemically induced fluorescence of azoxystrobin revealed another very recent (2007) paper by the Flores group in which they developed a photochemically induced fluorescence based trace detection of azoxystrobin in musts and wines.³⁰ To date, there have been no studies performed on the photochemically induced fluorescence of azoxystrobin in water. Also, there were no attempts at further enhancing the fluorescence of the newly generated fluorophore.

It was reported in the literature that the optimal excitation wavelength for a photolysed solution of AZO was 374 nm but work done during this project showed that an excitation wavelength of 369 nm produced a slightly higher maximum fluorescence intensity value than 374 nm. The maximum fluorescence intensity value was found to occur at 462 nm.

IV.2.1. Photochemically Induced Fluorescence

3 ml of the 1.5×10^{-5} M AZO stock solution was used in order to determine the total time needed to fully photolyze the AZO solution. A fluorescence spectrum was obtained prior to any UV exposure and then the solution was placed in the home-made photochemical reactor equipped with a handheld UV-C lamp (~254 nm) for 30 minute intervals with the fluorescence

measured after each interval for a total of 360 minutes. By this point, there was no further increase of fluorescence as the maximum intensity value stayed relatively constant for several 30 minute intervals. This proves that the photoproduct of AZO is stable at the UV wavelength that it is being exposed to and that it is fully photolyzed after approximately 2 hours of exposure. Figure 33 shows that there is no fluorescence of the unphotolyzed AZO solution along with the fluorescence band produced from the photolyzed solution.

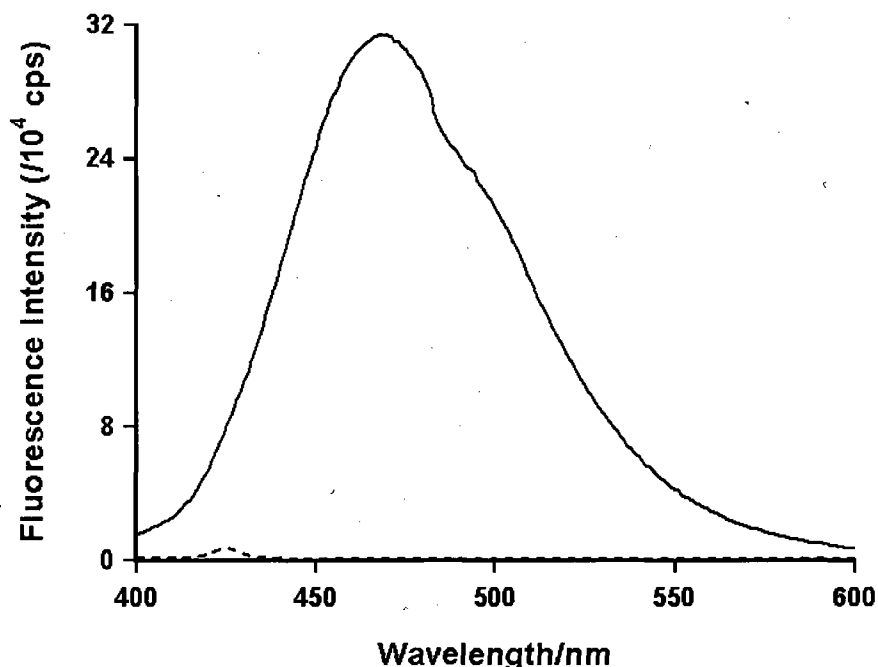


Figure 33. The fluorescence spectrum of AZO without any UV exposure (· · ·) and the fluorescence of photolyzed AZO (—).

Absorption measurements of the fully photolyzed solution showed that it maintained the same two broad peaks in the same wavelength region as the unphotolyzed solution,

however each peak approximately doubled in absorbance, thus illustrating that there likely was a change in the structure of the molecule. The absorption spectrum is shown in Figure 34.

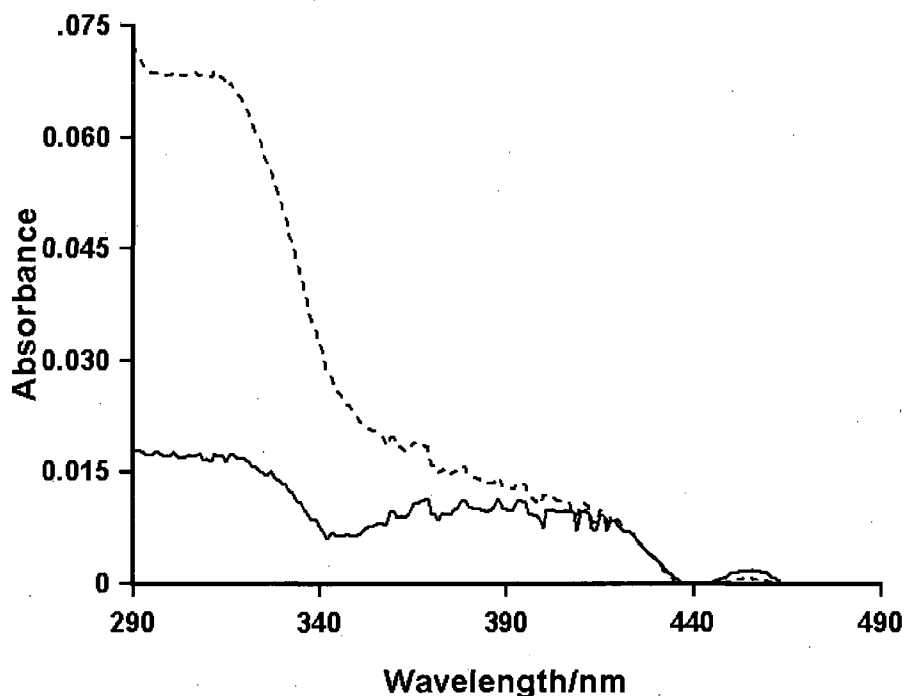


Figure 34. The absorption spectrum of unphotolyzed (—) and photolyzed (---) AZO.

IV.2.2. Fluorescence Enhancement by Cyclodextrin Inclusion

It was determined in the literature that azoxystrobin can be detected in trace amounts as low as 16 ppb via photochemically induced fluorescence in wine.³⁰ Once it was discovered that photolysis creates an extremely fluorescent fluorophore from a previously non-fluorescent molecule, it became a molecule of interest for host:guest inclusion with the addition of CD; to investigate which CDs could provide a more sensitive trace analysis technique.

The AZO solution was photolyzed for 2.5 hours until the photochemical reaction was completely finished. The fluorescence measurement of the fully photolyzed solution was performed using 369 nm as the excitation wavelength and 400 nm to 600 nm was the emission wavelength region, as was determined to be the optimal conditions for the fluorescence of this molecule in water. The integration of the fluorescence peak of the fully photolyzed solution without the presence of CD is used as F_0 in the fluorescence enhancement calculation. HP- γ -CD was added to the 3 ml aliquot of fully photolyzed AZO to create a 10mM solution of HP- γ -CD with the newly formed fluorophore. The AZO:HP- γ -CD solution was measured in the fluorimeter under identical settings and that fluorescence peak was integrated in order to determine if there was any enhancement of the fluorescence by host:guest inclusion. The results from the F/F_0 equation show that there is a large enhancement of fluorescence. It increased by a factor of approximately 2.9.

The same experiment was carried out again with HP- β -CD and resulted in an enhancement of a factor of 3.3. Both fluorescence peaks are shown in Figure 35, along with the fully photolyzed solution of AZO without the presence of either CD.

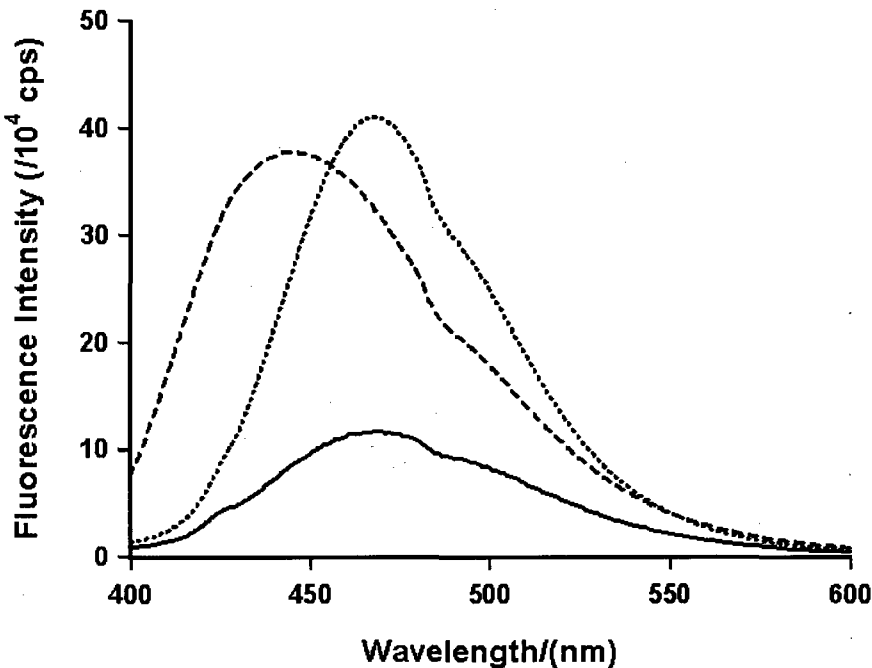


Figure 35. The fluorescence spectra of a photolyzed solution of AZO w/o CD (—), a photolyzed solution of AZO w/ HP- β -CD (---) and a photolyzed solution of AZO w/ HP- γ -CD (···). The enhancement of fluorescence by CD addition is illustrated.

It is interesting that the overall F/F_0 of AZO with HP- β -CD was larger than the F/F_0 of AZO with HP- γ -CD except the maximum fluorescence intensity at the peak was higher for HP- γ -CD. This is not something that was seen before in any other pesticide experiments. It was also unique that the addition of HP- β -CD resulted in a blue shift in the fluorescence spectra and there was no observed blue shift in the fluorescence spectra with the presence of HP- γ -CD as can be seen from the maximum fluorescence intensity wavelength of 462 nm remaining the same from the photolyzed solution without CD as the $\lambda_{\text{max},F}$ with HP- γ -CD. The $\lambda_{\text{max},F}$ of the photolyzed solution of AZO with HP- β -CD shifted to 444 nm. The reasons for the observed fluorescence enhancement of AZO by both HP- γ -CD and HP- β -CD was not investigated in detail, although by studying the spectra, it can be concluded from the visible blue shift of the

photolyzed AZO with HP- β -CD, that the photolyzed AZO is polarity sensitive and the change in polarity between environments greatly increased the fluorescence. There is also the potential of two different mechanisms existing between the photolyzed AZO solution and each of the CDs. The size differences of the two cavities could be producing alternate mechanisms or modes of inclusion causing the resulting blue-shift in one case but not the other. It would be difficult to elucidate these mechanisms without first knowing the structure of the new photoproduct. This unknown photoproduct has not previously been elucidated by Flores et al. or in this project.

IV.2.3. Determination of Binding Constants

Fluorescence titrations for the pesticide azoxystrobin with HP- γ -CD and HP- β -CD were performed using a slightly different procedure. Rather than create ten different solutions, all with different concentrations of CD from 1 mM to 10 mM, one photolyzed solution was created and enough CD was added to the solution to increase the solution concentration by 1 mM for each fluorescence measurement. The reasoning for this was the length of time it takes to fully photolyze one solution of AZO was two hours. Previous fluorescence titrations done in this project did not require the two hour photolysis for each solution and therefore experimental time was not an issue. Photolyzing 11 solutions of AZO for two hours each would be far too time consuming and unnecessary.

The fluorescence titration was performed by increasing the concentration of CD in the photolyzed AZO solution by 1 mM increments rather than by creating 11 solutions as was done

in all previous fluorescence experiments. Each peak was corrected for solvent and integrated. Those integration values were fitted to equation 1.2 to calculate the binding constant. For HP- γ -CD, the calculated binding constant is $550 \text{ M}^{-1} \pm 22 \text{ M}^{-1}$ (two trials). In comparison to the other binding constants in this project, this value is relatively large. It indicates that it is a very favourable situation for the guest pesticide molecule to become included within the cavity of the host.

The identical procedure was used to determine the binding constant for HP- β -CD. In this case, the calculated binding constant of $270 \text{ M}^{-1} \pm 44 \text{ M}^{-1}$ is not nearly as large as for HP- γ -CD but is still large compared to other pesticide binding constants in this project. This binding constant, in comparison to all the other pesticide molecules used in this project, is still a favourable result; however this difference in binding constants between hosts suggests that the photoproduct of AZO is still a relatively large pesticide molecule as it favours the larger cavity size of HP- γ -CD.

Figure 36 shows the integration values from the fluorescence titration with HP- γ -CD, along with the actual fit curve, calculated from Eq. 1.2.

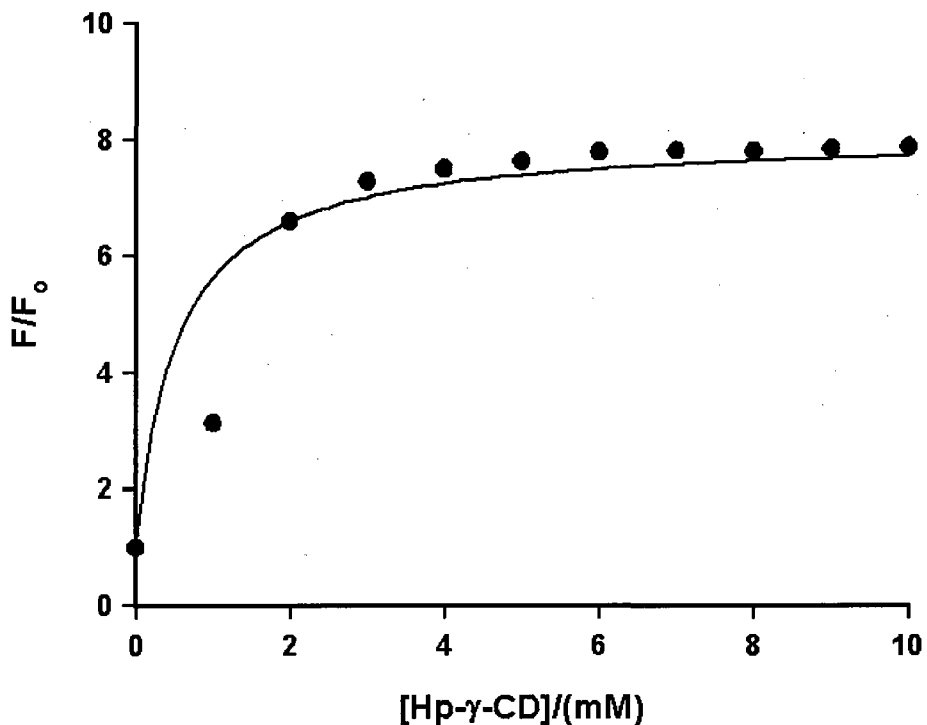


Figure 36. Fluorescence titration of photolyzed AZO with HP- γ -CD. The solid circles represent the F/F_0 vs [CD] data and the solid curve represents the calculated fit from equation 1.2. The binding constant was found to be $550\text{ M}^{-1} \pm 22\text{ M}^{-1}$ (average of two trials).

The data from the fluorescence titration was also used to create a double reciprocal plot to determine the host:guest complex that is formed. With both hosts, a 1:1 complex had formed with the fluorescent photoproduct of AZO. This was concluded from the plot of data showing a straight line with an r value of 0.981 for HP- γ -CD and an r value of 0.980 for HP- β -CD.

IV.2.4. Limit of Detection and Quantification

A calibration curve of photolyzed AZO solutions with HP- γ -CD was created from proper dilutions of the stock solution into concentrations of 20 ppb increments from 20 to 100 ppb.

Each solution was measured in the fluorimeter with an excitation wavelength of 369 nm and an emission region of 400 nm to 600 nm. The spectra for the five solutions were corrected for the solvent and the maximum peak intensity values were recorded at the maximum emission wavelength of 462 nm. These intensity values were plotted in *Fig. P.* and from that, the equation of the line was calculated. The equation for this calibration curve was $y = (2057.394 \text{cps/ppb})x + 11598.49 \text{ ppb}$. A solvent blank was run ten times and the intensity at 462 nm was recorded. A standard deviation of the blank solution was calculated to be 1018.74. A calibration curve of photolyzed AZO with HP- β -CD was not done only because the larger enhancement of HP- γ -CD made using HP- β -CD irrelevant, for the limit of detection and limit of quantification would not be as low as it is with HP- γ -CD.

Using equations 2.7 and 2.8 and the calculated values of the standard deviation of the solvent blank and slope of the calibration curve, the limit of detection and limit of quantification were found. The limit of quantification for photolyzed AZO in the presence of HP- γ -CD was 5.0 ppb and the limit of detection was 1.5 ppb. To date, as stated earlier, the only other published study on the detection of azoxystrobin using a photochemically induced fluorescence based trace detection method involved musts and grapes.³⁰ The authors reported a limit of detection level of 6 ppb in the extracts of musts, wines and grapes but did not report a limit of detection in water. The addition of HP- γ -CD substantially improved upon the detection limits that were reported in the literature by a factor of approximately 4.

The low limits of detection and quantification found in this project indicate that the photochemically induced fluorescence coupled with host:guest inclusion is a viable method of

detection for trace amounts of azoxystrobin in water. HPLC-MS studies have shown the ability to detect this pesticide in the range of 5 ppb in surface waters.⁵⁵ This new method, that has been developed in this project, that combines photochemically induced fluorescence and CD enhancement of fluorescence, improves upon the standard method of detection presently used. The lower limit of detection is important in fluorimetric based method but also by having less impact on the environment due to not having to use potentially harmful chemicals, this method can be considered worthwhile for further investigations. This method of combining UV photolysis with host inclusion has not been performed on AZO previous to this research. It also opens the door for the other pesticides that have been previously studied and concluded to have no measureable fluorescence, for further studies to combine UV photolysis with host inclusion including pesticides atrazine and metalochlor.

V. RESULTS AND DISCUSSION- UV-A Photochemistry of the Pesticide Azinphos-Methyl

As can be seen from Chapter 4, the identification of the highly fluorescent photoproduct- in the case of photochemically induced fluorescence of a pesticide would be extremely important and useful, for example, in predicting the best host for further enhancement of the PIF signal for trace detection applications. This has not yet been done for azoxystrobin which had been discussed in that chapter. However, the photochemistry of another pesticide, azinphos-methyl, which has been recently restricted on PEI, will be the focus of this chapter.

The fluorescence of azinphos-methyl (AZM, Fig. 7.c) has been extensively studied by the Wagner group in the past.^{15, 59} It has been a significant pesticide on Prince Edward Island for a number of years and has been directly linked to several fish kills.³⁹ Cyclodextrin inclusion, base hydrolysis of AZM and UV photolysis have been studied in detail with successful efforts to enhance the weak natural fluorescence of the pesticide molecule.¹⁶ Work on the UV photolysis of AZM as a means of enhancing the fluorescence had been undertaken by Lovely Yeasman, a previous graduate student in the Wagner group. In that work, the identity of the fluorescent photoproduct and a mechanism for its formation were proposed. However, the relative importance of the two competing photolysis pathways identified, only one of which leads to the highly fluorescent photoproduct, was not investigated. This chapter will examine, in more detail, the UV-A photolysis of AZM, identify/confirm the intermediates and products of the photolysis, as well as investigate the mechanism and pathway partition for the photolysis of AZM using fluorescence, HPLC and NMR spectroscopy as analytical tools. The results of the

work described in this chapter, combined with those of Yeasmin⁵⁹ were recently published in the *Journal of Photochemistry and Photobiology A: Chemistry*.²⁹ This work will also serve as a template for similar work carried out in the future on the photochemistry of azoxystrobin.

V.1. *Calibration Curve, LOD and LOQ of AZM*

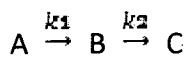
Although studies had been previously done on the enhancement of AZM with HP- β -CD,¹⁶ the limits of detection and limits of quantification using enhanced fluorescence based trace detection by CD addition had not been determined prior to this current project. The weak overall fluorescence of AZM even in the presence of HP- β -CD only allows for the calibration curve to go as low as 1 ppm. The calibration curve was successfully prepared with concentrations from 5 ppm to 1 ppm with an *r* value of 0.998. The standard deviation was calculated from the solvent blank to be 263.30 cps. The slope of the calibration curve line was calculated using Fig. P. to be 2.91 cps/ppm. Using equations 2.7 and 2.8, the LOD was calculated to be 270 ppb and the LOQ was calculated to be 900 ppb. The limit of detection is not low enough for this method of detection to replace any other methods of detection as the fluorescence signal of AZM, even with the enhanced fluorescence by CD addition, is not high enough to detect in low ppb levels.

V.2. *Fluorescence-Based Studies of the UV-A Photolysis of AZM.*

V.2.1. Previous Work

In experiments previously done in the Wagner group,^{16, 59} the fluorescence of fully irradiated samples of AZM in water and AZM in methanol were measured and the maximum fluorescence intensity values recorded. That work showed that the highly fluorescent species is in fact unstable to UV-A light, and undergoes subsequent photolysis to final photoproducts. Samples of proposed intermediates, N-methylantranilic acid (NMA, **Fig. 9.a**) and anthranilic acid (AA, **Fig. 10.b**) in both water and methanol were also measured under identical conditions and the resulting maximum fluorescence intensity values were compared. It was concluded through comparison of the maximum intensity values and the shape of the fluorescence spectra that the unknown fluorescent intermediate was N-methylantranilic acid, as both had identical maximum emission wavelengths (407 nm in water and 405 nm in methanol), and the spectra overlapped very closely.

Yerasmin⁵⁹ also studied the effects of UV-A exposure on AZM in both methanol and in water over a longer period of time and found the gradual production of the highly fluorescent intermediate and its subsequent decay to a photochemically stable final product, concluding that it follows a consecutive first order reaction mechanism as shown in Equation 5.10.



Eq. 5.10

In this equation, A is AZM, B is the highly fluorescent intermediate, and C is the relatively non-fluorescent final photoproducts. k_1 and k_2 are the rates of reaction between each of the steps in the reaction.

Based on the results of Yeasmin,⁵⁸ and other previous literature work,^{46, 60} a complete mechanism was proposed for the UV-A photolysis of AZM.⁵⁹ Two competing reaction pathways were proposed; one leading to the highly fluorescent intermediate NMA, and the other to the stable photoproduct, BA. The proposed mechanism is shown in Figure 37.

V.2.2. Goal of this Work

There were limitations to the work performed by Yeasmin. There was no other direct evidence of NMA besides that of the fluorescence studies. Using NMR and HPLC, it was investigated whether more evidence of the formation of the intermediate NMA could be provided, and to quantify the amount of the non-fluorescent product formed. Furthermore, by the fluorescence quantum yields of AZM and NMA, it would be possible to determine the concentration of NMA that is present in the photolyzed solution. This, combined with the determination of the concentration of BA in the final photolysis mixture using HPLC, will allow for the determination of the relative importance of the two photolysis pathways in Figure 37. This is important for the overall understanding of the photolysis mechanism and photochemically induced fluorescence for AZM.

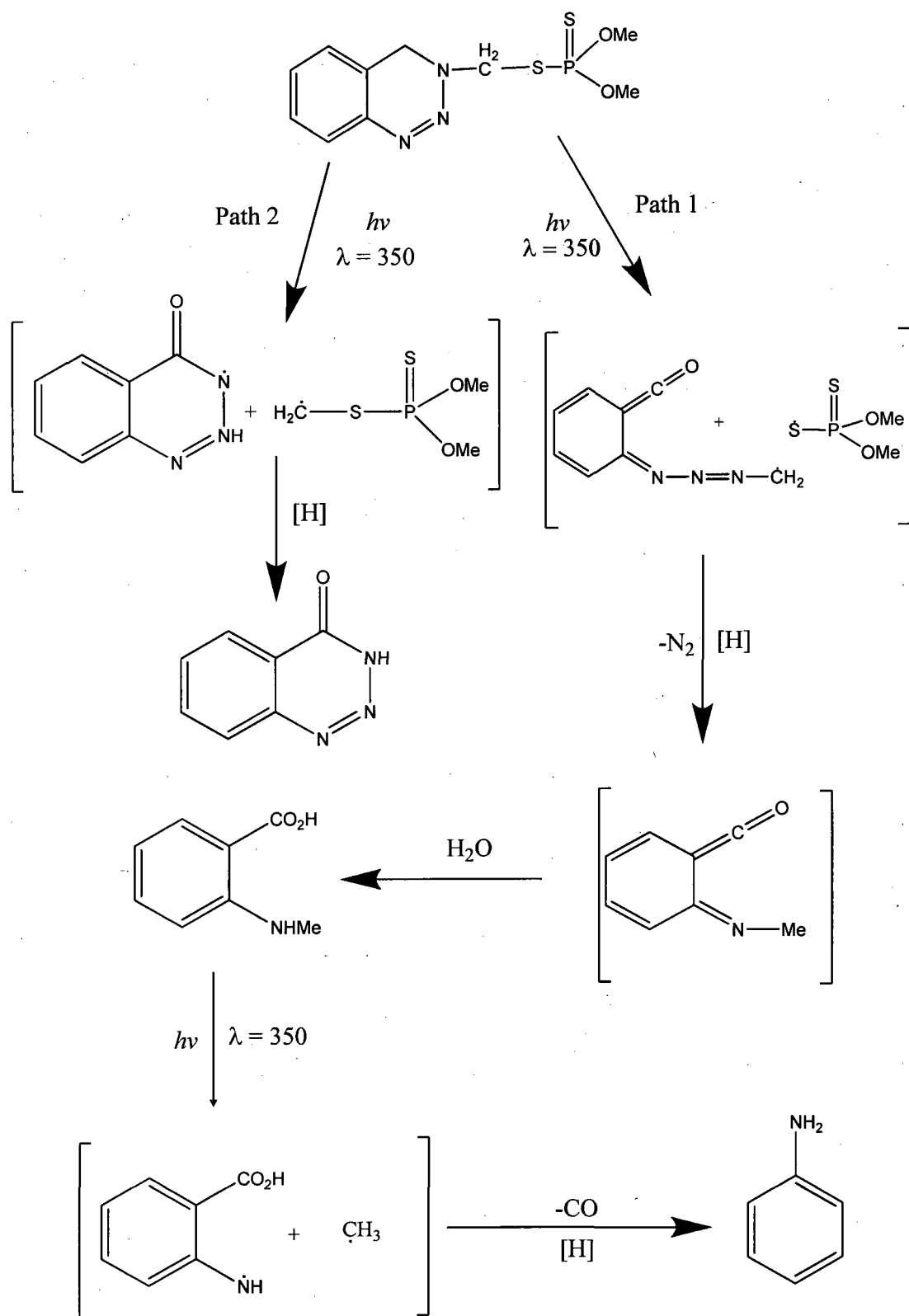


Figure 37. The proposed mechanism of AZM with both major and minor pathways.⁵⁹

V.3. Decay Rate of the Photolysis of the Highly Fluorescent Intermediate

Further studies were carried out during this Masters project in support of the identification of the intermediate as NMA through its photolytic cleavage properties. A new solution of NMA was photolyzed under UV-A light and its fluorescence was measured as a function of time exposed to the UV light. The fluorescence intensity was recorded at the maximum intensity wavelength every 30 minutes for a total time of 600 minutes. These values were plotted with the graphing program *Fig. P*, and fit to a single exponential decay equation: $I(t)=I_0 \exp\{-kt\}+\text{residual}$. The rate constant, k , obtained was $0.0041 \pm 0.0005 \text{ min}^{-1}$; the data and fit are shown in Figure 38.

This decay rate constant calculated from the measured intensity vs. time of irradiation of NMA matches extremely well with the rate constant of $0.0038 \pm 0.0008 \text{ min}^{-1}$ for the photolysis of the fluorescent intermediate of AZM to the stable photoproduct (k_2 in Eq. 5.10) in experiments previously completed by Yeasmin. This work provides further confirmation of the assignment of the intermediate as NMA. This work had originally been performed by Yeasmin but data was highly scattered. It was redone in this project to ensure reproducibility, and to obtain a more accurate measurement of the rate constant for the decay of NMA for a comparison to that obtained for the decay of the intermediates in the photolysis of AZM experiments obtained performed by Yeasmin.

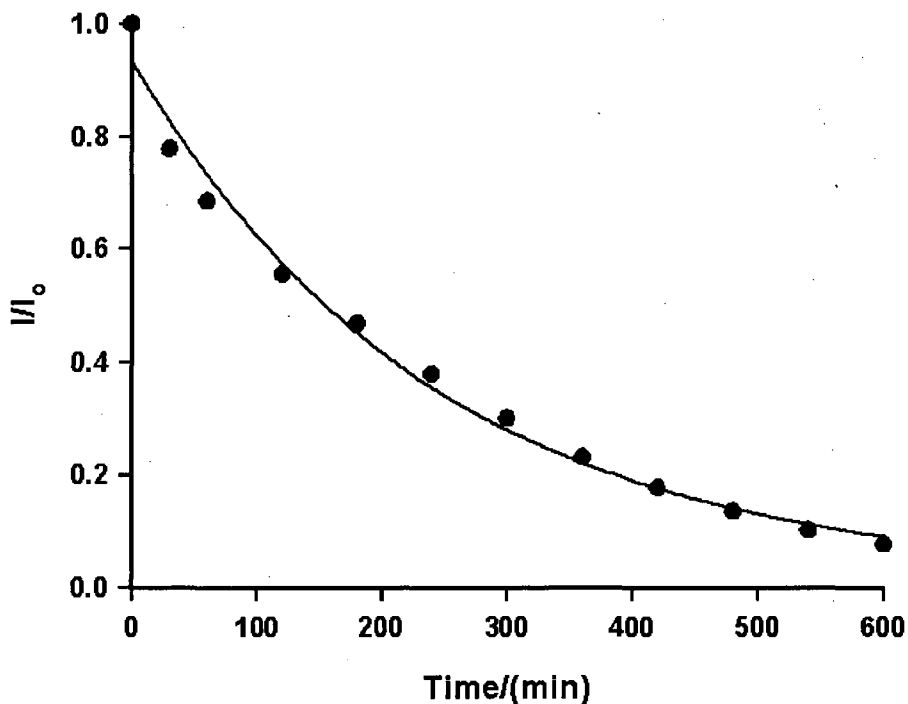


Figure 38. The fluorescence intensity of NMA vs. UV exposure time.

V.3.1. Quantum Yields and Extinction Coefficients

Using quantum yields and extinction coefficients of NMA and AZM, the concentration of NMA, the proposed highly fluorescent intermediate, in the solution of AZM that had been irradiated for 8 hours (peak enhancement time) can be calculated. This information can be used to investigate the relative efficiency of the process leading to enhanced fluorescence.

Solutions of 9.19×10^{-5} M AZM and 4.0×10^{-4} M NMA were prepared and the fluorescence of each was measured. The integrated fluorescence (area), the absorbance of the solution at the excitation wavelength (A) and the refractive index of the solution of AZM (n), combined with the quantum yield standard, 9,10-DPA ($\phi_{F,S}$), its absorbance at the excitation wavelength (A_S), the refractive index of its cyclohexane solution (n_S), and the integration of the fluorescence

peak (area_S) were all measured and recorded in order to calculate the quantum yield from Eq. 1.1.

In this experiment, the excitation wavelength that was used for the AZM and NMA solutions was 315 nm. The absorbance of each solution was measured using the UV-Vis spectrophotometer to give values of 0.301 for the NMA solution and 0.340 for the AZM solution. The fluorescence quantum yields were calculated to be $7.0 \pm 0.9 \times 10^{-4}$ for AZM and 0.25 ± 0.01 for NMA (average of 3 trials). These measurements were also performed on the Perkin Elmer fluorimeter using the corrected emission spectrum mode. In this case, the absorbance values were 0.339 for AZM and 0.340 for NMA and the quantum yield values were 0.30 for NMA and 6.0×10^{-4} for AZM. Thus excellent agreement was obtained using the two different fluorimeters.

The absorption data obtained for the quantum yield calculations can also be used with the solution concentrations to calculate the extinction coefficient for each of the two solutions. By rearranging the Beer-Lambert law (shown previously in Eq. 2.6.), it is possible solve for extinction coefficient (ϵ): $\epsilon = A/(cI)$, where c is the concentration and I is the path length. The extinction coefficients for AZM and NMA were calculated to be $575 \text{ M}^{-1}\text{cm}^{-1}$ and $1800 \text{ M}^{-1}\text{cm}^{-1}$ respectively.

Like the quantum yield calculations, the absorbance for the extinction coefficient is measured at the excitation wavelength (315 nm) that was used for the quantum yield calculations. The path length is the length of the quartz cuvette which was 1 cm and the concentrations were from each of the individual solutions. Combining the Beer-Lambert law

and the quantum yields, Equation 5.12 can be derived, where the enhancement is the measured increase in fluorescence at the maximum of the intermediate formation relative to that of AZM (a factor of 46).

$$[NMA] = [AZM] \times \text{Enhancement} \times \frac{\Phi_{AZM}}{\Phi_{NMA}} \times \frac{\epsilon_{AZM}}{\epsilon_{NMA}} \quad \text{Eq.5.12}$$

Using this equation, the concentration of NMA was calculated to be 1.6×10^{-5} M. Since the initial concentration of AZM was 2.5×10^{-4} M, this corresponds to only about a 4% conversion per mole. NMA has a quantum yield a factor of 360 times larger than AZM and this is what accounts for the large enhancement of 46, and results in such a small concentration of NMA resulting from the photolysis of AZM displaying such a large fluorescence signal. Thus, unfortunately the photolysis pathway leading to fluorescence enhancement (path 1 in Fig. 37) would seem to be the minor pathway; it is predicted that most of the photolysis produces the non-fluorescent product benzazimide. This will be further investigated and confirmed using HPLC as described in section V.3.3.

V.3.2. ^1H NMR Spectroscopy Studies of the UV-A Photolysis of AZM

^1H NMR spectroscopy was chosen as an alternate method for studying the photolysis of AZM and to possibly provide additional proof of the identity of the intermediate and photoproducts. AZM solutions, photolyzed and unphotolyzed, were prepared in methanol-d₄. Solutions of the possible intermediates, NMA and AA were prepared in methanol-d₄ and the stable final photoproduct, BA (refer to Fig.10.a) was also made in methanol-d₄.

The unphotolyzed AZM solution ^1H NMR spectrum showed that the four aromatic protons were found as expected at 8.35, 8.24, 8.11 and 7.98 ppm. The non-aromatic –CH₂ protons were at 5.81 ppm and the –OCH₃ protons were found at 3.76 ppm. ^1H NMR spectra were obtained for the solutions of NMA, AA and BA in order to compare with the photolyzed solution of AZM.

The AZM in methanol-d₄ solution was photolyzed for 6 hours in order to produce the highest concentration of NMA before subsequent decay to BA occurs. 6 hours was found to be the optimum irradiation time for a solution of AZM in methanol. This ^1H NMR spectrum revealed a new peak that was very weak in intensity and could not be identified by comparison to any of the expected intermediates or final product.

A third AZM in methanol-d₄ solution was irradiated for 36 hours in order to fully photolyze the solution. The ^1H NMR spectrum of the fully photolyzed solution showed that new aromatic peaks were present in the sample at 8.32, 8.19, 8.09, and 7.92 ppm and that the aromatic peaks from the AZM solution were no longer present and had been replaced by BA.

There were also peaks at 5.80 ppm and 3.79 ppm, and it was concluded that they were most likely from unidentified final products.

Unfortunately, there was no trace of either NMA or AA in the 6 hour irradiated solution. The large presence of BA in the 36 hour irradiated solution clearly shows that this is indeed the final product that is photochemically stable under UV-A irradiation. To prove this photochemical stability, a solution of BA in methanol-d₄ was irradiated for 12 hours and the ¹H NMR spectrum was compared to that of a ¹H NMR spectrum of a solution of BA that had no UV-A exposure. There was no change in the spectrum of the photolyzed solution thus confirming BA as a stable photoproduct of AZM under UV-A exposure and thus, a final product.

V.3.3. HPLC Studies of the UV-A Photolysis of AZM

HPLC analysis was done as a third method for identifying the intermediates and products in order to confirm or disprove the proposed mechanism of the photolysis of AZM under UV-A irradiation. Unexposed solutions of AZM, NMA, AA, and BA were run in the HPLC as standards in order to get accurate retention times in the column. They were prepared as 60/40 water/methanol solutions. A solution of AZM was photolyzed for 8 hours at 350 nm in an effort to produce the sought after intermediates at the highest possible concentration. Two major peaks showed up in the chromatogram with retention times of 3.1 and 8.8 min, which matched up perfectly with the standards of BA and AZM respectively. The concentration of the AZM remaining from the initial 2.5×10^{-4} M was found to be 1.2×10^{-4} M after the 8 hours of exposure. This represents a total of 52% conversion of AZM from 8 hours of UV-A exposure. The BA

concentration calculated from the HPLC chromatogram was 7.0×10^{-5} M. This concentration represents 54% of the total photolyzed AZM concentration and 28% of the overall initial concentration of AZM. This clearly indicates that BA is the major stable photoproduct of AZM under UV-A conditions, and that "path 2" in Fig. 37 is the major photolysis pathway. This is in agreement with the results from the quantum yield experiments, which indicate that formation of the highly fluorescent NMA at peak conversion represented only 4% conversion of AZM after 8 hours.

A third peak in the 8 hour solution, with a retention time of 1.5 min was not able to be accurately identified due to the fact that both NMA and AA standards shared that same approximate retention time. It was not possible to say with certainty which intermediate was present in the sample, only that it was most likely one of the two.

V.4. *Conclusions*

The work performed in this chapter, in conjunction with the previous work by Yeasmin²⁹ has resulted in a full understanding of the photochemistry and photochemically induced fluorescence of AZM. This combined work ultimately led to a publication in the *Journal of Photochemistry and Photobiology A: Chemistry*²⁹ on AZM photochemistry. The photolysis mechanism of AZM was proposed by Yeasmin and Wagner based on various fluorescence spectral and kinetic experiments. HPLC experiments that were performed in the work and described in this chapter provided information on the partition of the competing pathways; by comparing the concentration of BA in a fully photolyzed solution from the HPLC experiments to

the concentration of NMA from the fluorescence quantum yield experiment, it is clear that pathway 2 is the major photolysis pathway.

The work in this chapter is an illustration of the work that needs to be done in the future for the pesticide AZO as well as other pesticides that have not been identified in this thesis, that show photochemically induced fluorescence.

VI. CONCLUSIONS AND FUTURE WORK

Pesticides continue to find ways to enter water systems on Prince Edward Island and wreak havoc on the natural ecosystems. A fast, inexpensive method of pesticide detection that has potential preventative measures would be of high value, financially and environmentally. With no end in sight for industrialized farming practises including heavily mechanized methods and applications of large quantities of pesticides and fertilizers, the future of PEI's water systems looks as bleak as the past.

A total of eight pesticides were studied in this project encompassing a variety of insecticides, fungicides and herbicides, all of which are found in PEI's Non-Domestic Pesticide Sales Reports of 2007⁷

Fluorescence-based methods of trace detection of pesticides in water using supramolecular host:guest inclusion, photochemically induced fluorescence, or a combination of the two, were developed for various pesticides. PIF or host:guest inclusion was used to enhance the non- or weakly fluorescent band produced from a pesticide molecule to a degree at which it could be detected in low part per billion concentrations. The host molecules used for this type of supramolecular chemistry ranged from modified to native α -, β - and γ -cyclodextrins.

Carbofuran, carbaryl, azoxystrobin, imidacloprid, chlorothalonil, atrazine, metolachlor and azinphos-methyl with various CDs were all studied in detail in this thesis project. Work done by Pacioni et al.¹⁵ showed cyclodextrin enhanced fluorimetric-based trace detection of a pesticide in water could be used for carbofuran and carbaryl, two members of the carbamate

family of pesticides. Since one of the major goals of this project was to compile a list of valid candidates of pesticides used on PEI for this method of detection, both carbofuran and carbaryl were studied more extensively. From that starting point, binding constants, host:guest stoichiometry, and limits of detection and quantification were obtained and improved upon from that publication. Spiked samples with unknown concentrations for both carbofuran and carbaryl were analyzed with promising preliminary results.

Chlorothalonil, the highest selling pesticide used in Prince Edward Island and most controversial due to its persistence in the atmosphere, had a weak fluorescent band that increased substantially with the addition of α -CD. Binding constants with all six host CD molecules were obtained, a calibration curve was successfully created and limits of detection and quantification were found using α -CD as the host. Due to the weak natural fluorescence of the molecule however, even with the increase in the presence of CD, the fluorescence was not strong enough to detect the pesticide in low ppb concentrations. Spiked samples were not performed due to the difficulty in obtaining a calibration curve in the parts per billion range.

Metolachlor and atrazine are two pesticides that shows little or no natural fluorescence. The addition of CD did not increase the fluorescence to a point where it was worthwhile to continue therefore both pesticides were omitted from further experimentation.

Synchronous scanning was successfully used in efforts to separate broad fluorescent bands that overlapped when two or more pesticides were present in a solution. The work done by Ni and Cao⁵⁶ on carbofuran, carbaryl and propoxur paved the way for trials involving

synchronous scanning of a mixture of pesticides including chlorothalonil, azinphos-methyl, carbaryl and carbofuran with CDs that was completed in this project with excellent results.

Accidentally, the pesticides imidacloprid and azoxystrobin is both discovered to have highly fluorescent photoproducts when exposed to UV light. Both pesticides, when left in the fluorimeter for varying amounts of time under exposure to the lamp, showed that the photoproduct was highly fluorescent, so much so that it was reasonable to explore further the possibility of trace detection of these pesticides by photochemically induced fluorescence.

Literature reviews found that imidacloprid had previously been found to photolyze under UV light to a highly fluorescent photoproduct that has been extensively studied by Flores et al.^{30, 31} It was then attempted in this project to further enhance the fluorescent band of the photoproduct by host:guest inclusion by CD addition but no further enhancement occurred.

Initial fluorescence trials of azoxystrobin found that it was not a fluorescent molecule but after exposure to UV light and subsequent photolysis produced a highly fluorescent photoproduct. A literature paper found from a revamped literature search discussed the photolysis of azoxystrobin in grapes, wines and musts but no such paper was found on the photolysis of azoxystrobin in water. Studies revealed that under UV-C light, azoxystrobin photolyzed into an unknown fluorophore that was stable and did not undergo further photolysis. Further tests revealed that with the addition of CD, the photochemically-induced fluorescence could be significantly enhanced. Binding constants and calibration curves were successfully obtained as well as limits of detection and quantification. A preliminary spiked sample trial was performed with promising results.

Work on azinphos-methyl, a pesticide that had previously been studied extensively by Wagner et al.¹⁶ and Wagner and Yeasmin,⁵⁹ was undertaken in this project to complete work on the proposal of a mechanism for the UV-A photolysis of AZM in water. Through a series of experiments involving extinction coefficients, quantum yields, decay rates, HPLC, and ¹H NMR, a mechanism for the photolysis of AZM under UV-A conditions was successfully elucidated, involving a major pathway in which benzazimide is the final stable product and a minor pathway in which a highly fluorescence intermediate N-methylanthranilic acid is formed; and then subsequently photolyzed further, to a stable final product, aniline. Furthermore, the relative partitioning of the two proposed pathways was determined, with the pathway leading to non-fluorescent products dominating that lead to the highly fluorescent intermediate by a factor of 14:1. This work was subsequently published.²⁹

A calibration curve was successfully obtained for AZM as well as limits of detection and quantification using HP- β -CD as a host molecule. The limit of detection, due to the weak fluorescent signal, even in the presence of CD was not low enough to perform spiked sample experiments.

With the non-domestic pesticide sales report changing on a yearly basis and the continuous development of pesticides, there exists a significant need for a fast, inexpensive, environmentally friendly method of trace detection of pesticides in water. There is an even greater potential worth if this could also serve as a method of prevention. Fully developing this fluorescence-based method, firstly by creating an extensive list of pesticides used on PEI that exhibit natural fluorescence, and that can have this fluorescence enhanced photochemically or

by supramolecular host:guest chemistry and secondly by separating each fluorescence band of an individual pesticide using synchronous scanning that it can be distinguished from other pesticides present in a solution, are the main goals of this work. This work has successfully demonstrated that such enhanced fluorescence based detection methods have the potential to be useful for the detection of pesticides in natural waters.

Immediate future work will include performing more spiked sample trials with the pesticides that showed promise in this project as well as elucidating the mechanism of azoxystrobin photolysis under UV-C light. Expanding on the list of pesticides that form host:guest inclusion complexes that results in fluorescence enhancement would be a high priority. Other work that could be undertaken is the continuation of spiked sample trials with the addition of natural water and determining if there are any background effects from natural water itself. There is tremendous potential in photochemically induced fluorescence studies of pesticides and a list could be generated, consisting of pesticides that undergo photolysis and generate a highly fluorescent products.

Finally, and most importantly, the eventual use of a portable fluorimeter which we have in our lab, would allow for rapid on-site field testing, will be examined with the very recently obtained diodes for excitation at 290 – 300 nm. The portable fluorimeter can be controlled from a laptop computer and can easily be transported around in order to measure water samples in the field. The work done in this project will provide the foundation for moving forward with developing a portable method.

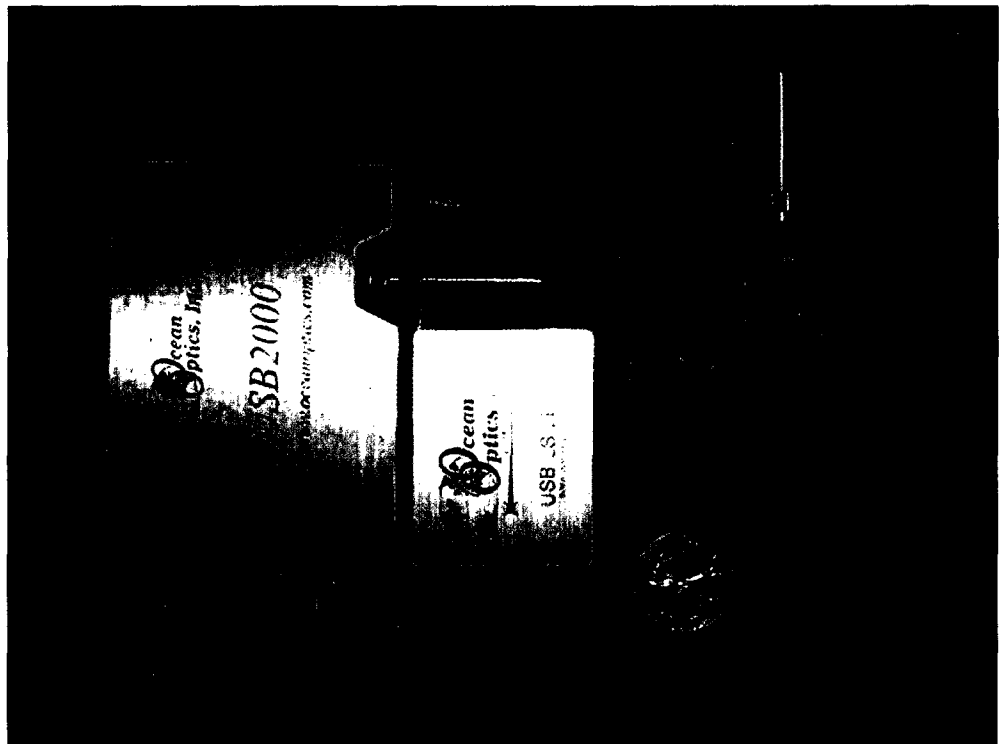


Figure 39. The portable fluorimeter. A quarter is included to give the reader a sense of the size of the fluorimeter.

In closing, the potential exists for a fluorimetric-based trace detection of pesticides using host:guest chemistry and this project illustrates the basic foundation and procedures behind it. There is also promise for photochemically induced fluorescence based trace detection as shown from the work done on imidacloprid and azoxystrobin. Using both methods in conjunction with one another, and the further inclusion of synchronous scanning to narrow the fluorescence bands, opens up a new door in the fluorescence based trace detection of pesticides.

VII. REFERENCES

1. Prince Edward Island Department of Agriculture and Forestry Roundtable Report. 2004.
2. Agriculture Information Document PDF. Department of Agriculture. Prince Edward Island Government. 2008.
3. White,L.M.; Ernst, W.R.; Julien, G.; Garron, C.; Leger,M. *Pest. Manag. Sci.* **2006**, 62, 126-136.
4. "State of Environment". Government of Prince Edward Island. Department of Fisheries, Aquaculture and Environment. 2003.
5. Tests Found Inconclusive on Two PEI Fish Kills. *The Guardian*. October15, 2007, Online.
6. Prince Edward Island Pesticide Control Act. Government of Prince Edward Island. Dec. 2008.
7. Reeves, D. Non-Domestic Sales Report of Prince Edward Island, Department of Environment, Government of Prince Edward Island, June 2007.
8. "Consumer Fact Sheet on CCl₄". United States Environmental Protection Agency. <http://www.epa.gov/safewater/contaminants/basicinformation/carbon-tetrachloride.html> (accessed September 2009).
9. Sundravadana, S.; Alice, D.; Samiyappan, R.; Kuttalam, S. *J. Braz. Chem. Soc.* **2008**, 19, 60-63.
10. Mickova, B.; Zrostlikova, J.; Hajslova, J.; Rauch, P.; Moreno, M.J.; Abad, A.; Montoya, A. *Anal. Chim. Acta*. **2003**, 495, 123-132.

11. Canadian Water Quality Guidelines. Environment Canada Webpage (Accessed Oct. 2009).
12. Wagner, B.D. *Handbook of Photochemistry and Photobiology*; Nalwa, H.S., Ed.; American Scientific Publishers: New York, 2003; 1-57.
13. Lakowicz, J.R. *Principles of Fluorescence Spectroscopy*, Third Edition, Springer US, Boston, MA, 2006.
14. Salinas, F.; Munoz de la Pena, A.; Munoz de la Pena, F. *Mikrochimica Acta*. 1985, 3, 361-368.
15. Pacioni, N.L.; Veglia, A.V. *Anal. Chim. Acta*. 2003, 488, 193-202.
16. Wagner, B.D.; Sherren A.C.; Rankin, M.A. *Can. J. Chem.* 2002, 80, 1210-1216.
17. Mbaye, M.; Seye, M. *Anal. Bioanal. Chem.* 2009, 394, 1089-1098.
18. Coly, A; Aaron, J.J. *Anal. Chim. Acta*. 1998, 360, 129-141.
19. Wagner, B.D. The Effects of Cyclodextrins on Guest fluorescence. *Cyclodextrin Materials Photochemistry, Photophysics, and Photobiology*. 2006. 27-57.
20. Lehn, J.M. *Angew. Chem. Int. Ed. Engl.* 1988, 27, 89-112
21. Munoz de la Pena, A.; Salinas, F.; Gomez, M.J.; Acedo, M.A.; Sanchez Pena, M. *J. Incl. Phenom. Mol. Rec. Chem.* 1993, 15, 131.
22. Sanrame, C.N.; de Rossi, R.H.; Arguello, G.A. *J. Phys. Chem.* 1996, 8151.
23. Szejtli, J.; *Chem. Rev.* 1998. 98, 1743-1753.
24. Li, S.; Purdy, W.C. *Chem. Rev.* 1992, 92, 1457-1470.
25. Paginton, J.S. *Chem. Bra.* 1987, 23, 455.
26. Khan, A.R.; Forgo, P.; Stine, K.J.; D'Souza, V.T. *Chem. Rev.* 1998, 98, 1977.

27. Englman, R.; Jortner, J. *Molec. Phys.* **1970**, *18*, 145.

28. Kim, Y.H.; Cho, D.W.; Yoon, M.; Kim, D. *J. Phys. Chem.* **1996**, *100*, 15670.

29. Yeasman, L.; MacDougall, S.A.; Wagner, B.D. *J. Photochem Photobiol: A.* **2009**, *204*, 217-223.

30. Flores, J.L.; Diaz, A.M.; Fernandez de Cordova, M.L. *Anal. Chim. Acta* **2007**, *585*, 185-191.

31. Flores, J.L.; Diaz, A.M.; Fernandez de Cordova, M.L. *Talanta* **2007**, *72*, 991-997.

32. Crosby, D.G. *Residue Rev.* **1969**, *25*, 1-12.

33. Mickova, B, et al. *Anal. Chim. Acta*, **2003**, *495*, 123-132.

34. "Chlorothalonil Fungicide Factsheet" *J. Pest. Reform.* **1997**, *17*, 15-20.

35. General Pesticides. Government of Canada's Occupational Health and Safety Webpage.
<http://www.ccohs.ca/oshanswers/chemicals/pesticides/general.html> (accessed Nov, 2009).

36. Pesticide Info Sheet. Azoxystrobin. Government of British Columbia. Ministry of Agriculture and Lands. January 2009.

37. Northwest Coalition for Alternatives to Pesticides. *J. Pest. Reform.* **2005**, *25*.

38. Canadian Water Quality Guidelines for the Protection of Agricultural Water Uses. Canadian Council of Ministers of the Environment, **1999**.

39. Tanner,D.K.; Knuth, M.L. *Ecotoxicol. Environ. Saf.* **1995**, *32*, 184-193.

40. Azinphos-methyl Fact Sheet. United States Environmental Protection Act. 2008.

41. Kulikova, N.A.; Perminova, I.V. *Environ. Sci. Technol.* **2002**, *36*, 3720-3724.

42. Extoxnet. Pesticide Information Profile. August 1993.

43. Renner, R. *Environ. Sci. Technol.* **2002**, *36*, 55-56.

44. Youbin, S.; Kazuhiro, T.; Iwasaki, A.; Zhou, D. *Pest. Manag. Sci.* **2009**, *65*, 956-962.

45. Eaton, D.F. *J. Photochem. Photobiol. B: Biol.* **1998**, *2*, 523-531.

46. MacDougall, D.; Crummett, W. *Anal. Chem.* **1980**, *52*, 2242-2249.

47. Cramer, F.; Saenger, W.; Spatz, H-Ch. *J. Am. Chem. Soc.* **1967**, *89*, 14.

48. Franke, J.; Merz, T; Losensky, W.; Muller, W.M.; Werner, V.; Vogtle, F. *J. Inclu. Phen. Mol. Rec. Chem.* **1985**, *3*, 471.

49. Rankin, M.A.; Wagner, B.D. *Supramol. Chem.* **2004**, *16*, 513-519.

50. A world compendium: A pesticide Manual. 12 ed.; Tomlin, C. D. S., Ed.; British Crop Protection Council: Farnham, UK, 2000; 67-68.

51. Veenhuis, S. "Fluorescence Based Trace Analysis of Pesticides Carbaryl and Azinphos-Methyl in Natural Waters", Honour's Thesis, UPEI, April 2004.

52. Eaton, D.F. *J. Photochem. Photobiol. B: Biol.* **1998**, *2*, 523-531.

53. Northwest Coalition for Alternatives to Pesticides. *J. Pest. Reform.* **2001**, *21*.

54. Rivard, Linda. Environmental Fate of Metolachlor. Environmental Monitoring Branch. Department of Pesticide Regulation.

55. Polati, S.; Bottaro, M.; Frascarolo, P.; Gosetti, F.; Gianotti, V.; Gennaro, M.C. *Anal. Chim. Acta.* **2006**, *579*, 146-151.

56. Bartlett, J.L.; Clough, J.M.; Godfrey, C.R.A.; Godwin, J.R.; Hall, A.A.; Heaney, S.P.; Maund, S.J. *Pest. Outlook.* **2001**, *143-147*.

57. Ni, Y.; Cao, D. *Spectroscopy Letters.* **2006**, *39*, 431-445.

58. Vilchez, J.L.; El-Khattabi, R.; Blanc, R.; Navalon, A. *Anal. Chim. Acta*, **1998**, *371*, 247-253.

59. Yeasman, L. "Investigations of the UV-A Photochemistry of the Pesticide Azinphos-Methyl". Master's Thesis, UPEI, 2006.

60. Gil-Garcia, M.D.; Martinez-Galera, M.; Parilla-Vazquez, P.; Mughari, A.R.; Ortiz-Rodriguez, I.M. *J. Fluoresc.* **2008**, *18*, 365-373.